Supplemental information

VAV1 mutations contribute to development of T-cell neoplasms in mice

Kota Fukumoto[1], Mamiko Sakata-Yanagimoto[1, 2, 3], Manabu Fujisawa[1], Tatsuhiro Sakamoto[1, 3], Hiroaki Miyoshi[4], Yasuhito Suehara[1], Tran B. Nguyen[1], Sakurako Suma[1], Shintaro Yanagimoto[5], Yuichi Shiraishi[6], Kenichi Chiba[6], Alyssa Bouska[7], Keisuke Kataoka[8, 9], Seishi Ogawa[8], Javeed Iqbal[7], Koichi Ohshima[4], and Shigeru Chiba[1, 2, 3]

[1] *Department of Hematology, Comprehensive Human Biosciences, University of Tsukuba.*
[2] *Department of Hematology, Faculty of Medicine, University of Tsukuba.*
[3] *Department of Hematology, University of Tsukuba Hospital.*
[4]*Department of Pathology, School of Medicine, Kurume University.*
[5]*Division for Health Service Promotion, University of Tokyo.*
[6]*Division of Cellular Signaling, National Cancer Center Research Institute*.
[7]*Department of Pathology and Microbiology, University of Nebraska Medical Center.*
[8]*Department of Pathology and Tumor Biology, Graduate School of Medicine, Kyoto University.*
[9]*Division of Molecular Oncology, National Cancer Center Research Institute.*

Supplemental Methods

Mice

All mice were maintained in specific pathogen-free conditions at the Laboratory Animal Resource Center of the University of Tsukuba. All experiments were performed according to guidelines of the Laboratory Animal Resource Center. *p53*$^{-/-}$ mice were provided by the RIKEN BioResource Center Acc. No.CDB 0001K (Tsukada, 1993 #730). BALB/c-nu (CAnN.Cg-*Foxn1*^{nu}/CrlCrlj, nude) mice were from Charles River Laboratory. Six genotypes of mice, including wild-type (WT), VAV1 mutant (V-Del or V-Fus) transgenic mice (*VAV1-Tg*), *Trp53*$^{+/-}$ mice (*p53*$^{+/-}$), *Trp53*$^{-/-}$ mice (*p53*$^{-/-}$), *p53*$^{+/-}$ *VAV1-Tg*, and *p53*$^{-/-}$ *VAV1-Tg* (*p53*$^{-/-}$ V-Del or *p53*$^{-/-}$ V-Fus) were analyzed arround 4 weeks of age. These mice were performed genomic polymerase chain reaction (PCR) of tail DNA to confirm transduction of the VAV1 mutant and *Trp53* loss, as shown in Figure S1d. Primers for VAV1 are 5'-GGCTGAGGCTGAACAGAACTGGTGG-3' (forward) and 5'-CAGGCTCCTTGAAGGGGAACTGCAA-3' (reverse). Primers for Tp53 are 5'-GTTATGCATCCATACAGTACA (forward) and 5'- CAGGATATCTTCTGGAGGAAG-3' (reverse).

Primary mouse tumor cells

Mice were sacrificed by cervical dislocation. Single cell suspensions from thymus, spleen, and abdominal lymph nodes were prepared in five ml phosphate-buffered saline supplemented with 2.5% fetal calf serum (Staining Medium; SM). Cells were washed in SM and centrifuged at 410 × g for 5 minutes at 4°C, subjected to NH_4Cl lysis to eliminate erythrocytes, resuspended in SM, and passed through a 70 μm cell strainer (Falcon, NY, USA). Cells were analyzed by FACS Aria II (Beckton Dickinson). Remaining cells were transplanted into nude mice to confirm cell autonomous activity and stored in CELL BANKER 1 plus (ZENOAQ

RESOURCE) or RLT Buffer (Qiagen) at -80°C prior to performing whole transcriptome analysis (WTA) and whole exome sequencing (WES).

Quantitative PCR

cDNA synthesis from total RNAs was performed with SuperScript III First-Strand Synthesis System for RT-PCR (ThermoFisher SCIENTIFIC) according to the manufacturer's instructions. Taqman Gene Expression Assays (Applied Biosystems) and FastStart Universal Probe Master (ROX) were used in each experiment. cDNA libraries were subjected to 7500 Fast System (Applied Biosystems) and analyzed using 7500 software. Relative expression was normalized to values of 18S rRNA. All assays were performed three times for each biological replicate.

Histology

Tissues were fixed in 10% formaldehyde in 0.01 mol/L phosphate-buffered saline solution (pH 7.2), paraffin-embedded, cut in 5µm sections and stained with hematoxylin and eosin (HE). Immunohistochemical analysis for CD3, CD4, CD8, CD45R, and phosphoVAV1 was performed on FFPE tissue sections. Sections were activated by Tris-EDTA (pH 9.0) for 20-40 minutes at room temperature (RT) and then incubated with primary antibodies against mouse-CD3 antibody (1:50, Clone: SP7, Cat. No. ab16669, abcam) for 60 minutes at RT, -CD4 antibody (1:500, Clone: EPR19514, Cat. ab183685, abcam) for 60 minutes at RT, -CD8a antibody (1:500, Clone: EPR20305, Cat. No. ab209775, abcam) for 30 minutes at RT, -CD45R (B220) biotinylated antibody (1:400, Clone: RA3-6B2, Cat. No. 553085, BD) for 30 minutes at RT, or -phospho-VAV1 (Tyr174) antibody (1:100, Clone: polyclonal Cat. PA5-36699, Thermofisher scientific) for overnight at 4°C. Secondary antibodies were EnVision+ System-HRP, Labelled Polymer (Rabbit) (DAKO) for anti -CD3, -CD4, and -CD8a antibody incubated

30 minutes at RT, ImmPRESS HRP Anti-Rat IgG Polymer (VECTOR) for anti -CD45R (B220) incubated 30 minutes at RT, and SignalStain Boost IHC Detection Reagent (HRP.Rabbit) (CST) for anti -phospho-VAV1 (Tyr174) incubated 30 minutes at RT. HE and immunohistochemically-stained sections were photographed with a Keyence BZ X710 microscope (Keyence Corporation, Osaka, Japan).

Other tissues were fixed in 4% paraformaldehyde for 5 hours at 4ºC and then embedded in OCT compound (Sakura Finetek Japan Co., Tokyo, Japan) at -80 ºC. OCT blocks were sliced into 5 μm sections using a cryostat and then incubated with primary antibodies against mouse-CD3 (1:500, Clone: 17A2, Cat. No. 100201, BioLegend), and -cMyc antibody (1:100, Cat. No. ab32072, Abcam) at 4 ºC overnight. All secondary antibodies were diluted 1:2000 and incubated with sections at RT for 60 minutes. After incubation with DAPI (Vectashield Mounting Medium; Vector laboratories, CA, USA), stained samples were photographed with a Leica TCS SP5 confocal laser scanning microscope (Leica Microsystems, Wetzlar, Germany).

T cell receptor (TCR) stimulation

Naïve T cells were sorted from splenocytes using EasySep Mouse Naïve T Cell Isolation Kit (VERITAS). Soted naïve T cells were cultured in RPMI-1640 (Sigma) supplemented with 10% FCS, 1% Penicillin-Streptomycin-L-glutamine (Wako), 1% sodium pyruvate (gibco), 1% nonessential amino acids (gibco), 1% HEPES (gibco), 50μM 2-MercaptoEthanol (Wako), and recombinant mouse interleukin-2 (20 ng/ml) (Wako). TCR were stimulated 2 hours by PMA/Ionomycin for checking phospho-VAV1 or 8 days Dynabeads Mouse T-activator CD3/CD28 (VERITAS) for checking transcription factor GATA3.

Flow cytometry

Single cell suspensions of tissues were stained with combinations of phycoerythrin - Cyanin 7- (PE-Cy7, Cat. No. 25-0042-82) labeled antibody to CD4; fluorescein isothiocyanate- (FITC, Cat. No. 11-0081-82), or allophycocyanin- (APC, Cat. No. 17-0081-82) labeled antibodies to CD8a; phycoerythrin-labeled (PE, Cat. No. 12-0031-82) antibody to CD3e; PE-labeled (Cat. No. 12-5961-82) antibody to TCR_{β}; APC-labeled (Cat. No. 17-0242-82) antibody to CD24; FITC-labeled (Cat. No. 11-0441-82) antibody to CD44; PE-labeled (Cat. No. 12-9981-82) antibody to CD279 (PD-1); FITC-labeled (Cat. No. 11-9949-82) antibody to CD278 (ICOS); APC-labeled (Cat. No. 17-0621-82) antibody to CD62L (L-Selectin); PE-labeled (Cat. No. 12-0251-82) antibody to CD25; or perinidin chlorophyll-labeled (PerCP, Cat. No. 00-6993-50) antibody to 7AAD. Cells were also stained using Phosflow Lyse/Fix Buffer (BD) and Phosflow Perm Buffer III (BD) with Alexa Fluor 488-labeled (Cat. Ab237470) antibody to VAV1 (phosphor Y174) or Foxp3/Transcription Factor Staining Buffer Set (eBioscience) with Alexa Fluor 488-labeled (Cat. 53-9966-42) antibody to GATA3. Stained cells were analyzed using a FACS Aria II or III flow cytometer (BD Biosciences) and data were analyzed using FlowJo software.

We defined tumors as immature T-cell neoplasms (TCN) corresponding to human T-lymphoblastic lymphoma (T-LBL) when thymuses were enlarged and tumor cells exhibited TCR_{β}^{low} $CD24^{+}$ cell-surface patterns, indicative of immature T cells; by contrast, we defined TCN (Lym) as mature when spleens were enlarged and tumor cells exhibited TCR_{β}^{high} $CD24^{-}$ cell-surface patterns indicative of mature T cells.

Mouse tumor transplantation

2×10^7 cells of a single cell suspension prepared from whole thymocytes of T-LBL tumor or whole splenocytes of Lym tumor were intraperitoneally injected into 5-week-old nude mice that had undergone 2 Gy irradiation before injection. Tumor cell engraftment was checked in peripheral blood at 14 days after transplantation and defined as a percentage of donor H-$2K^b$ (MHC class I alloantigen of C57BL/6 mice, Cat. No. 116606) -positive cells > 0.01% of peripheral blood mononuclear cells.

Whole transcriptome analysis (WTA)

Total RNAs were extracted from fresh frozen cells using the RNeasy mini kit (Qiagen). RNA integrity number (RIN) values and size distribution and concentration of libraries were examined using the Agilent 2100 Bioanalyzer (Agilent). Sequencing reads were mapped on the mm10 mouse reference genome and quantified using CLC Genomics Workbench version 9.5.1 (Qiagen, Hilden, Germany). Normalized to reads per kilobase of exon per million mapped sequence reads (RPKM) were estimated for each gene and filtered by the Empirical Analysis of Digital Gene Expression tool. To identify significantly enriched pathways in each group, Gene Set Enrichment Analysis (GSEA: v.4.0.1) [1,2] (https://www.gsea-msigdb.org/gsea/index.jsp) with the Molecular Signatures Database (MSigDB) gene sets (hallmark and C2: v7.0) was performed for genes expressed at >1 RPKM in two or more samples. Gene Ontology enrichment analysis was performed using Metascape [3] (https://metascape.org/gp/index.html#/main/step1).

Whole exome sequencing (WES)

Genomic DNAs were extracted from fresh frozen tumor cells using QIAamp DNA Blood Mini Kit (Qiagen). DNA integrity number (DIN) values were examined using Agilent TapeStation 2200 (Agilent). Libraries were made using SureSelect XT Mouse All Exon kits (Agilent

Technologies). Sequencing was performed by standard 150 bp paired-end protocol. The Genomon2 pipeline (https://github.com/Genomon-Project) was used for sequence alignment and mutation calling. Putative somatic mutations with Fisher's exact *P*-value <0.01 and an EB call *P*-value >2.0 were adopted. Mapping errors were excluded by visual inspection with Integrative Genomics Viewer (IGV) (http://software.broadinstitute.org/software/igv/). Copy number analysis using WES data were performed using CopywriteR (https://github.com/PeeperLab/CopywriteR). Significant focal CNVs for CopywriteR output were identified using GISTIC 2.0 software (https://github.com/genepattern/GISTIC_2.0).

Protocol for mouse injections

Cells were harvested from whole splenocytes of tumor-bearing nude mice that had been transplanted with T-LBL or Lym tumors and then intraperitoneally injected again into 2 Gy-irradiated nude mice. JQ1 (Selleck chemicals) at 3 mg/kg body weight or vehicle was intraperitoneally injected once every two days from day 7. As diluent we used 2 % DMSO/30 % PEG300/5 % Tween 80 in distilled water (Wako).

Supplementary Figure 1

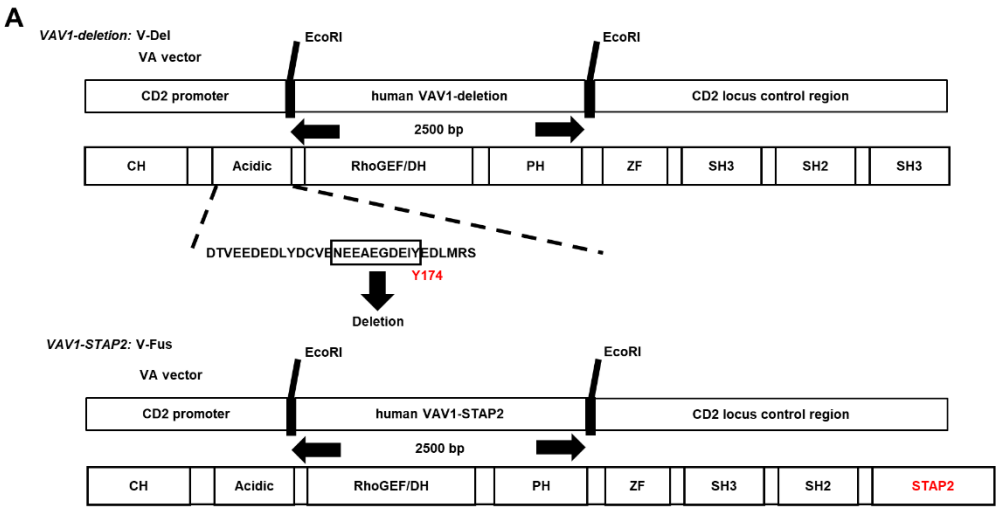

B

Line ID	Sample	VAV1 Copy/cell	Actin Quantity	VAV1/Actin copy number/cell	Average VAV1/Actin copy number/cell
V-Del Line A	VDEL A-1	4.2	9.191	1.0	1.0
	VDEL A-2	4.2	9.161	1.0	
	VDEL A-3	3.2	7.030	1.0	
V-Del Line B	VDEL B-1	2.4	2.693	1.9	1.97
	VDEL B-2	2.2	2.512	1.9	
	VDEL B-3	4.3	4.339	2.1	
V-Del Line C	VDEL C-1	16.1	11.846	2.9	3.03
	VDEL C-2	13.1	10.038	2.8	
	VDEL C-3	12.8	8.08	3.4	
V-Fus Line A	VS2 A-1	0.5	2.129	0.5	0.53
	VS2 A-2	0.6	2.379	0.5	
	VS2 A-3	0.8	3.062	0.6	
V-Fus Line B	VS2 B-1	3.9	13.132	0.6	0.57
	VS2 B-2	4.6	15.986	0.6	
	VS2 B-3	0.6	2.964	0.5	
V-Fus Line C	VS2 C-1	4.7	7.535	1.3	1.37
	VS2 C-2	6.3	9.356	1.4	
	VS2 C-3	2.6	4.021	1.4	

v.s. Jurkat cell

C

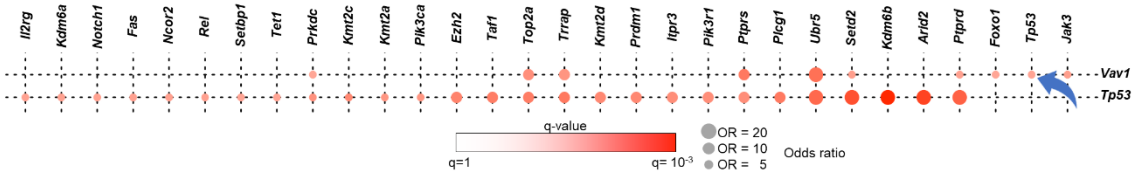

D (i)

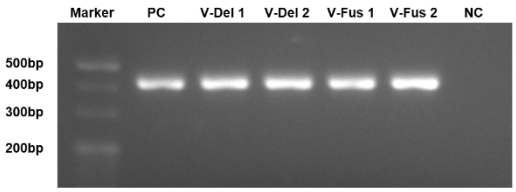

(ii)

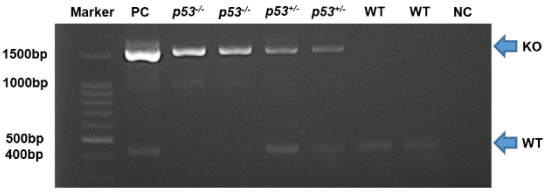

Supplementary Figure 1: Generation of VAV1 mutant-expressing mice on a *p53*-null

background.

A. Structure of VA vector constructs harboring human *VAV1*-Δ165-174 (V-Del) and *VAV1-STAP2* (V-Fus) cDNAs driven by the *CD2* promoter.

B. Average copy number of human VAV1 mutant transgenes, as detected by analysis of tail DNAs from three lines (Lines A, B, and C) of V-Del or V-Fus mice. Line C from each genotype was used for subsequent analyses. Amplification values were normalized to those of mouse *Actin*, a housekeeping gene.

C. Alterations in *TP53* and *VAV1* in PTCLs [4]. Pairwise correlations between mutations were assessed using a pairwise Fisher's exact test with Benjamini-Hochberg correction ($q < 0.1$).

D. Genomic PCR analysis of (i) human V-Del and V-Fus transgenes, and (ii) bands indicative of *Trp53* deletion in tail DNA from mice with conventional *Trp53* knockout ($p53^{-/-}$) or $p53^{+/-}$ mice expressing V-Del or V-Fus transgenes ($p53^{-/-}$ V-Del or $p53^{-/-}$ V-Fus mice) at 4 weeks of age. N=2 for each. KO, knockout; WT, wild type; PC, positive control; NC, negative control.

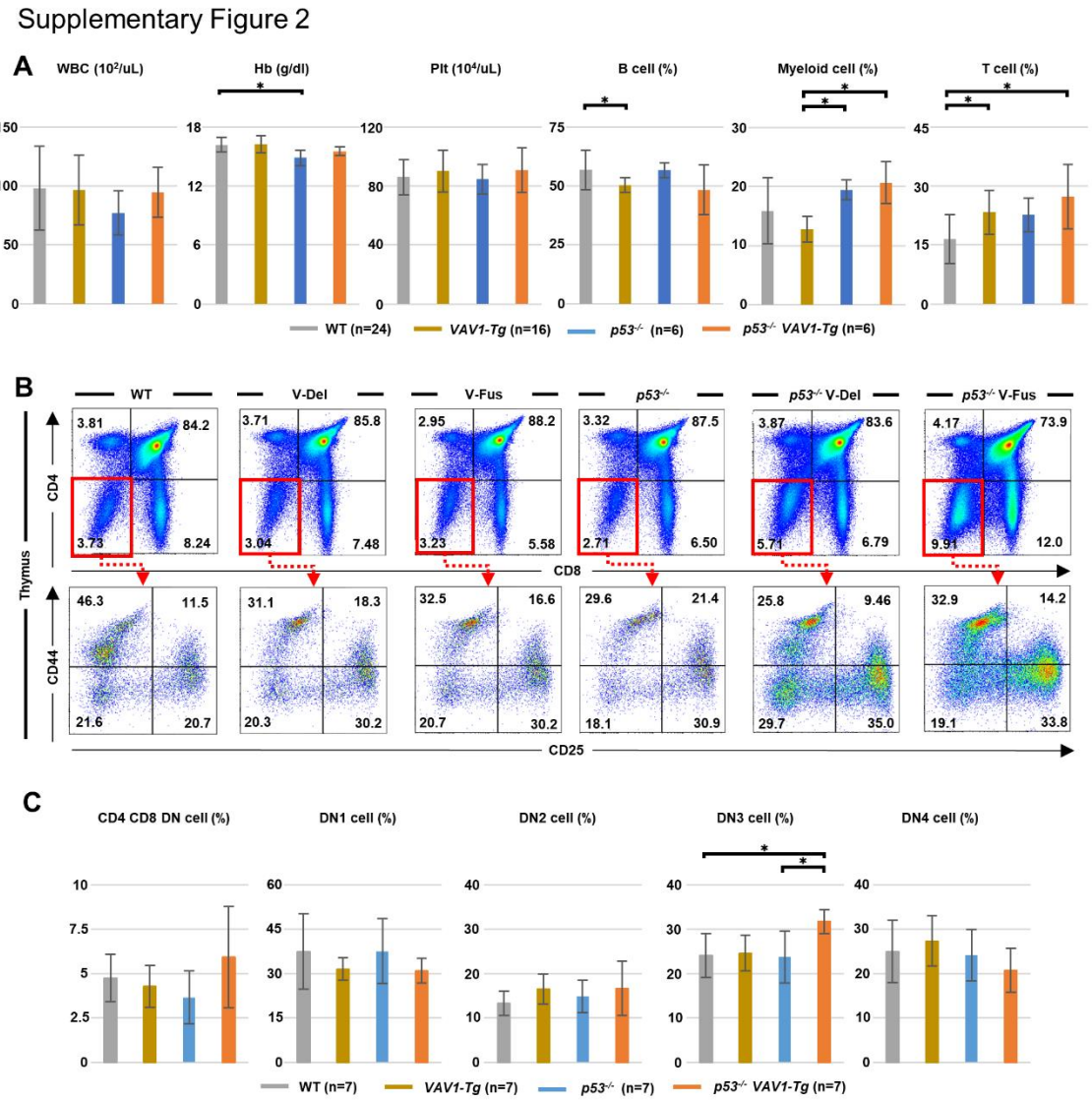

Supplementary Figure 2: Function of VAV1 mutants in physiological T-cell differentiation.

A. White blood cells (WBC), hemoglobin (Hb), and platelet (Plt) counts in peripheral blood (PB), and percentages of B, Myeloid, and T cells based on flow cytometric analysis of mice of indicated genotypes. The number of mice analyzed 24 WT, 16 *VAV1-Tg*, 6 $p53^{-/-}$, and 6 $p53^{-/-}$ *VAV1-Tg* mice. * indicates $p<0.05$.

B. Representative data analyzing CD4- and CD8- double negative (DN) thymocytes from indicated mice at 12 weeks of age. DN1 is characterized by $CD44^{+}CD25^{-}$, DN2 by $CD44^{+}CD25^{+}$, DN3 by $CD44^{-}CD25^{+}$, and DN4 by $CD44^{-}CD25^{-}$.

C. Shown are the percentage of the DN fraction and percentages of DN1, DN2, DN3, and DN4 cells in the DN fraction (right 4 graphs). The number of mice analyzed is as follows: WT, n=7; *VAV1-Tg*, n=7; $p53^{-/-}$, n=7; $p53^{-/-}$ *VAV1-Tg*, n=7. * indicates $p<0.05$.

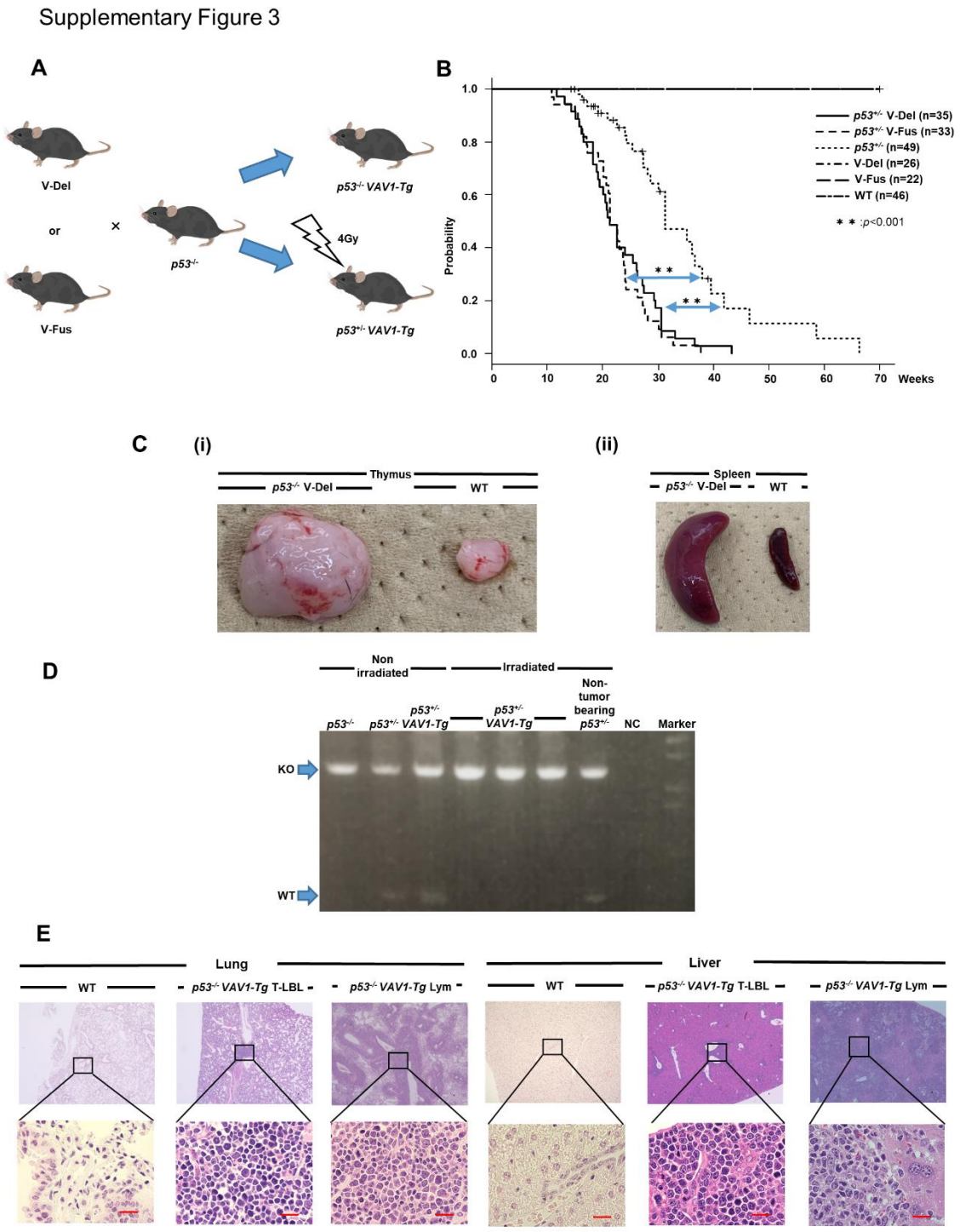

Supplementary Figure 3, related to Figure 3: Function of *VAV1* mutations in tumorigenicity.

A. Schematic showing generation of mouse models. Two *VAV1-Tg* mice lines, V-Del and V-Fus, were crossed with $p53^{-/-}$ or $p53^{+/-}$ mice to generate $p53^{-/-}$ *VAV1-Tg* ($p53^{-/-}$ V-Del or $p53^{-/-}$ V-

Fus mice) and *p53*$^{+/-}$ *VAV1-Tg* mice (*p53*$^{+/-}$ V-Del or *p53*$^{+/-}$ V-Fus mice). We observed the natural course of tumor development in *p53*$^{-/-}$ *VAV1-Tg* mice, and also we irradiated *p53*$^{+/-}$ *VAV1-Tg* mice with 4Gy at 8 weeks of age.

B. Overall survival of mice of indicated genotypes after irradiation. Shown are results derived from *p53*$^{+/-}$ V-Del and *p53*$^{+/-}$ V-Fus mice, as well as *p53*$^{+/-}$ mice, *VAV1-Tg* mice on a WT background (V-Del and V-Fus mice), or WT mice. Both types of *p53*$^{+/-}$ *VAV1-Tg* mice showed significantly shorter survival after 4 Gy irradiation than did *p53*$^{+/-}$ mice, *VAV1-Tg* mice on a WT background, and WT mice.

C. Macroscopic analysis of representative thymuses (i) at 12 weeks of age and spleens (ii) at 24 weeks of age from tumor-bearing *p53*$^{-/-}$ V-Del or WT mice.

D. Genomic PCR analysis of *Trp53* for genomic DNA extracted from T-LBL tumor cells of irradiated *p53*$^{+/-}$ *VAV1-Tg* mice (n=3). PC, positive control; NC, negative control.

E. Hematoxylin eosin (HE)-stained sections of indicated tissues from WT and *p53*$^{-/-}$ *VAV1-Tg* mice. Both T-LBL and Lym tumor cells massively infiltrated lung and liver tissue. Lower magnification is x4 and higher magnification is x100. The length of scale bars is 20 μm.

Supplementary Figure 4

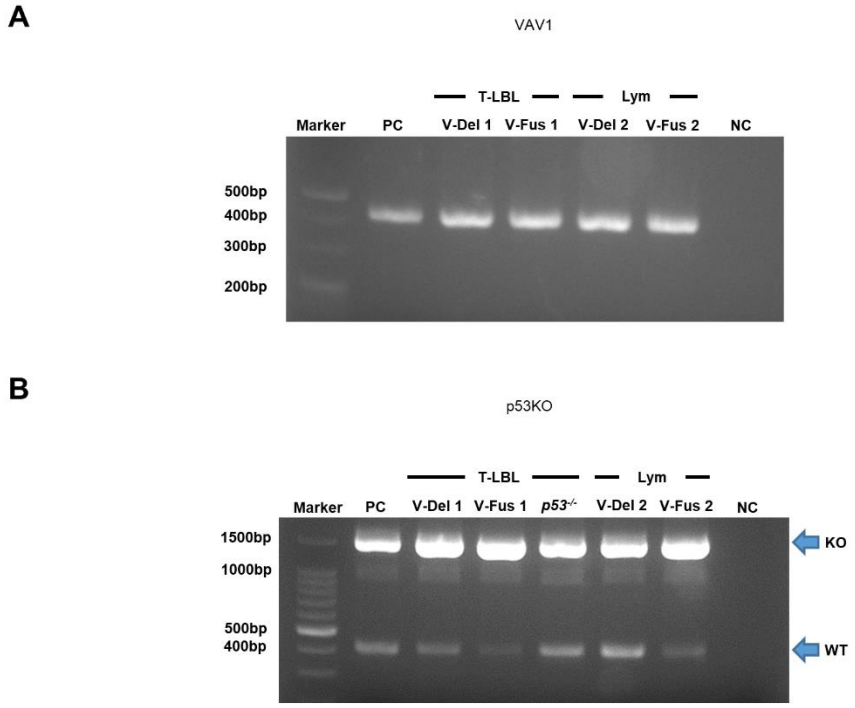

Supplementary Figure 4, related to Figure 4: Characteristics of engrafted nude mice

Genomic PCR analysis of (A) human V-Del and V-Fus transgenes, and (B) bands indicative of *Trp53* deletion in genomic DNA extracted from tumors of nude mice transplanted with donor tumor cells from indicated samples. n=1 each. PC, positive control; NC, negative control.

Supplementary Figure 5

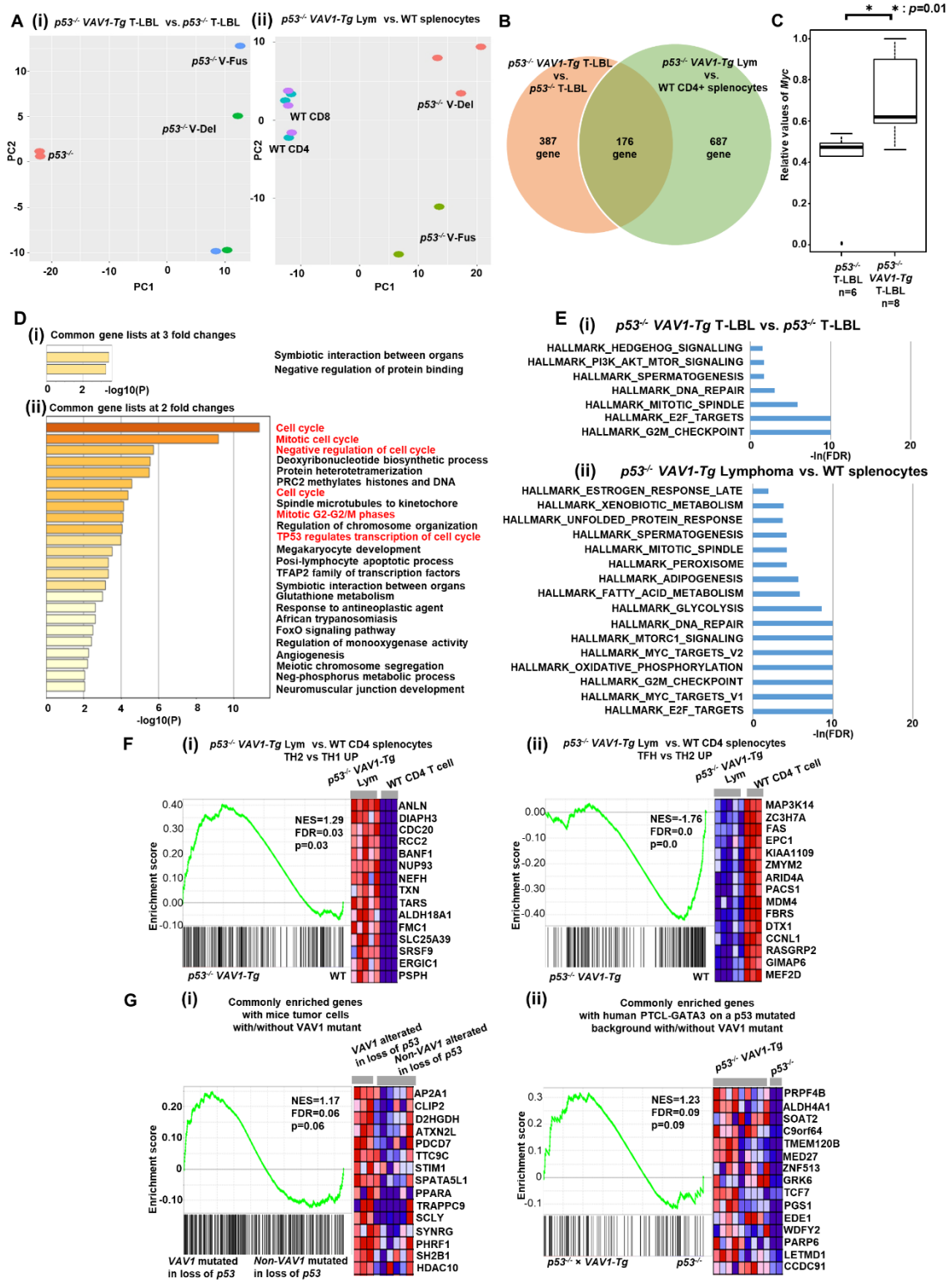

Supplementary Figure 5, related to Figure 5: Details of whole transcriptome analyses

(WTAs) of tumors found in *p53*$^{-/-}$ *VAV1-Tg* and *p53*$^{-/-}$ mice.

A. Principal component analysis (PCA) of T-LBL from *p53*$^{-/-}$ V-Del, *p53*$^{-/-}$ V-Fus and *p53*$^{-/-}$ mice and whole thymocytes from WT mice (i), and tumor cells sorted from Lym from *p53*$^{-/-}$ V-Del and *p53*$^{-/-}$ V-Fus mice and CD4^{+} or CD8^{+} splenocytes from WT mice (ii).

B. Venn diagram showing genes more highly expressed by at least two-fold in T-LBL from *p53*$^{-/-}$ *VAV1-Tg* relative to *p53*$^{-/-}$ mice, or those in Lym from *p53*$^{-/-}$ *VAV1-Tg* mice relative to CD4^{+} splenocytes.

C. Quantitative PCR analysis of *Myc* expression using T-LBL from *p53*$^{-/-}$ mice and *p53*$^{-/-}$ *VAV1-Tg* mice. The number of mice analyzed: *p53*$^{-/-}$ mice, n=6; *p53*$^{-/-}$ *VAV1-Tg* mice, n=8. * indicates p=0.01.

D. Metascape analysis of gene ontology of genes (i) upregulated at least three-fold in T-LBL and Lym tumors from *p53*$^{-/-}$ *VAV1-Tg* mice relative to controls, or (ii) upregulated at least two-fold in T-LBL and Lym tumors from *p53*$^{-/-}$ *VAV1-Tg* relative to control mice.

E. Gene set enrichment analysis (GSEA) of tumor cells of T-LBL from *p53*$^{-/-}$ *VAV1-Tg* mice compared with T-LBL from *p53*$^{-/-}$ mice (i) and sorted from Lym from *p53*$^{-/-}$ *VAV1-Tg* mice compared with CD4 splenocytes from WT mice (ii) performed using gene sets of Hallmark gene sets in the Molecular Signatures Database (MSigDB).

F. GSEA of tumor cells sorted from Lym from *p53*$^{-/-}$ *VAV1-Tg* mice compared with CD4 splenocytes from WT mice performed using gene sets of T-helper 2 (TH2) vs TH1 cells (i), and T follicular helper (TFH) vs TH2 cells (ii) in the MSigDB.

G. Comparison of WTAs from human PTCL-GATA3 with *VAV1* mutation and *Tp53* loss and WTAs from our mouse tumors harboring *VAV1* mutations. GSEA was performed for WTA data from tumors of *p53*$^{-/-}$ *VAV1-Tg* vs. *p53*$^{-/-}$ mice using the gene lists that were significantly enriched in PTCL-GATA3 samples with *VAV1* mutations (i) or from PTCL-GATA3 samples

with *VAV1* and *Tp53* alterations vs loss of *Tp53* without VAV1 mutations using the gene lists that were significantly enriched in tumors from *p53*$^{-/-}$ *VAV1-Tg* relative to *p53*$^{-/-}$ mice (ii).

Supplementary Figure 6

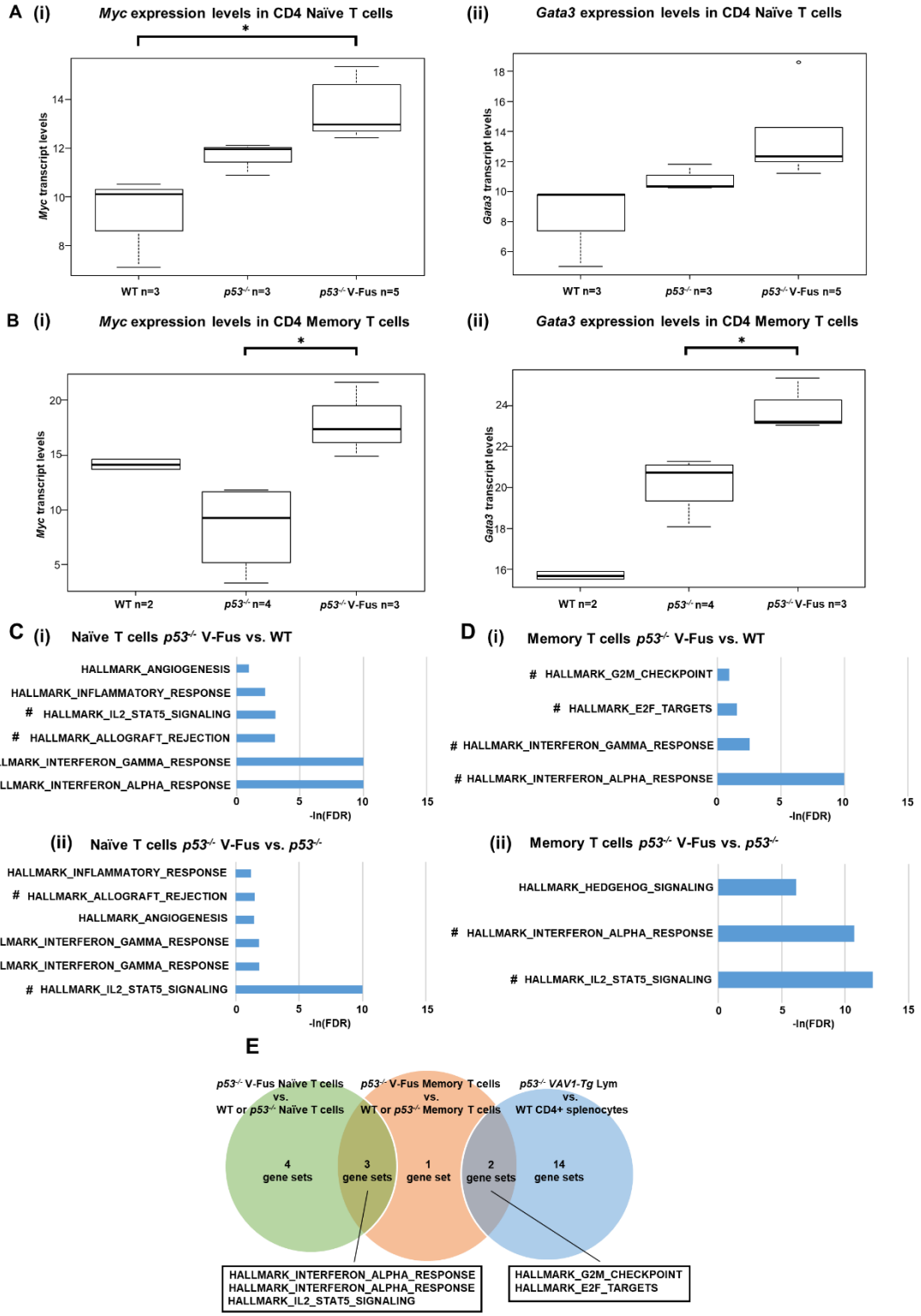

Supplementary Figure 6, related to Figure 5: Details of WTAs CD4 naïve T cells and CD4 memory T cells found in *p53*$^{-/-}$ V-Fus and *p53*$^{-/-}$ mice at 12 weeks of age.

A-B. *Myc* (i) and *Gata3* (ii) expression levels in CD4 naïve T cells from WT mice (n=3), *p53*$^{-/-}$ mice of (n=3), and *p53*$^{-/-}$ V-Fus mice (n=5) (A), and in CD4 memory T cells from WT mice (n=2), *p53*$^{-/-}$ mice of (n=4), and *p53*$^{-/-}$ V-Fus mice (n=3) (B).

C-D. Gene set enrichment analysis (GSEA) of CD4 naïve T cells (C) and CD4 memory T cells (D) from *p53*$^{-/-}$ V-Fus mice compared with those from WT mice (i), and CD4 naïve T cells (C) and CD4 memory T cells (D) from *p53*$^{-/-}$ V-Fus mice compared with those from *p53*$^{-/-}$ mice (ii) performed using gene sets of Hallmark gene sets in MSigDB.

E. Venn diagram showing common gene sets significantly enriched in CD4 naïve T cells from *p53*$^{-/-}$ V-Fus mice (green), CD4 memory T cells from *p53*$^{-/-}$ V-Fus mice (red), and tumor cells sorted from Lym from *p53*$^{-/-}$ *VAV1-Tg* mice (blue).

Supplementary Figure 7

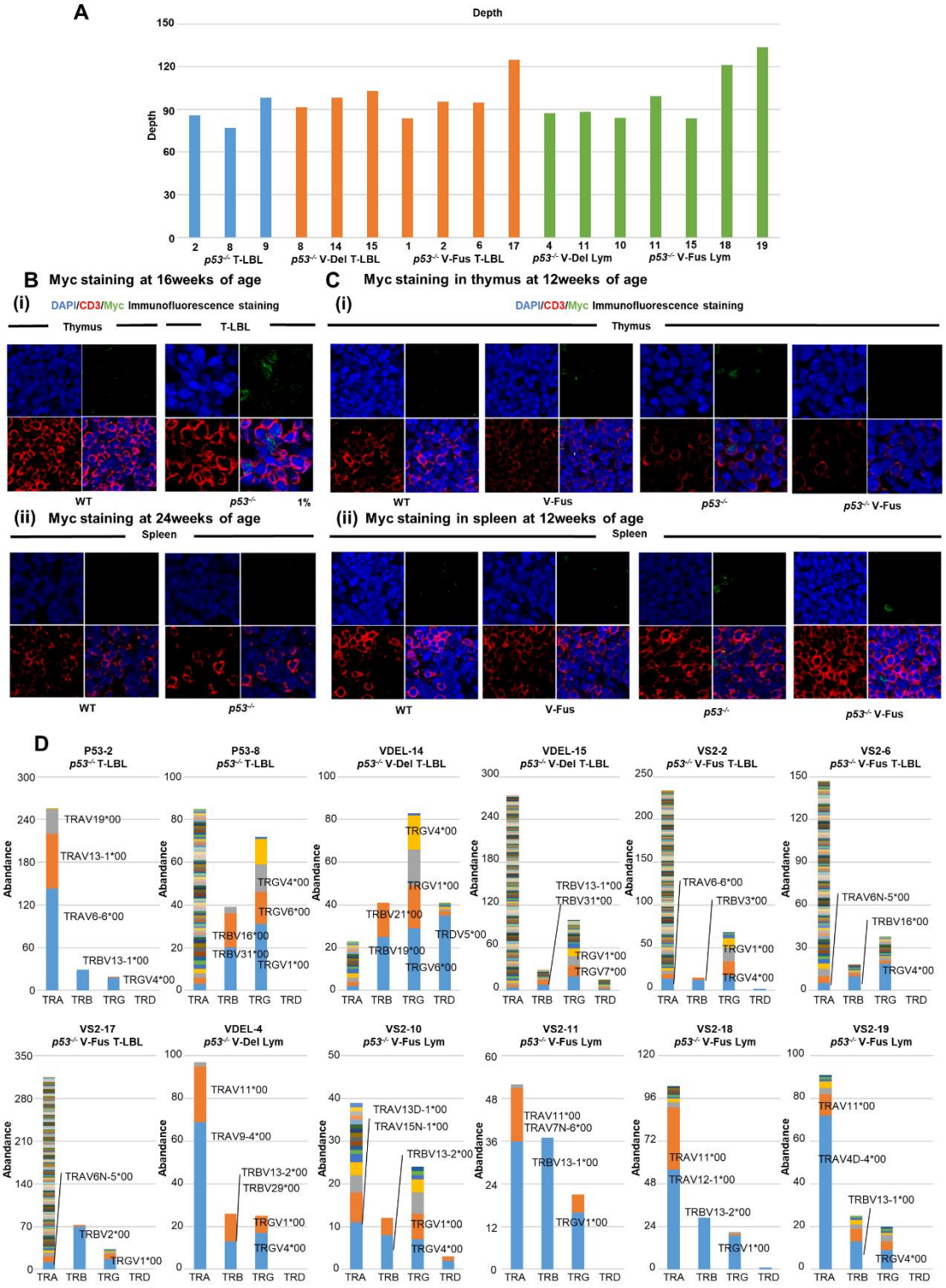

Supplementary Figure 7, related to Figure 6: Details relevant to whole exome sequencing

analyses (WES) of tumors found in *p53*$^{-/-}$ *VAV1-Tg* and *p53*$^{-/-}$ mice.

A. Comparison of average read depth among WES data for tumors from *p53*$^{-/-}$ *VAV1-Tg* and *p53*$^{-/-}$ mice.

B. Immunofluorescent staining for indicated markers in thymus from WT and *p53*$^{-/-}$ mice harboring T-LBL at 16 weeks of age (i), and in spleens from WT and *p53*$^{-/-}$ mice without harboring T-LBL at 24 weeks of age (ii). The percentage at the bottom right corner on T-LBL from *p53*$^{-/-}$ mice is positivity in the tumor cells. CD3, red; Myc, green; DAPI, blue.

C. Immunofluorescent staining for indicated markers in thymus (i) and in spleen (ii) from WT, V-Fus, *p53*$^{-/-}$, and *p53*$^{-/-}$ V-Fus mice at 12 weeks of age. CD3, red; Myc, green; DAPI, blue.

D. Rearrangements of *T-cell receptor (TCR)* genes identified through the MiXCR algorithm using WES data. The y axis indicates each rearranged *TCR* gene with a certain CDR3 sequence. Distinct CDR3 regions are indicated by alternating colors within each sample; colors matched across samples are coincidental and do not indicate sequence identity.

Supplementary Table 1: Distribution and immunophenotype of each tumor found in mice of indicated genotype

ID	Genotype	Onset	Infiltrated organ	Diagnosis
P53-1	*p53*$^{-/-}$	18	Abdominal Tumor	Non-hematological malignancy
P53-2	*p53*$^{-/-}$	23.4	Thymus, Lung	CD8 SP T-LBL
P53-3	*p53*$^{-/-}$	20.1	Thymus	CD4 CD8 DP T-LBL
P53-4	*p53*$^{-/-}$	26.6	Thymus	CD4 CD8 DP T-LBL
P53-5	*p53*$^{-/-}$	33.7	Chest Tumor	Non-hematological malignancy
P53-6	*p53*$^{-/-}$	36	Thymus	CD4 CD8 DP T-LBL
P53-7	*p53*$^{-/-}$	29.1	Thymus	CD4 CD8 DP T-LBL
P53-8	*p53*$^{-/-}$	13.7	Thymus, Lung	CD8 SP T-LBL
P53-9	*p53*$^{-/-}$	15.3	Thymus, Lung	CD4 CD8 DP T-LBL
P53-10	*p53*$^{-/-}$	28.4	Abdominal Tumor	Non-hematological malignancy
P53-11	*p53*$^{-/-}$	20.9	Thymus, Lung	CD8 SP T-LBL
P53-12	*p53*$^{-/-}$	27	Thymus, Lung	CD4 CD8 DP T-LBL
P53-13	*p53*$^{-/-}$	23.3	Thymus, Lung	CD4 CD8 DP T-LBL
P53-14	*p53*$^{-/-}$	35.6	Abdominal Tumor	Non-hematological malignancy
P53-15	*p53*$^{-/-}$	30.9	Thymus, Lung	CD4 CD8 DP T-LBL
P53-16	*p53*$^{-/-}$	20.6	Thymus, Lung	CD4 CD8 DP T-LBL
VDEL-1	*p53*$^{-/-}$ V-Del	28	Chest Tumor	Non-hematological malignancy
VDEL-2	*p53*$^{-/-}$ V-Del	14.4	Thymus, Lung	CD8 SP T-LBL
VDEL-3	*p53*$^{-/-}$ V-Del	13.6	Thymus, Lung	CD8 SP T-LBL
VDEL-4	*p53*$^{-/-}$ V-Del	24.9	Liver, Thymus, Lung, Lymph, BM, Spleen	DN Lym
VDEL-5	*p53*$^{-/-}$ V-Del	20.7	Thymus, Lung	CD4 CD8 DP T-LBL
VDEL-6	*p53*$^{-/-}$ V-Del	18.3	Thymus, Lung, Liver, Spleen	CD8 SP T-LBL

VDEL-7	*p53*$^{-/-}$ V-Del	19.1	Thymus, Lung	CD8 SP T-LBL
VDEL-8	*p53*$^{-/-}$ V-Del	15.4	Thymus, Lung, Liver	CD4 CD8 DP T-LBL
VDEL-9	*p53*$^{-/-}$ V-Del	27	Abdominal Tumor	Non-hematological malignancy
VDEL-10	*p53*$^{-/-}$ V-Del	14.6	Thymus, Lung	CD8 SP T-LBL
VDEL-11	*p53*$^{-/-}$ V-Del	29.3	Spleen, Liver, Lung, BM	DN Lym
VDEL-12	*p53*$^{-/-}$ V-Del	27.1	Spleen, Liver, Lung, BM, Lymph	CD4 SP Lym
VDEL-13	*p53*$^{-/-}$ V-Del	13	Thymus	CD8 SP T-LBL
VDEL-14	*p53*$^{-/-}$ V-Del	16.4	Thymus, Lung	CD4 CD8 DP T-LBL
VDEL-15	*p53*$^{-/-}$ V-Del	16.1	Thymus, Lung, Liver	CD8 SP T-LBL
VDEL-16	*p53*$^{-/-}$ V-Del	19	Thymus	CD8 SP T-LBL
VDEL-17	*p53*$^{-/-}$ V-Del	14.7	Thymus, Lung, Liver	CD8 SP T-LBL
VDEL-18	*p53*$^{-/-}$ V-Del	14.6	Thymus, Lung, Liver	CD8 SP T-LBL
VDEL-19	*p53*$^{-/-}$ V-Del	18.7	Thymus, Lung, Liver	CD8 SP T-LBL
VDEL-20	*p53*$^{-/-}$ V-Del	13.3	Thymus, Lung	CD4 CD8 DP T-LBL
VDEL-21	*p53*$^{-/-}$ V-Del	20.6	Spleen, Liver, Lung, BM, Lymph	CD4 SP Lym
VS2-1	*p53*$^{-/-}$ V-Fus	16.1	Thymus, Lung	CD8 SP T-LBL
VS2-2	*p53*$^{-/-}$ V-Fus	14.7	Thymus, Lung	CD8 SP T-LBL
VS2-3	*p53*$^{-/-}$ V-Fus	18.6	Thymus, Lung, Chest Tumor	CD8 SP T-LBL
VS2-4	*p53*$^{-/-}$ V-Fus	17.6	Chest Tumor	Non-hematological malignancy
VS2-5	*p53*$^{-/-}$ V-Fus	14	Thymus	CD8 SP T-LBL
VS2-6	*p53*$^{-/-}$ V-Fus	16.9	Thymus, Lung, Liver	CD8 SP T-LBL
VS2-7	*p53*$^{-/-}$ V-Fus	21.9	Thymus, Lung	CD8 SP T-LBL
VS2-8	*p53*$^{-/-}$ V-Fus	11.6	Thymus	CD8 SP T-LBL
VS2-9	*p53*$^{-/-}$ V-Fus	22.9	Thymus	CD8 SP T-LBL
VS2-10	*p53*$^{-/-}$ V-Fus	27.6	Spleen, Liver	CD4 SP Lym

VS2-11	*p53*$^{-/-}$ V-Fus	32.6	Spleen, Liver, Lymph	DN Lym
VS2-12	*p53*$^{-/-}$ V-Fus	14.9	Thymus, Lung, Liver	CD8 SP T-LBL
VS2-13	*p53*$^{-/-}$ V-Fus	14.1	Thymus, Lung	CD8 SP T-LBL
VS2-14	*p53*$^{-/-}$ V-Fus	20.1	Thymus	CD8 SP T-LBL
VS2-15	*p53*$^{-/-}$ V-Fus	21.6	Spleen, Lymph	DN Lym
VS2-16	*p53*$^{-/-}$ V-Fus	25.7	Spleen, Lymph, Liver	DN Lym
VS2-17	*p53*$^{-/-}$ V-Fus	17.1	Thymus, Lung, Liver	CD4 CD8 DP T-LBL
VS2-18	*p53*$^{-/-}$ V-Fus	27.6	Spleen, Lymph, Liver	DN Lym
VS2-19	*p53*$^{-/-}$ V-Fus	27.6	Spleen, Lymph, Liver	DN Lym
VS2-20	*p53*$^{-/-}$ V-Fus	21.1	Thymus, Lung	CD8 SP T-LBL
VS2-21	*p53*$^{-/-}$ V-Fus	26	Spleen, Liver, Lung, BM	CD4 SP Lym
VS2-22	*p53*$^{-/-}$ V-Fus	15	Thymus, Lung	CD8 SP T-LBL
VS2-23	*p53*$^{-/-}$ V-Fus	32	Spleen, Liver, Lung, BM, Lymph	DN Lym

Supplementary Table 2: Genes commonly upregulated in T-LBL from *p53*$^{-/-}$ *VAV1-Tg* mice compared with T-LBL from *p53*$^{-/-}$ mice and Lym tumors from *p53*$^{-/-}$ *VAV1-Tg* compared with CD4 splenocytes from WT mice.

Common genes showing at least a 3-fold change						
1700080G11Rik	Cdkn2c	Hemgn	Mapk13	Ngp	Sord	Tcrg-V6
5830411N06Rik	Chdh	Ighg2c	Mt2	Padi3	Spats2	Tedc1
Als2	Cmtm7	Igkv4-61	Mxd3	Ptprf	Stmn1	Trav9d-4
Bex4	Fbln1	Il17rb	Myc	Sh2d1a	Tcrg-C1	Trbv2
Camp	Gm4316	Itm2a	Myl10	Smtn	Tcrg-V4	Tyms
Ccr4						
Common genes showing at least 2-fold change						
0610010F05Rik	Cby1	Depdc1a	Gmnn	Lsr	Prc1	Stom
1700080G11Rik	Ccnb1	Dhfr	Gsta4	Mapk13	Prkar2b	Tbc1d31
1700097N02Rik	Ccne2	Dleu7	Gstm1	Marcksl1	Ptgr1	Tcrg-C1
2010300C02Rik	Ccr4	Drosha	Gtse1	Mki67	Ptov1	Tcrg-V4
4930471C06Rik	Cdk2ap1	Dut	Hba-a1	Mns1	Ptprf	Tcrg-V6
5830411N06Rik	Cdkn2b	E2f3	Hbb-bt	Mt2	Pxmp2	Tedc1
9630013D21Rik	Cdkn2c	E2f8	Hemgn	Mtf2	Rab44	Tfrc
AA467197	Cenpf	Egfl7	Hist1h2ai	Mxd3	Rcbtb2	Tmem59l
Aco2	Cenpk	Egln3	Hist1h2ap	Mybl2	Rrm1	Top2a
Acot7	Cenpm	Eng	Hist1h3h	Myc	Rrm2	Tpx2
Adgrg1	Cenpv	Enkd1	Hist1h3i	Myl10	Rwdd2a	Trav7n-6

Adssl1	Chdh	Etv5	Ighg2c	Myl6b	Sgsm3	Trav9-4
Aif1l	Cited4	Ezh2	Igkv4-61	Nabp1	Sh2d1a	Trav9d-4
Als2	Ckap2l	Fads2	Igsf23	Ngp	Ska1	Trbv12-2
Anxa2	Clspn	Fam216a	Il10	Nsd2	Ska2	Trbv2
Apol10b	Cmc2	Fam69b	Il17rb	Nsl1	Slc43a3	Troap
Arhgef39	Cmtm7	Fbln1	Il9r	Nuf2	Slc9a9	Tuba1b
Atad2	Colq	Fkbp5	Islr	Padi3	Slfn4	Tyms
Atp1b2	Coro2a	Foxm1	Itm2a	Padi4	Slfn9	Xrcc6
Aurka	Cox6b2	Gfi1	Jdp2	Parm1	Smtn	Zfp428
Bex4	Cpa3	Gm10451	Jup	Parvg	Soat2	
Bub1b	Crip2	Gm15915	Kif20a	Pdcd1	Sord	
C1qtnf12	Crip2	Gm28942	Knl1	Phf5a	Spats2	
Camp	Cym	Gm34093	Knstrn	Pik3r3	Spc25	
Cbx5	Ddah2	Gm4316	Lockd	Pimreg	Stil	
Cbx6	Ddit4	Gm47459	Lrr1	Ppp1r1b	Stmn1	

Supplementary Table 3: Metascape analysis based on list of commonly upregulated genes.

Common gene list at 3 fold changes						
Terms	**Category**	**Description**	**LogP**	**Enrichment**	**Z-score**	**Log(q-value)**
GO:0051817	GO Biological Processes	modification of morphology or physiology of other organism involved in symbiotic interaction	-3.420156077	21.14672216	7.611326004	0
GO:0032091	GO Biological Processes	negative regulation of protein binding	-3.2537605	18.55325624	7.082142651	0
Common gene list at 2 fold changes						
Terms	**Category**	**Description**	**LogP**	**Enrichment**	**Z-score**	**Log(q-value)**
R-MMU-1640170	Reactome Gene Sets	Cell Cycle	-11.35710387	5.747849247	9.873244324	-7.095365318
GO:1903047	GO Biological Processes	mitotic cell cycle process	-9.175240508	4.705587436	8.35716471	-5.515561952
GO:0045786	GO Biological Processes	negative regulation of cell cycle	-5.716463305	4.369570827	6.337780115	-2.727255839
GO:0009263	GO Biological Processes	deoxyribonucleotide biosynthetic process	-5.523972573	37.70315399	12.00425765	-2.584453321
GO:0051290	GO Biological Processes	protein heterotetramerization	-5.483387593	14.66233766	8.784517832	-2.564071727
R-MMU-212300	Reactome Gene Sets	PRC2 methylates histones and DNA	-4.550706193	10.15084915	7.075579504	-1.751365644
mmu04110	KEGG Pathway	Cell cycle	-4.347659986	7.44941349	6.2947482	-1.563042693

GO:0008608	GO Biological Processes	attachment of spindle microtubules to kinetochore	-4.127586661	17.59480519	7.948255901	-1.44563171
R-MMU-453274	Reactome Gene Sets	Mitotic G2-G2/M phases	-4.092958681	6.792112299	5.922195981	-1.422284741
GO:0033044	GO Biological Processes	regulation of chromosome organization	-4.054589859	4.077447833	5.118841089	-1.394911303
R-MMU-6791312	Reactome Gene Sets	TP53 Regulates Transcription of Cell Cycle Genes	-3.961154433	15.99527745	7.533254446	-1.332884342
R-MMU-983231	Reactome Gene Sets	Factors involved in megakaryocyte development and platelet production	-3.49160128	6.543522593	5.344333541	-0.970225422
GO:0070230	GO Biological Processes	positive regulation of lymphocyte apoptotic process	-3.289494653	18.85157699	7.152024626	-0.833936079
R-MMU-8864260	Reactome Gene Sets	Transcriptional regulation by the AP-2 (TFAP2) family of transcription factors	-3.289494653	18.85157699	7.152024626	-0.833936079
GO:0051817	GO Biological Processes	modification of morphology or physiology of other organism involved in symbiotic interaction	-3.14757454	7.094679514	5.147621694	-0.718344905
mmu00480	KEGG Pathway	Glutathione metabolism	-2.981249083	8.946511116	5.341363211	-0.594571799
GO:0097327	GO Biological Processes	response to antineoplastic agent	-2.616512386	7.133029133	4.618503781	-0.407852282
mmu05143	KEGG Pathway	African trypanosomiasis	-2.595747159	10.99675325	5.245821325	-0.390913463
mmu04068	KEGG Pathway	FoxO signaling pathway	-2.475116557	4.998524203	4.027355966	-0.30224575
GO:0032768	GO Biological Processes	regulation of monooxygenase activity	-2.403889454	9.425788497	4.776422167	-0.255925474

GO:0001525	GO Biological Processes	angiogenesis	-2.235179278	2.572339941	3.151921082	-0.152417678
GO:0045132	GO Biological Processes	meiotic chromosome segregation	-2.195867705	5.441692328	3.831700504	-0.127253756
GO:0010563	GO Biological Processes	negative regulation of phosphorus metabolic process	-2.053407337	2.416868845	2.932636447	-0.037181457
GO:0007528	GO Biological Processes	neuromuscular junction development	-2.033385317	6.94531784	3.927721473	-0.029325345

Supplementary Table 4: Pathways enriched in *p53*$^{-/-}$ *VAV1-Tg* T-LBL relative to *p53*$^{-/-}$ T-LBL or Lym relative to WT mice, as analyzed by GSEA with the Hallmark matrix.

***p53*$^{-/-}$ *VAV1-Tg* T-LBL vs *p53*$^{-/-}$ T-LBL**	**NES**	**NOM p-val**	**FDR q-val**	**FWER p-val**
HALLMARK_G2M_CHECKPOINT	2.3501885	0	0	0
HALLMARK_E2F_TARGETS	1.9904214	0	0	0
HALLMARK_MITOTIC_SPINDLE	1.7532481	0	0.00276138	0.008
HALLMARK_DNA_REPAIR	1.4463986	0.00990099	0.047589343	0.176
HALLMARK_SPERMATOGENESIS	1.2666688	0.053892214	0.18260913	0.591
HALLMARK_PI3K_AKT_MTOR_SIGNALING	1.2462898	0.063400574	0.1768789	0.643
HALLMARK_HEDGEHOG_SIGNALING	1.1981287	0.1883289	0.22175923	0.781
***p53*$^{-/-}$ *VAV1-Tg* Lym vs WT T splenocytes**	**NES**	**NOM p-val**	**FDR q-val**	**FWER p-val**
HALLMARK_E2F_TARGETS	2.558755	0	0	0
HALLMARK_MYC_TARGETS_V1	2.3682046	0	0	0
HALLMARK_G2M_CHECKPOINT	2.3399968	0	0	0
HALLMARK_OXIDATIVE_PHOSPHORYLATION	2.211721	0	0	0
HALLMARK_MYC_TARGETS_V2	2.132254	0	0	0
HALLMARK_MTORC1_SIGNALING	1.998908	0	0	0
HALLMARK_DNA_REPAIR	1.804022	0	8.93E-05	0.001
HALLMARK_GLYCOLYSIS	1.7896651	0	7.81E-05	0.001
HALLMARK_FATTY_ACID_METABOLISM	1.6952677	0	5.76E-04	0.008
HALLMARK_ADIPOGENESIS	1.6419766	0	0.001280819	0.02
HALLMARK_UNFOLDED_PROTEIN_RESPONSE	1.512732	0.003218884	0.007342448	0.118

HALLMARK_MITOTIC_SPINDLE	1.5051714	0.001021451	0.007314903	0.129
HALLMARK_SPERMATOGENESIS	1.4469849	0.010660981	0.014756831	0.262
HALLMARK_PEROXISOME	1.4406089	0.006465518	0.015148852	0.286
HALLMARK_XENOBIOTIC_METABOLISM	1.3807272	0.003064351	0.032415345	0.533
HALLMARK_REACTIVE_OXYGEN_SPECIES_PATHWAY	1.322251	0.06317044	0.06153159	0.795
HALLMARK_ESTROGEN_RESPONSE_LATE	1.2429414	0.055158325	0.13925622	0.986
***p53*$^{-/-}$ V-Fus CD4 naïve T cells vs WT CD4 naïve T cells at non-tumor bearing status**	**NES**	**NOM p-val**	**FDR q-val**	**FWER p-val**
HALLMARK_INTERFERON_ALPHA_RESPONSE	2.7964284	0	0	0
HALLMARK_INTERFERON_GAMMA_RESPONSE	2.6829524	0	0	0
HALLMARK_ALLOGRAFT_REJECTION	1.9574037	0	2.44E-04	0.001
HALLMARK_IL2_STAT5_SIGNALING	1.8979421	0	0.00118635	0.006
HALLMARK_INFLAMMATORY_RESPONSE	1.677466	0	0.006421625	0.042
HALLMARK_ANGIOGENESIS	1.3543328	0.08969466	0.11393599	0.607
***p53*$^{-/-}$ V-Fus CD4 naïve T cells vs *p53*$^{-/-}$ CD4 naïve T cells at non-tumor bearing status**	**NES**	**NOM p-val**	**FDR q-val**	**FWER p-val**
HALLMARK_IL2_STAT5_SIGNALING	1.9698863	0	0	0
HALLMARK_INTERFERON_ALPHA_RESPONSE	1.6037624	0	0.013664926	0.042
HALLMARK_INTERFERON_GAMMA_RESPONSE	1.5591754	0	0.014285092	0.065
HALLMARK_ANGIOGENESIS	1.4229727	0.042857144	0.03809379	0.218
HALLMARK_ALLOGRAFT_REJECTION	1.4157016	0.002923977	0.03276637	0.236
HALLMARK_INFLAMMATORY_RESPONSE	1.3260729	0.029315962	0.062172648	0.467
***p53*$^{-/-}$ V-Fus CD4 memory T cells vs WT CD4 memory T cells at non-tumor bearing status**	**NES**	**NOM p-val**	**FDR q-val**	**FWER p-val**

HALLMARK_INTERFERON_ALPHA_RESPONSE	2.2760396	0	0	0
HALLMARK_INTERFERON_GAMMA_RESPONSE	1.7543682	0	0.004138116	0.013
HALLMARK_E2F_TARGETS	1.513492	0.005249344	0.035874285	0.161
HALLMARK_G2M_CHECKPOINT	1.3215445	0.015625	0.12918386	0.582
***p53*$^{-/-}$ V-Fus CD4 memory T cells vs *p53*$^{-/-}$ CD4 memory T cells at non-tumor bearing status**	**NES**	**NOM p-val**	**FDR q-val**	**FWER p-val**
HALLMARK_IL2_STAT5_SIGNALING	1.623906	0	0.06021363	0.066
HALLMARK_INTERFERON_ALPHA_RESPONSE	1.5426632	0	0.08491196	0.177
HALLMARK_HEDGEHOG_SIGNALING	1.4112917	0.05970149	0.24272242	0.566

Supplementary Table 5: Pathways enriched in *p53*$^{-/-}$ *VAV1-Tg* T-LBL relative to *p53*$^{-/-}$ T-LBL or Lym relative to WT mice, as analyzed by GSEA with curated gene sets.

***p53*$^{-/-}$ *VAV1-Tg* T-LBL vs *p53*$^{-/-}$ T-LBL**	**NES**	**NOM p-val**	**FDR q-val**	**FWER p-val**
MORI_IMMATURE_B_LYMPHOCYTE_DN	2.4418066	0	0	0
MORI_LARGE_PRE_BII_LYMPHOCYTE_UP	2.4258852	0	0	0
CROONQUIST_IL6_DEPRIVATION_DN	2.3914618	0	0	0
ZHOU_CELL_CYCLE_GENES_IN_IR_RESPONSE_24HR	2.3874774	0	0	0
ISHIDA_E2F_TARGETS	2.337184	0	0	0
BURTON_ADIPOGENESIS_3	2.3053317	0	0	0
ROSTY_CERVICAL_CANCER_PROLIFERATION_CLUSTER	2.2952988	0	0	0
KONG_E2F3_TARGETS	2.29428	0	0	0
CROONQUIST_NRAS_SIGNALING_DN	2.2648106	0	0	0
ODONNELL_TFRC_TARGETS_DN	2.25795	0	0	0
LI_INDUCED_T_TO_NATURAL_KILLER_DN	2.252859	0	0	0
HOFFMANN_LARGE_TO_SMALL_PRE_BII_LYMPHOCYTE_UP	2.2306979	0	0	0
ZHOU_CELL_CYCLE_GENES_IN_IR_RESPONSE_6HR	2.222351	0	0	0
FISCHER_G2_M_CELL_CYCLE	2.2221959	0	0	0
ZHAN_MULTIPLE_MYELOMA_PR_UP	2.2020533	0	0	0
WHITFIELD_CELL_CYCLE_G2	2.2007034	0	0	0
REACTOME_MITOTIC_PROMETAPHASE	2.1997523	0	0	0

PUJANA_BRCA2_PCC_NETWORK	2.1975908	0	0	0
MORI_MATURE_B_LYMPHOCYTE_DN	2.1769059	0	1.18E-04	0.002
KOBAYASHI_EGFR_SIGNALING_24HR_DN	2.1751773	0	1.12E-04	0.002
FLORIO_NEOCORTEX_BASAL_RADIAL_GLIA_DN	2.1657133	0	1.06E-04	0.002
ODONNELL_TARGETS_OF_MYC_AND_TFRC_DN	2.1607919	0	1.53E-04	0.003
KANG_DOXORUBICIN_RESISTANCE_UP	2.141991	0	1.46E-04	0.003
SOTIRIOU_BREAST_CANCER_GRADE_1_VS_3_UP	2.1369905	0	1.87E-04	0.004
PYEON_HPV_POSITIVE_TUMORS_UP	2.128333	0	1.80E-04	0.004
WHITEFORD_PEDIATRIC_CANCER_MARKERS	2.1164424	0	1.73E-04	0.004
WHITFIELD_CELL_CYCLE_LITERATURE	2.110056	0	2.09E-04	0.005
REACTOME_CELL_CYCLE_MITOTIC	2.094323	0	2.82E-04	0.007
PUJANA_XPRSS_INT_NETWORK	2.0942852	0	2.72E-04	0.007
FURUKAWA_DUSP6_TARGETS_PCI35_DN	2.0842986	0	3.37E-04	0.009
LEE_EARLY_T_LYMPHOCYTE_UP	2.0842857	0	3.26E-04	0.009
DUTERTRE_ESTRADIOL_RESPONSE_24HR_UP	2.0839722	0	3.16E-04	0.009
WINNEPENNINCKX_MELANOMA_METASTASIS_UP	2.0779808	0	3.76E-04	0.011
REACTOME_ESTROGEN_DEPENDENT_GENE_EXPRESSION	2.0615895	0	5.98E-04	0.018
REACTOME_RESOLUTION_OF_SISTER_CHROMATID_COHESION	2.0573964	0	6.13E-04	0.019
REACTOME_MITOTIC_SPINDLE_CHECKPOINT	2.0537755	0	6.27E-04	0.02
REACTOME_CONDENSATION_OF_PROPHASE_CHROMOSOMES	2.0329497	0.002493766	8.25E-04	0.026
LE_EGR2_TARGETS_UP	2.0322502	0	8.03E-04	0.026

REACTOME_ANCHORING_OF_THE_BASAL_BODY_TO_THE_PLASMA_MEMBRANE	2.0306015	0	7.83E-04	0.026
EGUCHI_CELL_CYCLE_RB1_TARGETS	2.0282447	0	8.20E-04	0.028
SCIAN_CELL_CYCLE_TARGETS_OF_TP53_AND_TP73_DN	1.9873399	0	0.001951208	0.068
PID_PLK1_PATHWAY	1.9849504	0	0.001958002	0.07
FRASOR_RESPONSE_TO_SERM_OR_FULVESTRANT_DN	1.9819345	0	0.00193893	0.071
MARKEY_RB1_ACUTE_LOF_UP	1.9786162	0	0.002127043	0.08
VILLANUEVA_LIVER_CANCER_KRT19_UP	1.9650404	0	0.002630246	0.101
BOYLAN_MULTIPLE_MYELOMA_C_CLUSTER_UP	1.9550147	0	0.003185076	0.123
REACTOME_CILIUM_ASSEMBLY	1.9529334	0	0.003307866	0.131
REACTOME_RECRUITMENT_OF_NUMA_TO_MITOTIC_CENTROSOMES	1.9505787	0	0.003333106	0.135
MISSIAGLIA_REGULATED_BY_METHYLATION_DN	1.9478755	0	0.003494632	0.144
BIDUS_METASTASIS_UP	1.9473819	0	0.00344734	0.145
MORI_PRE_BI_LYMPHOCYTE_UP	1.9455134	0	0.003512422	0.149
KAMMINGA_EZH2_TARGETS	1.9434797	0	0.003598506	0.155
REACTOME_AURKA_ACTIVATION_BY_TPX2	1.940215	0	0.003806792	0.165
REACTOME_CENTROSOME_MATURATION	1.9398818	0	0.003756979	0.166
KEGG_CELL_CYCLE	1.9375675	0	0.003810356	0.169
SARRIO_EPITHELIAL_MESENCHYMAL_TRANSITION_UP	1.9238694	0	0.004790256	0.21
REICHERT_MITOSIS_LIN9_TARGETS	1.921107	0	0.004803975	0.215

LEE_INTRATHYMIC_T_PROGENITOR	1.8992349	0	0.006741544	0.284
PUJANA_BREAST_CANCER_WITH_BRCA1_MUTATED_UP	1.8976082	0	0.006740341	0.29
REACTOME_M_PHASE	1.8946149	0	0.00677858	0.294
REACTOME_G0_AND_EARLY_G1	1.8726703	0	0.009422476	0.385
NIKOLSKY_BREAST_CANCER_11Q12_Q14_AMPLICON	1.8725457	0	0.009307027	0.386
REACTOME_REGULATION_OF_PLK1_ACTIVITY_AT_G2_M_TRANSITION	1.870187	0	0.009624373	0.404
REN_BOUND_BY_E2F	1.858378	0	0.011130267	0.458
LI_WILMS_TUMOR_ANAPLASTIC_UP	1.8537245	0	0.011687769	0.483
PUJANA_BRCA_CENTERED_NETWORK	1.8514025	0	0.012107926	0.502
NIKOLSKY_BREAST_CANCER_5P15_AMPLICON	1.8511715	0	0.011944018	0.502
PID_FOXM1_PATHWAY	1.8493605	0	0.012051641	0.509
YU_MYC_TARGETS_UP	1.8487412	0	0.011942365	0.511
BIOCARTA_CELLCYCLE_PATHWAY	1.8475375	0.002136752	0.012029561	0.519
REACTOME_RHO_GTPASES_ACTIVATE_FORMINS	1.8474107	0	0.011860131	0.519
GRAHAM_CML_DIVIDING_VS_NORMAL_QUIESCENT_UP	1.8428758	0	0.012288833	0.532
PID_E2F_PATHWAY	1.8269681	0	0.01509128	0.611
VANTVEER_BREAST_CANCER_METASTASIS_DN	1.8199339	0.002985075	0.016383277	0.655
REACTOME_POLO_LIKE_KINASE_MEDIATED_EVENTS	1.8165848	0.002386635	0.017061645	0.673
GREENBAUM_E2A_TARGETS_UP	1.8112606	0	0.017858397	0.697
WHITFIELD_CELL_CYCLE_S	1.8105603	0	0.017846128	0.701

MITSIADES_RESPONSE_TO_APLIDIN_DN	1.808101	0	0.018284362	0.711
LI_WILMS_TUMOR_VS_FETAL_KIDNEY_1_DN	1.8059185	0	0.018564407	0.718
FERRANDO_HOX11_NEIGHBORS	1.7990166	0	0.020123536	0.754
XU_HGF_TARGETS_INDUCED_BY_AKT1_48HR_DN	1.7990162	0.002267574	0.019875098	0.754
REACTOME_MEIOTIC_RECOMBINATION	1.7980156	0	0.01999018	0.76
MOLENAAR_TARGETS_OF_CCND1_AND_CDK4_DN	1.796716	0	0.02010384	0.764
REACTOME_PHASE_2_PLATEAU_PHASE	1.7954106	0.006864989	0.020266967	0.77
REACTOME_CELL_CYCLE_CHECKPOINTS	1.7784805	0	0.024970304	0.837
WU_APOPTOSIS_BY_CDKN1A_VIA_TP53	1.7737756	0	0.026327986	0.853
REACTOME_RUNX1_REGULATES_GENES_INVOLVED_IN_MEGAKARYOCYTE_DIFFERENTIATION_AND_PLATELET_FUNCTION	1.7736678	0	0.026089817	0.855
BLUM_RESPONSE_TO_SALIRASIB_DN	1.7711926	0	0.026590629	0.866
SHEDDEN_LUNG_CANCER_POOR_SURVIVAL_A6	1.7616456	0	0.029729892	0.896
DAZARD_RESPONSE_TO_UV_SCC_DN	1.7609289	0	0.02973926	0.897
CHEN_ETV5_TARGETS_TESTIS	1.754247	0	0.03230947	0.919
STEIN_ESRRA_TARGETS_RESPONSIVE_TO_ESTROGEN_DN	1.7515812	0.002463054	0.032910872	0.927
FUJII_YBX1_TARGETS_DN	1.7509458	0	0.032835007	0.928
NIKOLSKY_BREAST_CANCER_6P24_P22_AMPLICON	1.748601	0.009090909	0.033489812	0.934
SMID_BREAST_CANCER_RELAPSE_IN_BRAIN_UP	1.7485241	0	0.03318446	0.936
BIOCARTA_NKCELLS_PATHWAY	1.739608	0	0.036701787	0.951
BIOCARTA_CARDIACEGF_PATHWAY	1.7379438	0.004535148	0.036893185	0.951

REACTOME_SUMOYLATION_OF_TRANSCRIPTION_COFACTORS	1.7321919	0	0.03914541	0.957
FERREIRA_EWINGS_SARCOMA_UNSTABLE_VS_STABLE_UP	1.7315838	0	0.0390006	0.958
CHIARETTI_T_ALL_REFRACTORY_TO_THERAPY	1.7312571	0	0.038733505	0.961
SHEPARD_CRUSH_AND_BURN_MUTANT_DN	1.722888	0	0.042453364	0.97
REACTOME_MICRORNA_MIRNA_BIOGENESIS	1.7225937	0.00248139	0.042181052	0.971
REACTOME_CHROMOSOME_MAINTENANCE	1.7223829	0.002915452	0.04190224	0.972
REACTOME_TRANSCRIPTIONAL_REGULATION_OF_GRANULOPOIESIS	1.715618	0.0025	0.044637498	0.983
BENPORATH_PROLIFERATION	1.7127804	0	0.046000637	0.985
CHICAS_RB1_TARGETS_GROWING	1.7126993	0	0.045619912	0.985
HOEGERKORP_CD44_TARGETS_TEMPORAL_DN	1.7074517	0.006993007	0.048055124	0.988
REACTOME_RUNX1_INTERACTS_WITH_CO_FACTORS_WHOSE_PRECISE_EFFECT_ON_RUNX1_TARGETS_IS_NOT_KNOWN	1.7073276	0.004914005	0.047703367	0.988
GRAHAM_NORMAL_QUIESCENT_VS_NORMAL_DIVIDING_DN	1.7072449	0	0.04728654	0.988
BIOCARTA_LIS1_PATHWAY	1.7056676	0.002336449	0.047585946	0.988
FISCHER_G1_S_CELL_CYCLE	1.7047962	0	0.047531232	0.988
REACTOME_DNA_METHYLATION	1.7047569	0.007125891	0.04711706	0.988
WNT_SIGNALING	1.7043931	0	0.046819713	0.988
WANG_METASTASIS_OF_BREAST_CANCER_ESR1_UP	1.6963913	0.004926108	0.050687183	0.992
CAFFAREL_RESPONSE_TO_THC_24HR_5_DN	1.692208	0	0.052713137	0.995
BIOCARTA_CXCR4_PATHWAY	1.6916965	0	0.052560955	0.995

ZHAN_MULTIPLE_MYELOMA_MF_DN	1.6913755	0.010362694	0.05219893	0.995
REACTOME_ORGANELLE_BIOGENESIS_AND_MAINTENANCE	1.6909205	0	0.05204177	0.995
REACTOME_ACTIVATION_OF_HOX_GENES_DURING_DIFFERENTIATION	1.6895152	0.002793296	0.052467946	0.995
PID_ATR_PATHWAY	1.6883637	0	0.052640475	0.996
NIKOLSKY_BREAST_CANCER_8Q23_Q24_AMPLICON	1.6838452	0	0.054611012	0.997
REACTOME_RHO_GTPASE_EFFECTORS	1.6827174	0	0.054791074	0.997
REACTOME_G1_S_SPECIFIC_TRANSCRIPTION	1.6811156	0.007462686	0.055318553	0.997
REACTOME_ACTIVATED_PKN1_STIMULATES_TRANSCRIPTION_OF_AR_ANDROGEN_RECEPTOR_REGULATED_GENES_KLK2_AND_KLK3	1.6802119	0.004415011	0.05538973	0.997
BURTON_ADIPOGENESIS_PEAK_AT_24HR	1.6788143	0	0.055775832	0.997
PID_MYC_REPRESS_PATHWAY	1.6785774	0	0.055449203	0.997
WHITFIELD_CELL_CYCLE_G2_M	1.676484	0	0.05639429	0.997
REACTOME_KINESINS	1.6761293	0.005347594	0.056181654	0.997
GEORGES_CELL_CYCLE_MIR192_TARGETS	1.6724656	0	0.057818405	0.998
PID_ATM_PATHWAY	1.6714168	0.00511509	0.057935867	0.999
REACTOME_MITOTIC_G2_G2_M_PHASES	1.6704264	0	0.058111954	0.999
SIMBULAN_PARP1_TARGETS_DN	1.6699834	0.015384615	0.057909016	0.999
BURTON_ADIPOGENESIS_12	1.6697768	0.007633588	0.057625193	0.999
REACTOME_SUMOYLATION	1.6678945	0	0.058314055	0.999

SHEPARD_BMYB_TARGETS	1.6676042	0	0.058073737	0.999
REACTOME_NUCLEOSOME_ASSEMBLY	1.6660588	0.002604167	0.058556043	0.999
BIOCARTA_SHH_PATHWAY	1.6604596	0.008714597	0.061482407	0.999
LY_AGING_MIDDLE_DN	1.660082	0.015765766	0.061240334	0.999
PID_ILK_PATHWAY	1.6566696	0.005347594	0.06287279	1
KAUFFMANN_DNA_REPAIR_GENES	1.6562961	0	0.062689595	1
BENPORATH_ES_CORE_NINE_CORRELATED	1.6551712	0	0.062923044	1
FARMER_BREAST_CANCER_CLUSTER_2	1.655091	0.004683841	0.06251131	1
REACTOME_ACTIVATION_OF_THE_PRE_REPLICATIVE_COMPLEX	1.6548798	0.007594937	0.062215112	1
PETROVA_PROX1_TARGETS_UP	1.6544493	0.011655011	0.062149927	1
REACTOME_PRC2_METHYLATES_HISTONES_AND_DNA	1.6540163	0.007894737	0.061977513	1
REACTOME_ACTIVATION_OF_ATR_IN_RESPONSE_TO_REPLICATION_STRESS	1.6532259	0.002512563	0.062039282	1
RHODES_UNDIFFERENTIATED_CANCER	1.6511396	0.005263158	0.063217536	1
LINDGREN_BLADDER_CANCER_CLUSTER_3_UP	1.6496192	0	0.06366764	1
WEST_ADRENOCORTICAL_TUMOR_MARKERS_DN	1.6472436	0.006564552	0.064753406	1
REACTOME_GENE_SILENCING_BY_RNA	1.64006	0.006514658	0.06893448	1
REACTOME_ESR_MEDIATED_SIGNALING	1.6396973	0	0.06875286	1
KORKOLA_EMBRYONIC_CARCINOMA_VS_SEMINOMA_DN	1.634234	0.013605442	0.07187294	1
REACTOME_SIRT1_NEGATIVELY_REGULATES_RRNA_EXPRESSION	1.6316618	0.007712083	0.07315243	1

SAGIV_CD24_TARGETS_UP	1.6301597	0.011337869	0.0738318	1
CHANDRAN_METASTASIS_UP	1.6294489	0	0.07380701	1
REACTOME_HSP90_CHAPERONE_CYCLE_FOR_STEROID_HORMONE_RECEPTORS_SHR	1.6257005	0.010610079	0.07584289	1
HU_GENOTOXIN_ACTION_DIRECT_VS_INDIRECT_4HR	1.6213319	0.010282776	0.0785933	1
RIZ_ERYTHROID_DIFFERENTIATION_CCNE1	1.6201108	0.010075566	0.079067774	1
FINETTI_BREAST_CANCER_KINOME_RED	1.619923	0.033333335	0.0787259	1
CROONQUIST_NRAS_VS_STROMAL_STIMULATION_DN	1.6176969	0	0.07995545	1
SONG_TARGETS_OF_IE86_CMV_PROTEIN	1.6154827	0.00511509	0.081220165	1
REACTOME_TRANSCRIPTIONAL_REGULATION_BY_E2F6	1.6137792	0.002444988	0.08219328	1
BOYAULT_LIVER_CANCER_SUBCLASS_G23_UP	1.6132226	0.002717391	0.08222023	1
REACTOME_PHOSPHORYLATION_OF_THE_APC_C	1.6118261	0.017777778	0.082826175	1
NAKAYAMA_SOFT_TISSUE_TUMORS_PCA2_UP	1.6100723	0	0.08377997	1
HORIUCHI_WTAP_TARGETS_DN	1.6099924	0	0.08336327	1
PID_ERA_GENOMIC_PATHWAY	1.6074307	0.005617978	0.08497857	1
REACTOME_SENESCENCE_ASSOCIATED_SECRETORY_PHENOTYPE_SASP	1.6054115	0.002739726	0.0860741	1
KRIGE_AMINO_ACID_DEPRIVATION	1.6037489	0.005037783	0.08698351	1
REACTOME_CHROMATIN_ORGANIZATION	1.6037115	0	0.08650477	1
REACTOME_MITOTIC_METAPHASE_AND_ANAPHASE	1.5977839	0	0.09052724	1
JEON_SMAD6_TARGETS_DN	1.5936985	0.013392857	0.093604736	1

CHIARETTI_T_ALL_RELAPSE_PROGNOSIS	1.5930629	0.020454545	0.09359729	1
TANG_SENESCENCE_TP53_TARGETS_DN	1.5907834	0.005333333	0.09506076	1
REACTOME_TRANSCRIPTIONAL_REGULATION_BY_SMALL_RNAS	1.5905825	0.00591716	0.09469149	1
WELCH_GATA1_TARGETS	1.5902011	0.012195122	0.09440494	1
REACTOME_CELLULAR_SENESCENCE	1.588542	0	0.095247634	1
REACTOME_INHIBITION_OF_THE_PROTEOLYTIC_ACTIVITY_OF_APC_C_REQUIRED_FOR_THE_ONSET_OF_ANAPHASE_BY_MITOTIC_SPINDLE_CHECKPOINT_COMPONENTS	1.5860171	0.017817372	0.09694301	1
REACTOME_PHOSPHORYLATION_OF_CD3_AND_TCR_ZETA_CHAINS	1.5841858	0.030023094	0.098165356	1
GROSS_HYPOXIA_VIA_ELK3_UP	1.5833834	0	0.09826684	1
KAUFFMANN_MELANOMA_RELAPSE_UP	1.5814794	0.007915568	0.09944139	1
PID_CMYB_PATHWAY	1.580526	0.002941177	0.099725515	1
BOYLAN_MULTIPLE_MYELOMA_C_UP	1.576728	0.007853403	0.10263729	1
REACTOME_CONVERSION_FROM_APC_C:CDC20_TO_APC_C:CDH1_IN_LATE_ANAPHASE	1.5759332	0.030588236	0.10295391	1
PYEON_CANCER_HEAD_AND_NECK_VS_CERVICAL_UP	1.5739174	0	0.104110666	1
BIOCARTA_CREB_PATHWAY	1.5722034	0.021327015	0.10528702	1
REACTOME_MECP2_REGULATES_NEURONAL_RECEPTORS_AND_CHANNELS	1.5711719	0.029279279	0.10557187	1
PID_AURORA_B_PATHWAY	1.569718	0.01058201	0.1063805	1

REACTOME_RMTS_METHYLATE_HISTONE_ARGININES	1.5687277	0.005420054	0.10676791	1
REACTOME_HOMOLOGOUS_DNA_PAIRING_AND_STRAND_EXCHANGE	1.5664504	0.013297873	0.108192705	1
PID_BETA_CATENIN_DEG_PATHWAY	1.5660653	0.030303031	0.10809131	1
NADERI_BREAST_CANCER_PROGNOSIS_UP	1.5643373	0.007832898	0.109244905	1
BIOCARTA_STATHMIN_PATHWAY	1.5635334	0.03736264	0.10941621	1
TSENG_ADIPOGENIC_POTENTIAL_UP	1.5599707	0.015463918	0.11208535	1
REACTOME_SUMOYLATION_OF_CHROMATIN_ORGANIZATION_PROTEINS	1.5592587	0.013333334	0.11218353	1
SMID_BREAST_CANCER_LUMINAL_A_DN	1.5567867	0.022988506	0.11385774	1
REACTOME_TRANSCRIPTION_OF_E2F_TARGETS_UNDER_NEGATIVE_CONTROL_BY_DREAM_COMPLEX	1.5550869	0.01904762	0.11487337	1
BOYLAN_MULTIPLE_MYELOMA_D_CLUSTER_DN	1.5533974	0.02184466	0.11595088	1
REACTOME_TELOMERE_MAINTENANCE	1.5480257	0.00862069	0.12052504	1
RIZ_ERYTHROID_DIFFERENTIATION	1.5470319	0.012048192	0.12102276	1
SCIBETTA_KDM5B_TARGETS_DN	1.5458677	0.002857143	0.12158328	1
REACTOME_EPHRIN_SIGNALING	1.5457683	0.033707865	0.12106481	1
VECCHI_GASTRIC_CANCER_EARLY_UP	1.5449321	0	0.12127242	1
REACTOME_FACTORS_INVOLVED_IN_MEGAKARYOCYTE_DEVELOPMENT_AND_PLATELET_PRODUCTION	1.5443289	0.003355705	0.12138854	1
MAGRANGEAS_MULTIPLE_MYELOMA_IGLL_VS_IGLK_UP	1.5432917	0.009501188	0.1219693	1

REACTOME_VEGFR2_MEDIATED_CELL_PROLIFERATION	1.5422083	0.029017856	0.12244837	1
KARAKAS_TGFB1_SIGNALING	1.5401033	0.018691588	0.124279805	1
ZHANG_BREAST_CANCER_PROGENITORS_UP	1.5354903	0	0.12847817	1
BIOCARTA_TPO_PATHWAY	1.5343614	0.03422983	0.12902795	1
FOURNIER_ACINAR_DEVELOPMENT_LATE_DN	1.5322347	0.025056947	0.13076764	1
REACTOME_MITOTIC_PROPHASE	1.531475	0.003367003	0.13094416	1
REACTOME_REGULATION_OF_TP53_ACTIVITY_THROUGH_PHOSPHORYLATION	1.5299132	0.002890173	0.13203731	1
REACTOME_DNA_STRAND_ELONGATION	1.5287586	0.019512195	0.1326577	1
PID_AURORA_A_PATHWAY	1.5284656	0.012755103	0.13237298	1
SENGUPTA_NASOPHARYNGEAL_CARCINOMA_UP	1.5274581	0	0.13293129	1
GOLUB_ALL_VS_AML_UP	1.5245302	0.019138755	0.13562489	1
REACTOME_SIGNALING_BY_NTRK2_TRKB	1.5206816	0.030303031	0.13926364	1
BIOCARTA_GH_PATHWAY	1.51834	0.026190476	0.14131416	1
KEGG_AXON_GUIDANCE	1.5182483	0.003194888	0.14075078	1
REACTOME_G2_M_DNA_DAMAGE_CHECKPOINT	1.5175227	0.009118541	0.140959	1
REACTOME_FORMATION_OF_THE_BETA_CATENIN:TCF_TRANSACTIVATING_COMPLEX	1.5169766	0.005555556	0.14098907	1
WHITFIELD_CELL_CYCLE_G1_S	1.5166395	0.002994012	0.1407393	1
REACTOME_DNA_DOUBLE_STRAND_BREAK_REPAIR	1.5163386	0.006557377	0.14042047	1
GUTIERREZ_CHRONIC_LYMPHOCYTIC_LEUKEMIA_DN	1.5148233	0.008108108	0.14150903	1

BIOCARTA_MCALPAIN_PATHWAY	1.5142745	0.045652173	0.14143796	1
REACTOME_PROCESSING_OF_DNA_DOUBLE_STRAND_BREAK_ENDS	1.5121379	0.020057306	0.14328359	1
ROVERSI_GLIOMA_COPY_NUMBER_UP	1.5104823	0.002881844	0.14459954	1
REACTOME_TRAFFICKING_OF_GLUR2_CONTAINING_AMPA_RECEPTORS	1.5092916	0.03167421	0.14536539	1
REACTOME_PLATELET_SENSITIZATION_BY_LDL	1.5081981	0.04017857	0.14594518	1
PID_WNT_CANONICAL_PATHWAY	1.5066061	0.037444934	0.14707907	1
XU_HGF_SIGNALING_NOT_VIA_AKT1_48HR_DN	1.5029361	0.057268724	0.15095648	1
MORI_EMU_MYC_LYMPHOMA_BY_ONSET_TIME_UP	1.5018317	0	0.15167251	1
PUJANA_BREAST_CANCER_LIT_INT_NETWORK	1.5014455	0.014880952	0.15151377	1
REACTOME_SYNAPTIC_ADHESION_LIKE_MOLECULES	1.5014001	0.028199567	0.15093343	1
REACTOME_DEPURINATION	1.5003222	0.04157044	0.15166713	1
REACTOME_DOWNSTREAM_SIGNAL_TRANSDUCTION	1.4998354	0.025114154	0.15158042	1
REACTOME_OXIDATIVE_STRESS_INDUCED_SENESCENCE	1.4995217	0.005747126	0.15128733	1
PID_NCADHERIN_PATHWAY	1.4991837	0.024570024	0.15101169	1
NAKAMURA_CANCER_MICROENVIRONMENT_DN	1.4988761	0.024937656	0.15075211	1
CHIANG_LIVER_CANCER_SUBCLASS_PROLIFERATION_UP	1.4972266	0	0.15206458	1
REACTOME_HOMOLOGY_DIRECTED_REPAIR	1.4954607	0.003389831	0.15340045	1
REACTOME_ONCOGENE_INDUCED_SENESCENCE	1.4954339	0.028571429	0.15281305	1
LIU_VAV3_PROSTATE_CARCINOGENESIS_DN	1.4953685	0.043956045	0.15222575	1

MARIADASON_RESPONSE_TO_BUTYRATE_SULINDAC_6	1.4947386	0.013333334	0.15232939	1
BIOCARTA_WNT_PATHWAY	1.4933034	0.029411765	0.1535057	1
PID_FANCONI_PATHWAY	1.4918599	0.007653061	0.15474224	1
GENTILE_UV_RESPONSE_CLUSTER_D2	1.4904152	0.023684211	0.15589976	1
KEGG_WNT_SIGNALING_PATHWAY	1.4893903	0	0.15638044	1
BIOCARTA_MCM_PATHWAY	1.4848855	0.041394334	0.1611302	1
VERNELL_RETINOBLASTOMA_PATHWAY_UP	1.4847324	0.016	0.16073398	1
REACTOME_SIGNALING_BY_RHO_GTPASES	1.4835545	0	0.16144314	1
PID_VEGFR1_PATHWAY	1.4834596	0.0315534	0.16091837	1
ACEVEDO_LIVER_CANCER_WITH_H3K9ME3_DN	1.483	0.008450705	0.16080742	1
DUAN_PRDM5_TARGETS	1.4822111	0.013736264	0.16112813	1
REACTOME_GOLGI_TO_ER_RETROGRADE_TRANSPORT	1.479953	0	0.16347022	1
REACTOME_HDR_THROUGH_SINGLE_STRAND_ANNEALING_SSA	1.4793144	0.03640777	0.16356106	1
CHIN_BREAST_CANCER_COPY_NUMBER_UP	1.4787121	0.03678161	0.16356882	1
LINDGREN_BLADDER_CANCER_WITH_LOH_IN_CHR9Q	1.4779822	0.006493507	0.16385132	1
BIOCARTA_GLEEVEC_PATHWAY	1.4769732	0.044705883	0.1645649	1
CREIGHTON_ENDOCRINE_THERAPY_RESISTANCE_2	1.4768361	0	0.16410033	1
REACTOME_HIV_LIFE_CYCLE	1.4758247	0	0.16491452	1
STANELLE_E2F1_TARGETS	1.4753851	0.04450262	0.16485977	1
CHAUHAN_RESPONSE_TO_METHOXYESTRADIOL_UP	1.4751319	0.034946237	0.16458799	1
LE_NEURONAL_DIFFERENTIATION_DN	1.4746631	0.046563193	0.16455829	1

REACTOME_SIGNALING_BY_SCF_KIT	1.4713645	0.029776676	0.16827428	1
REACTOME_HATS_ACETYLATE_HISTONES	1.4699416	0.005988024	0.16943872	1
BIOCARTA_G1_PATHWAY	1.4690872	0.04398148	0.16986549	1
WEST_ADRENOCORTICAL_TUMOR_UP	1.468066	0	0.17048253	1
BIOCARTA_BIOPEPTIDES_PATHWAY	1.4676942	0.031007752	0.17036776	1
REACTOME_NONHOMOLOGOUS_END_JOINING_NHEJ	1.4667764	0.018229166	0.17093731	1
HUMMEL_BURKITTS_LYMPHOMA_UP	1.4660558	0.02116402	0.17113338	1
WILCOX_RESPONSE_TO_PROGESTERONE_UP	1.4656479	0.003205128	0.17108202	1
CAFFAREL_RESPONSE_TO_THC_UP	1.464835	0.0495283	0.17155428	1
BIOCARTA_PITX2_PATHWAY	1.4641731	0.06726457	0.17185321	1
REACTOME_INTRAFLAGELLAR_TRANSPORT	1.4634087	0.031088082	0.17227033	1
DAZARD_RESPONSE_TO_UV_NHEK_DN	1.4624263	0	0.17307858	1
PID_HDAC_CLASSIII_PATHWAY	1.4619179	0.035955057	0.17318751	1
BROWNE_HCMV_INFECTION_10HR_UP	1.46061	0.008219178	0.17430879	1
HOFFMANN_SMALL_PRE_BII_TO_IMMATURE_B_LYMPHOCYTE_DN	1.4593273	0.020356234	0.17534634	1
TONKS_TARGETS_OF_RUNX1_RUNX1T1_FUSION_ERYTHROCYTE_DN	1.457568	0.038990825	0.176979	1
REACTOME_MEIOSIS	1.4545375	0.019886363	0.18024829	1
PID_CD8_TCR_PATHWAY	1.4522064	0.022922637	0.18272774	1
PID_P38_ALPHA_BETA_PATHWAY	1.4516759	0.040963855	0.18280987	1

REACTOME_SIGNALING_BY_FGFR_IN_DISEASE	1.4512995	0.010958904	0.18265928	1
SHEN_SMARCA2_TARGETS_UP	1.4511172	0	0.18221654	1
REACTOME_RNA_POLYMERASE_II_TRANSCRIPTION_PRE_INITIATION_AND_PROMOTER_OPENING	1.451114	0.027777778	0.18158324	1
BROWNE_HCMV_INFECTION_14HR_UP	1.44946	0.003289474	0.183082	1
TOYOTA_TARGETS_OF_MIR34B_AND_MIR34C	1.448047	0	0.18437932	1
BIOCARTA_MET_PATHWAY	1.4468422	0.044665013	0.18531907	1
HOLLEMAN_PREDNISOLONE_RESISTANCE_B_ALL_UP	1.4466814	0.065375306	0.18487023	1
KIM_WT1_TARGETS_DN	1.4441772	0	0.18754812	1
AFFAR_YY1_TARGETS_DN	1.4435756	0	0.18759575	1
RIZ_ERYTHROID_DIFFERENTIATION_HEMGN	1.4413624	0.06026786	0.19010872	1
NUNODA_RESPONSE_TO_DASATINIB_IMATINIB_UP	1.441174	0.06188119	0.18973751	1
REACTOME_TRANSCRIPTIONAL_REGULATION_BY_THE_AP_2_TFAP2_FAMILY_OF_TRANSCRIPTION_FACTORS	1.4411255	0.06855792	0.1891561	1
REACTOME_TP53_REGULATES_TRANSCRIPTION_OF_CELL_CYCLE_GENES	1.4398594	0.043715846	0.19032942	1
MCCLUNG_DELTA_FOSB_TARGETS_8WK	1.4394022	0.01946472	0.19030033	1
SU_TESTIS	1.4380478	0.028735632	0.19131704	1
HASLINGER_B_CLL_WITH_MUTATED_VH_GENES	1.4372569	0.07111111	0.19181342	1
GENTILE_RESPONSE_CLUSTER_D3	1.4367853	0.031007752	0.1918333	1
REACTOME_MITOTIC_G1_G1_S_PHASES	1.4360384	0	0.19223604	1

PID_EPHRINB_REV_PATHWAY	1.4357646	0.052757792	0.19198298	1
MMS_MOUSE_LYMPH_HIGH_4HRS_UP	1.4349953	0.037593983	0.1924327	1
REACTOME_DNA_DAMAGE_TELOMERE_STRESS_INDUCED_SENESCENCE	1.4321328	0.024657534	0.19572963	1
REACTOME_METABOLISM_OF_ANGIOTENSINOGEN_TO_ANGIOTENSINS	1.4313797	0.091116175	0.19612467	1
REACTOME_DAP12_SIGNALING	1.4296994	0.06896552	0.19797783	1
KEGG_BLADDER_CANCER	1.4292397	0.04197531	0.19798788	1
REACTOME_LAGGING_STRAND_SYNTHESIS	1.4287214	0.046357617	0.19805093	1
HOEBEKE_LYMPHOID_STEM_CELL_UP	1.4284127	0.013927577	0.19778211	1
REACTOME_COPI_DEPENDENT_GOLGI_TO_ER_RETROGRADE_TRAFFIC	1.4275863	0.008982036	0.198326	1
REACTOME_BASE_EXCISION_REPAIR_AP_SITE_FORMATION	1.4268004	0.04040404	0.19879141	1
PID_ERBB1_RECEPTOR_PROXIMAL_PATHWAY	1.4266664	0.050890584	0.19834228	1
REACTOME_DEACTIVATION_OF_THE_BETA_CATENIN_TRANSACTIVATING_COMPLEX	1.4263501	0.041666668	0.19813924	1
REACTOME_RESOLUTION_OF_D_LOOP_STRUCTURES_THROUGH_SYNTHESIS_DEPENDENT_STRAND_ANNEALING_SDSA	1.425471	0.058295965	0.19871856	1
REACTOME_HDACS_DEACETYLATE_HISTONES	1.423769	0.02259887	0.20053054	1
REACTOME_POST_CHAPERONIN_TUBULIN_FOLDING_PATHWAY	1.4230014	0.05689278	0.20096856	1
CLIMENT_BREAST_CANCER_COPY_NUMBER_UP	1.4218708	0.067307696	0.2020477	1

DUTERTRE_ESTRADIOL_RESPONSE_6HR_DN	1.4208399	0.021943573	0.20303978	1
NIKOLSKY_BREAST_CANCER_15Q26_AMPLICON	1.4198278	0.06142506	0.2037498	1
KEGG_BASAL_TRANSCRIPTION_FACTORS	1.4168243	0.04134367	0.20728956	1
IVANOVA_HEMATOPOIESIS_STEM_CELL_SHORT_TERM	1.4160458	0.06928407	0.20796885	1
PEART_HDAC_PROLIFERATION_CLUSTER_DN	1.4153479	0.019354839	0.20828418	1
REACTOME_SIGNALING_BY_CYTOSOLIC_FGFR1_FUSION_MUTANTS	1.4153244	0.066176474	0.2076811	1
WONG_EMBRYONIC_STEM_CELL_CORE	1.4147296	0	0.20791125	1
PID_DNA_PK_PATHWAY	1.4145497	0.06950673	0.20755574	1
DACOSTA_UV_RESPONSE_VIA_ERCC3_COMMON_DN	1.4144108	0	0.20716344	1
BROWNE_HCMV_INFECTION_30MIN_DN	1.4138294	0.01875	0.20737779	1
REACTOME_SIGNALING_BY_NUCLEAR_RECEPTORS	1.4135284	0	0.20717359	1
BAELDE_DIABETIC_NEPHROPATHY_UP	1.4125602	0.025	0.20797229	1
KENNY_CTNNB1_TARGETS_UP	1.4124477	0.04187192	0.20751956	1
REACTOME_ER_QUALITY_CONTROL_COMPARTMENT_ERQC	1.4121948	0.052009456	0.20727703	1
KEGG_SPLICEOSOME	1.4112482	0.00619195	0.20811354	1
MAYBURD_RESPONSE_TO_L663536_UP	1.4090205	0.049411766	0.21066718	1
ZWANG_DOWN_BY_2ND_EGF_PULSE	1.4082764	0.007407407	0.21118157	1
REACTOME_DISASSEMBLY_OF_THE_DESTRUCTION_COMPLEX_AND_RECRUITMENT_OF_AXIN_TO_THE_MEMBRANE	1.4062579	0.06382979	0.21359189	1
SIMBULAN_UV_RESPONSE_NORMAL_DN	1.4053004	0.065375306	0.21445394	1

REACTOME_RNA_POLYMERASE_II_TRANSCRIBES_SNRNA_GENES	1.4019783	0.017391304	0.21872343	1
LAU_APOPTOSIS_CDKN2A_UP	1.4009312	0.032432433	0.21952456	1
MOOTHA_GLUCONEOGENESIS	1.3988253	0.08607595	0.22203135	1
KIM_LIVER_CANCER_POOR_SURVIVAL_DN	1.397823	0.047169812	0.22300732	1
KEGG_MELANOGENESIS	1.3977323	0.01510574	0.22251855	1
BIOCARTA_PDGF_PATHWAY	1.3948914	0.06407323	0.22633305	1
NICK_RESPONSE_TO_PROC_TREATMENT_DN	1.391878	0.055045873	0.23040329	1
WANG_RESPONSE_TO_GSK3_INHIBITOR_SB216763_DN	1.3895698	0	0.23352943	1
REACTOME_BASE_EXCISION_REPAIR	1.3893163	0.040572792	0.23326649	1
YIH_RESPONSE_TO_ARSENITE_C1	1.3889551	0.08604651	0.23317336	1
PID_KIT_PATHWAY	1.3885494	0.049586777	0.2331761	1
RICKMAN_TUMOR_DIFFERENTIATED_WELL_VS_POORLY_UP	1.3885194	0	0.23257095	1
BIOCARTA_TCR_PATHWAY	1.3884908	0.05854801	0.23192717	1
REACTOME_SUMOYLATION_OF_DNA_DAMAGE_RESPONSE_AND_REPAIR_PROTEINS	1.387775	0.04249292	0.23238707	1
VANTVEER_BREAST_CANCER_POOR_PROGNOSIS	1.3877238	0.034391534	0.23180902	1
BIOCARTA_CCR5_PATHWAY	1.386472	0.103837475	0.23310743	1
REACTOME_S_PHASE	1.3846642	0.010309278	0.23510893	1
BIOCARTA_ECM_PATHWAY	1.3840556	0.098280095	0.23537073	1
KAMIKUBO_MYELOID_MN1_NETWORK	1.3831667	0.087804876	0.23608328	1

KYNG_NORMAL_AGING_UP	1.3822101	0.09803922	0.23713116	1
KAUFFMANN_DNA_REPLICATION_GENES	1.3811927	0.010067114	0.23809291	1
BIOCARTA_SPPA_PATHWAY	1.37905	0.0864745	0.24089652	1
DACOSTA_UV_RESPONSE_VIA_ERCC3_TTD_DN	1.3784735	0.029239766	0.24117665	1
REACTOME_TRANSCRIPTION_OF_E2F_TARGETS_UNDER_NEGATIVE_CONTROL_BY_P107_RBL1_AND_P130_RBL2_IN_COMPLEX_WITH_HDAC1	1.3778335	0.089411765	0.2416344	1
AGUIRRE_PANCREATIC_CANCER_COPY_NUMBER_DN	1.3777686	0.004291846	0.24109215	1
BIOCARTA_PPARA_PATHWAY	1.3775231	0.035230353	0.24079657	1
KEGG_ERBB_SIGNALING_PATHWAY	1.3766342	0.031518623	0.24152501	1
PID_NETRIN_PATHWAY	1.3764923	0.052369077	0.24106778	1
PROVENZANI_METASTASIS_UP	1.374452	0.007843138	0.24371994	1
BIOCARTA_PYK2_PATHWAY	1.374447	0.06422018	0.2430634	1
REACTOME_CELLULAR_RESPONSES_TO_STRESS	1.3739411	0	0.24317424	1
KYNG_WERNER_SYNDROM_UP	1.3738102	0.10933941	0.24274366	1
VERHAAK_GLIOBLASTOMA_PRONEURAL	1.3719566	0.01010101	0.24496758	1
REACTOME_TRANSCRIPTIONAL_REGULATION_BY_TP53	1.3710549	0	0.24576965	1
WU_HBX_TARGETS_3_UP	1.3709662	0.10185185	0.24527662	1
REACTOME_REGULATION_OF_KIT_SIGNALING	1.3681691	0.10909091	0.24911894	1
REACTOME_PD_1_SIGNALING	1.3675845	0.10067114	0.2494455	1
CEBALLOS_TARGETS_OF_TP53_AND_MYC_UP	1.3675374	0.094339624	0.24886025	1

PURBEY_TARGETS_OF_CTBP1_AND_SATB1_UP	1.3671309	0.039660055	0.24894658	1
PID_HDAC_CLASSII_PATHWAY	1.3661007	0.057971016	0.24990797	1
REACTOME_RNA_POLYMERASE_II_PRE_TRANSCRIPTION_EVENTS	1.365983	0.04191617	0.24942668	1
***p53*$^{-/-}$ *VAV1-Tg* Lym vs WT T splenocytes**	**NES**	**NOM p-val**	**FDR q-val**	**FWER p-val**
ROSTY_CERVICAL_CANCER_PROLIFERATION_CLUSTER	2.6744897	0	0	0
FLORIO_NEOCORTEX_BASAL_RADIAL_GLIA_DN	2.6566577	0	0	0
SOTIRIOU_BREAST_CANCER_GRADE_1_VS_3_UP	2.6321936	0	0	0
DUTERTRE_ESTRADIOL_RESPONSE_24HR_UP	2.5826893	0	0	0
KOBAYASHI_EGFR_SIGNALING_24HR_DN	2.5650227	0	0	0
CROONQUIST_IL6_DEPRIVATION_DN	2.5500708	0	0	0
ZHOU_CELL_CYCLE_GENES_IN_IR_RESPONSE_24HR	2.5440145	0	0	0
GRAHAM_CML_DIVIDING_VS_NORMAL_QUIESCENT_UP	2.5255225	0	0	0
KANG_DOXORUBICIN_RESISTANCE_UP	2.5253317	0	0	0
KONG_E2F3_TARGETS	2.52217	0	0	0
BURTON_ADIPOGENESIS_3	2.52092	0	0	0
WINNEPENNINCKX_MELANOMA_METASTASIS_UP	2.5142796	0	0	0
WHITEFORD_PEDIATRIC_CANCER_MARKERS	2.5127528	0	0	0
GRAHAM_NORMAL_QUIESCENT_VS_NORMAL_DIVIDING_DN	2.5038695	0	0	0
HOFFMANN_LARGE_TO_SMALL_PRE_BII_LYMPHOCYTE_UP	2.4811053	0	0	0
ISHIDA_E2F_TARGETS	2.4793837	0	0	0

LEE_EARLY_T_LYMPHOCYTE_UP	2.4585104	0	0	0
MORI_IMMATURE_B_LYMPHOCYTE_DN	2.4569979	0	0	0
ZHOU_CELL_CYCLE_GENES_IN_IR_RESPONSE_6HR	2.4499333	0	0	0
CROONQUIST_NRAS_SIGNALING_DN	2.4451854	0	0	0
WONG_EMBRYONIC_STEM_CELL_CORE	2.4449446	0	0	0
RUIZ_TNC_TARGETS_DN	2.4445546	0	0	0
ODONNELL_TFRC_TARGETS_DN	2.4390328	0	0	0
RHODES_UNDIFFERENTIATED_CANCER	2.4366643	0	0	0
MISSIAGLIA_REGULATED_BY_METHYLATION_DN	2.4317544	0	0	0
ZHAN_MULTIPLE_MYELOMA_PR_UP	2.4252977	0	0	0
GAVIN_FOXP3_TARGETS_CLUSTER_P6	2.403247	0	0	0
MORI_LARGE_PRE_BII_LYMPHOCYTE_UP	2.4003036	0	0	0
CHIANG_LIVER_CANCER_SUBCLASS_PROLIFERATION_UP	2.3944933	0	0	0
SHEDDEN_LUNG_CANCER_POOR_SURVIVAL_A6	2.3875186	0	0	0
WHITFIELD_CELL_CYCLE_LITERATURE	2.3838873	0	0	0
SARRIO_EPITHELIAL_MESENCHYMAL_TRANSITION_UP	2.3785024	0	0	0
NAKAYAMA_SOFT_TISSUE_TUMORS_PCA2_UP	2.3715634	0	0	0
PUJANA_BRCA_CENTERED_NETWORK	2.3687584	0	0	0
MANALO_HYPOXIA_DN	2.3649817	0	0	0
KAUFFMANN_MELANOMA_RELAPSE_UP	2.3636096	0	0	0
REACTOME_DNA_REPLICATION	2.3594742	0	0	0

REACTOME_CELL_CYCLE_CHECKPOINTS	2.3540342	0	0	0
MOLENAAR_TARGETS_OF_CCND1_AND_CDK4_DN	2.3510475	0	0	0
FRASOR_RESPONSE_TO_SERM_OR_FULVESTRANT_DN	2.348594	0	0	0
REACTOME_MITOCHONDRIAL_TRANSLATION	2.34375	0	0	0
MARKEY_RB1_ACUTE_LOF_UP	2.3429909	0	0	0
LE_EGR2_TARGETS_UP	2.3379867	0	0	0
MORI_PRE_BI_LYMPHOCYTE_UP	2.3336105	0	0	0
BENPORATH_PROLIFERATION	2.3314748	0	0	0
PUJANA_XPRSS_INT_NETWORK	2.3296735	0	0	0
REACTOME_DNA_STRAND_ELONGATION	2.3292868	0	0	0
VECCHI_GASTRIC_CANCER_EARLY_UP	2.3265474	0	0	0
BLUM_RESPONSE_TO_SALIRASIB_DN	2.3238804	0	0	0
FERREIRA_EWINGS_SARCOMA_UNSTABLE_VS_STABLE_UP	2.3194742	0	0	0
TANG_SENESCENCE_TP53_TARGETS_DN	2.3175657	0	0	0
REACTOME_DNA_REPLICATION_PRE_INITIATION	2.3158824	0	0	0
REICHERT_MITOSIS_LIN9_TARGETS	2.314824	0	0	0
BURTON_ADIPOGENESIS_PEAK_AT_24HR	2.3102262	0	0	0
FUJII_YBX1_TARGETS_DN	2.3064797	0	0	0
REN_BOUND_BY_E2F	2.299302	0	0	0
ODONNELL_TARGETS_OF_MYC_AND_TFRC_DN	2.2962534	0	0	0
SONG_TARGETS_OF_IE86_CMV_PROTEIN	2.2886176	0	0	0

WU_APOPTOSIS_BY_CDKN1A_VIA_TP53	2.287919	0	0	0
REACTOME_MITOTIC_SPINDLE_CHECKPOINT	2.2847168	0	0	0
REACTOME_G2_M_CHECKPOINTS	2.282097	0	0	0
TARTE_PLASMA_CELL_VS_PLASMABLAST_DN	2.2727005	0	0	0
CHICAS_RB1_TARGETS_GROWING	2.2657628	0	0	0
MUELLER_PLURINET	2.261173	0	0	0
LI_WILMS_TUMOR_VS_FETAL_KIDNEY_1_DN	2.2583716	0	0	0
LINDGREN_BLADDER_CANCER_CLUSTER_3_UP	2.2565873	0	0	0
CHEMNITZ_RESPONSE_TO_PROSTAGLANDIN_E2_UP	2.254501	0	0	0
REACTOME_MITOTIC_G1_G1_S_PHASES	2.2515328	0	0	0
SHEPARD_BMYB_TARGETS	2.2491589	0	0	0
VERNELL_RETINOBLASTOMA_PATHWAY_UP	2.2442465	0	0	0
LY_AGING_OLD_DN	2.243453	0	0	0
FURUKAWA_DUSP6_TARGETS_PCI35_DN	2.2404664	0	0	0
BASAKI_YBX1_TARGETS_UP	2.2383056	0	0	0
MOOTHA_VOXPHOS	2.2380688	0	0	0
REACTOME_MITOTIC_METAPHASE_AND_ANAPHASE	2.2354906	0	0	0
REACTOME_SWITCHING_OF_ORIGINS_TO_A_POST_REPLICATIVE_STATE	2.2324812	0	0	0
YU_MYC_TARGETS_UP	2.231363	0	0	0
HORIUCHI_WTAP_TARGETS_DN	2.222936	0	0	0

EGUCHI_CELL_CYCLE_RB1_TARGETS	2.221455	0	0	0
REACTOME_RESOLUTION_OF_SISTER_CHROMATID_COHESION	2.2213376	0	0	0
WONG_MITOCHONDRIA_GENE_MODULE	2.2187243	0	0	0
PID_ATR_PATHWAY	2.2160182	0	0	0
REACTOME_ASSEMBLY_OF_THE_PRE_REPLICATIVE_COMPLEX	2.2155342	0	0	0
REACTOME_CHROMOSOME_MAINTENANCE	2.215452	0	0	0
REACTOME_ORC1_REMOVAL_FROM_CHROMATIN	2.2138958	0	0	0
REACTOME_S_PHASE	2.211845	0	0	0
NAKAMURA_CANCER_MICROENVIRONMENT_DN	2.21011	0	0	0
REACTOME_REGULATION_OF_MITOTIC_CELL_CYCLE	2.2094111	0	0	0
REACTOME_ACTIVATION_OF_ATR_IN_RESPONSE_TO_REPLICATION_STRESS	2.208499	0	0	0
KEGG_DNA_REPLICATION	2.2056086	0	0	0
FOURNIER_ACINAR_DEVELOPMENT_LATE_2	2.2032926	0	0	0
GARGALOVIC_RESPONSE_TO_OXIDIZED_PHOSPHOLIPIDS_TURQUOISE_DN	2.2015016	0	0	0
FISCHER_G2_M_CELL_CYCLE	2.2003596	0	0	0
REACTOME_CELL_CYCLE_MITOTIC	2.194111	0	0	0
KEGG_OXIDATIVE_PHOSPHORYLATION	2.1899414	0	0	0
KAMMINGA_EZH2_TARGETS	2.1876495	0	0	0
BURTON_ADIPOGENESIS_PEAK_AT_16HR	2.1809392	0	0	0

REACTOME_HDR_THROUGH_HOMOLOGOUS_RECOMBINATION_HRR	2.1744378	0	0	0
PID_PLK1_PATHWAY	2.1738136	0	0	0
REACTOME_RESPIRATORY_ELECTRON_TRANSPORT_ATP_SYNTHESIS_BY_CHEMIOSMOTIC_COUPLING_AND_HEAT_PRODUCTION_BY_UNCOUPLING_PROTEINS	2.170476	0	0	0
ZHENG_GLIOBLASTOMA_PLASTICITY_UP	2.170293	0	0	0
REACTOME_HOMOLOGOUS_DNA_PAIRING_AND_STRAND_EXCHANGE	2.168943	0	0	0
FINETTI_BREAST_CANCER_KINOME_RED	2.1672335	0	0	0
REACTOME_RHO_GTPASES_ACTIVATE_FORMINS	2.1655781	0	0	0
REACTOME_ACTIVATION_OF_APC_C_AND_APC_C:CDC20_MEDIATED_DEGRADATION_OF_MITOTIC_PROTEINS	2.163194	0	0	0
BOYAULT_LIVER_CANCER_SUBCLASS_G3_UP	2.1591141	0	0	0
GOLDRATH_ANTIGEN_RESPONSE	2.1588256	0	0	0
PUJANA_BREAST_CANCER_WITH_BRCA1_MUTATED_UP	2.1585572	0	0	0
REACTOME_VIF_MEDIATED_DEGRADATION_OF_APOBEC3G	2.149222	0	0	0
SCIAN_CELL_CYCLE_TARGETS_OF_TP53_AND_TP73_DN	2.146048	0	0	0
DANG_MYC_TARGETS_UP	2.144505	0	0	0
SCHUHMACHER_MYC_TARGETS_UP	2.1438723	0	0	0
REACTOME_ACTIVATION_OF_THE_PRE_REPLICATIVE_COMPLEX	2.14348	0	0	0

REACTOME_RESPIRATORY_ELECTRON_TRANSPORT	2.1383324	0	0	0
REACTOME_THE_CITRIC_ACID_TCA_CYCLE_AND_RESPIRATORY_ELECTRON_TRANSPORT	2.1379685	0	0	0
REACTOME_LAGGING_STRAND_SYNTHESIS	2.1370711	0	0	0
PUJANA_BRCA2_PCC_NETWORK	2.136102	0	0	0
PID_FANCONI_PATHWAY	2.136061	0	0	0
REACTOME_CROSS_PRESENTATION_OF_SOLUBLE_EXOGENOUS_ANTIGENS_ENDOSOMES	2.1358488	0	0	0
YAO_TEMPORAL_RESPONSE_TO_PROGESTERONE_CLUSTER_14	2.1335976	0	0	0
AFFAR_YY1_TARGETS_DN	2.133369	0	0	0
YAO_TEMPORAL_RESPONSE_TO_PROGESTERONE_CLUSTER_13	2.132426	0	0	0
SMID_BREAST_CANCER_LUMINAL_A_DN	2.1247997	0	0	0
REACTOME_COMPLEX_I_BIOGENESIS	2.1235638	0	0	0
RHEIN_ALL_GLUCOCORTICOID_THERAPY_DN	2.12279	0	0	0
REACTOME_MITOTIC_PROMETAPHASE	2.1215334	0	0	0
PAL_PRMT5_TARGETS_UP	2.1201618	0	0	0
MOOTHA_HUMAN_MITODB_6_2002	2.1170757	0	0	0
GREENBAUM_E2A_TARGETS_UP	2.1118834	0	0	0
KEGG_PROTEASOME	2.1113586	0	0	0
MITSIADES_RESPONSE_TO_APLIDIN_DN	2.1096537	0	0	0
REACTOME_CDK_MEDIATED_PHOSPHORYLATION_AND_REMOVA	2.1086025	0	0	0

L_OF_CDC6				
FARMER_BREAST_CANCER_CLUSTER_2	2.1041853	0	0	0
LY_AGING_MIDDLE_DN	2.1035728	0	0	0
REACTOME_SCF_SKP2_MEDIATED_DEGRADATION_OF_P27_P21	2.1031206	0	0	0
REACTOME_DEGRADATION_OF_GLI1_BY_THE_PROTEASOME	2.0989466	0	0	0
REACTOME_APC_C:CDH1_MEDIATED_DEGRADATION_OF_CDC20_AND_OTHER_APC_C:CDH1_TARGETED_PROTEINS_IN_LATE_MITOSIS_EARLY_G1	2.096979	0	0	0
REACTOME_M_PHASE	2.0953948	0	0	0
REACTOME_NEGATIVE_REGULATION_OF_NOTCH4_SIGNALING	2.0942156	0	0	0
CHIANG_LIVER_CANCER_SUBCLASS_UNANNOTATED_DN	2.0920138	0	0	0
REACTOME_FBXL7_DOWN_REGULATES_AURKA_DURING_MITOTIC_ENTRY_AND_IN_EARLY_MITOSIS	2.0888557	0	0	0
REACTOME_EXTENSION_OF_TELOMERES	2.0841465	0	0	0
YAO_TEMPORAL_RESPONSE_TO_PROGESTERONE_CLUSTER_17	2.0827553	0	0	0
WANG_RESPONSE_TO_GSK3_INHIBITOR_SB216763_DN	2.0827463	0	0	0
PID_AURORA_B_PATHWAY	2.080214	0	0	0
REACTOME_HEDGEHOG_LIGAND_BIOGENESIS	2.0790641	0	0	0
VILLANUEVA_LIVER_CANCER_KRT19_UP	2.0789685	0	0	0
CROONQUIST_NRAS_VS_STROMAL_STIMULATION_DN	2.0784411	0	0	0
RHODES_CANCER_META_SIGNATURE	2.0755713	0	0	0

CONCANNON_APOPTOSIS_BY_EPOXOMICIN_DN	2.0743277	0	0	0
REACTOME_AUF1_HNRNP_D0_BINDS_AND_DESTABILIZES_MRNA	2.0741105	0	0	0
REACTOME_HOMOLOGY_DIRECTED_REPAIR	2.0733159	0	0	0
REACTOME_REGULATION_OF_APOPTOSIS	2.069861	0	0	0
KEGG_PARKINSONS_DISEASE	2.0690665	0	0	0
REACTOME_TELOMERE_MAINTENANCE	2.0683303	0	0	0
PID_BARD1_PATHWAY	2.0678487	0	0	0
SHIPP_DLBCL_VS_FOLLICULAR_LYMPHOMA_UP	2.067816	0	0	0
ZHANG_RESPONSE_TO_CANTHARIDIN_DN	2.0666094	0	0	0
LI_WILMS_TUMOR_ANAPLASTIC_UP	2.066475	0	0	0
NADERI_BREAST_CANCER_PROGNOSIS_UP	2.065104	0	0	0
KEGG_CELL_CYCLE	2.0625377	0	0	0
MOOTHA_MITOCHONDRIA	2.0619895	0	0	0
REACTOME_TRNA_PROCESSING	2.0594084	0	0	0
NAKAMURA_TUMOR_ZONE_PERIPHERAL_VS_CENTRAL_UP	2.0560803	0	0	0
CHICAS_RB1_TARGETS_LOW_SERUM	2.0524695	0	0	0
KEGG_PYRIMIDINE_METABOLISM	2.052319	0	0	0
KAUFFMANN_DNA_REPLICATION_GENES	2.0520437	0	0	0
REACTOME_RESOLUTION_OF_D_LOOP_STRUCTURES_THROUGH_SYNTHESIS_DEPENDENT_STRAND_ANNEALING_SDSA	2.0504234	0	0	0

MOREAUX_B_LYMPHOCYTE_MATURATION_BY_TACI_DN	2.0498405	0	0	0
REACTOME_TELOMERE_C_STRAND_LAGGING_STRAND_SYNTHESIS	2.048853	0	0	0
REACTOME_HDR_THROUGH_SINGLE_STRAND_ANNEALING_SSA	2.0488265	0	0	0
FERRANDO_T_ALL_WITH_MLL_ENL_FUSION_DN	2.0480037	0	0	0
HESS_TARGETS_OF_HOXA9_AND_MEIS1_UP	2.0479505	0	0	0
REACTOME_METABOLISM_OF_POLYAMINES	2.044844	0	0	0
CUI_TCF21_TARGETS_2_UP	2.0442848	0	0	0
FOURNIER_ACINAR_DEVELOPMENT_LATE_DN	2.039204	0	0	0
REACTOME_HOST_INTERACTIONS_OF_HIV_FACTORS	2.0388427	0	0	0
REACTOME_REGULATION_OF_MRNA_STABILITY_BY_PROTEINS_THAT_BIND_AU_RICH_ELEMENTS	2.0377343	0	0	0
REACTOME_CYCLIN_A_B1_B2_ASSOCIATED_EVENTS_DURING_G2_M_TRANSITION	2.0327559	0	0	0
GRADE_COLON_AND_RECTAL_CANCER_UP	2.032194	0	0	0
REACTOME_ABC_TRANSPORTER_DISORDERS	2.0314193	0	0	0
SHEPARD_BMYB_MORPHOLINO_DN	2.0279143	0	0	0
REACTOME_RECOGNITION_OF_DNA_DAMAGE_BY_PCNA_CONTAINING_REPLICATION_COMPLEX	2.0265033	0	0	0
REACTOME_DEFECTIVE_CFTR_CAUSES_CYSTIC_FIBROSIS	2.0257123	0	0	0
REACTOME_RESOLUTION_OF_D_LOOP_STRUCTURES	2.0229213	0	0	0

BOYAULT_LIVER_CANCER_SUBCLASS_G23_UP	2.0227163	0	0	0
REACTOME_CYTOSOLIC_TRNA_AMINOACYLATION	2.0225718	0	0	0
REACTOME_MITOCHONDRIAL_PROTEIN_IMPORT	2.0196936	0	0	0
REACTOME_DNA_DOUBLE_STRAND_BREAK_REPAIR	2.0174983	0	0	0
REACTOME_METABOLISM_OF_NON_CODING_RNA	2.0172477	0	0	0
VANTVEER_BREAST_CANCER_METASTASIS_DN	2.0157063	0	0	0
PETROVA_ENDOTHELIUM_LYMPHATIC_VS_BLOOD_UP	2.0153422	0	0	0
REACTOME_DEGRADATION_OF_DVL	2.0147104	0	0	0
RAHMAN_TP53_TARGETS_PHOSPHORYLATED	2.0144978	0	0	0
WHITFIELD_CELL_CYCLE_G2	2.0129697	0	0	0
REACTOME_TRNA_PROCESSING_IN_THE_NUCLEUS	2.0120451	0	0	0
REACTOME_THE_ROLE_OF_GTSE1_IN_G2_M_PROGRESSION_AFTER_G2_CHECKPOINT	2.011895	0	0	0
LY_AGING_PREMATURE_DN	2.0111415	0	0	0
ZHANG_BREAST_CANCER_PROGENITORS_UP	2.010389	0	0	0
MORI_MATURE_B_LYMPHOCYTE_DN	2.0079799	0	0	0
XU_HGF_SIGNALING_NOT_VIA_AKT1_48HR_DN	2.0062904	0	0	0
REACTOME_CYCLIN_A:CDK2_ASSOCIATED_EVENTS_AT_S_PHASE_ENTRY	2.0061798	0	0	0
REACTOME_MITOTIC_G2_G2_M_PHASES	2.0029516	0	0	0
REACTOME_TRANSLATION	1.9989636	0	0	0

SHEPARD_CRUSH_AND_BURN_MUTANT_DN	1.9927734	0	3.50E-06	0.001
REACTOME_PCNA_DEPENDENT_LONG_PATCH_BASE_EXCISION_REPAIR	1.992499	0	3.48E-06	0.001
GARCIA_TARGETS_OF_FLI1_AND_DAX1_DN	1.989329	0	3.46E-06	0.001
OUELLET_OVARIAN_CANCER_INVASIVE_VS_LMP_UP	1.9888312	0	3.45E-06	0.001
MORI_EMU_MYC_LYMPHOMA_BY_ONSET_TIME_UP	1.9886312	0	3.43E-06	0.001
WAKASUGI_HAVE_ZNF143_BINDING_SITES	1.9876219	0	3.41E-06	0.001
REACTOME_STABILIZATION_OF_P53	1.9841857	0	6.82E-06	0.002
KAUFFMANN_DNA_REPAIR_GENES	1.982272	0	1.02E-05	0.003
REACTOME_RESOLUTION_OF_ABASIC_SITES_AP_SITES	1.9822711	0	1.02E-05	0.003
PID_FOXM1_PATHWAY	1.9805388	0	1.01E-05	0.003
REACTOME_G1_S_DNA_DAMAGE_CHECKPOINTS	1.9795591	0	1.01E-05	0.003
REACTOME_G2_M_DNA_DAMAGE_CHECKPOINT	1.9790661	0	1.00E-05	0.003
KEGG_HOMOLOGOUS_RECOMBINATION	1.9754503	0	9.98E-06	0.003
KEGG_MISMATCH_REPAIR	1.9724494	0	1.33E-05	0.004
MALONEY_RESPONSE_TO_17AAG_DN	1.9690928	0	1.65E-05	0.005
REACTOME_RESOLUTION_OF_AP_SITES_VIA_THE_MULTIPLE_NUCLEOTIDE_PATCH_REPLACEMENT_PATHWAY	1.968144	0	1.64E-05	0.005
REACTOME_RUNX1_REGULATES_TRANSCRIPTION_OF_GENES_INVOLVED_IN_DIFFERENTIATION_OF_HSCS	1.9679836	0	1.64E-05	0.005
STEIN_ESRRA_TARGETS_RESPONSIVE_TO_ESTROGEN_DN	1.9659294	0	1.63E-05	0.005

REACTOME_DNA_DAMAGE_BYPASS	1.9643656	0	1.62E-05	0.005
REACTOME_E2F_MEDIATED_REGULATION_OF_DNA_REPLICATION	1.9642984	0	1.61E-05	0.005
DANG_REGULATED_BY_MYC_UP	1.963527	0	1.93E-05	0.006
REACTOME_ASYMMETRIC_LOCALIZATION_OF_PCP_PROTEINS	1.9633052	0	1.92E-05	0.006
LEE_LIVER_CANCER_SURVIVAL_DN	1.9628794	0	1.91E-05	0.006
SU_TESTIS	1.9605289	0	1.90E-05	0.006
ZAMORA_NOS2_TARGETS_UP	1.9603077	0	1.89E-05	0.006
REACTOME_PROCESSING_OF_DNA_DOUBLE_STRAND_BREAK_ENDS	1.9598241	0	1.88E-05	0.006
KEGG_HUNTINGTONS_DISEASE	1.9581851	0	1.88E-05	0.006
BHATI_G2M_ARREST_BY_2METHOXYESTRADIOL_UP	1.9559795	0	1.87E-05	0.006
REACTOME_MEIOTIC_RECOMBINATION	1.9545407	0	1.86E-05	0.006
SCHLOSSER_MYC_TARGETS_REPRESSED_BY_SERUM	1.9540824	0	1.85E-05	0.006
REACTOME_DNA_REPAIR	1.9519141	0	2.15E-05	0.007
REACTOME_CRISTAE_FORMATION	1.9514234	0	2.14E-05	0.007
SENGUPTA_NASOPHARYNGEAL_CARCINOMA_UP	1.9508607	0	2.13E-05	0.007
PEART_HDAC_PROLIFERATION_CLUSTER_DN	1.9497911	0	2.13E-05	0.007
REACTOME_ABC_FAMILY_PROTEINS_MEDIATED_TRANSPORT	1.948837	0	2.12E-05	0.007
REACTOME_G1_S_SPECIFIC_TRANSCRIPTION	1.9463863	0	2.41E-05	0.008
WEST_ADRENOCORTICAL_TUMOR_MARKERS_UP	1.9460038	0	2.40E-05	0.008

WANG_CISPLATIN_RESPONSE_AND_XPC_UP	1.9445832	0	2.39E-05	0.008
REACTOME_BASE_EXCISION_REPAIR	1.9441931	0	2.38E-05	0.008
HU_GENOTOXIC_DAMAGE_4HR	1.9432565	0	2.37E-05	0.008
YAO_TEMPORAL_RESPONSE_TO_PROGESTERONE_CLUSTER_11	1.9420053	0	2.36E-05	0.008
REACTOME_TRNA_AMINOACYLATION	1.9416152	0	2.35E-05	0.008
SCHLOSSER_MYC_TARGETS_AND_SERUM_RESPONSE_UP	1.940687	0	2.63E-05	0.009
REACTOME_METABOLISM_OF_NUCLEOTIDES	1.9329923	0	3.20E-05	0.011
GRAHAM_CML_QUIESCENT_VS_NORMAL_QUIESCENT_UP	1.9304248	0	4.06E-05	0.014
REACTOME_NUCLEOSOME_ASSEMBLY	1.9304224	0	4.04E-05	0.014
REACTOME_HIV_INFECTION	1.930257	0	4.03E-05	0.014
EPPERT_PROGENITOR	1.9297442	0	4.01E-05	0.014
BIOCARTA_ATRBRCA_PATHWAY	1.9262701	0	4.28E-05	0.015
YAO_TEMPORAL_RESPONSE_TO_PROGESTERONE_CLUSTER_10	1.9256686	0	4.26E-05	0.015
DUTERTRE_ESTRADIOL_RESPONSE_6HR_UP	1.9233431	0	4.25E-05	0.015
MOREAUX_MULTIPLE_MYELOMA_BY_TACI_DN	1.9212053	0	4.23E-05	0.015
PUJANA_BREAST_CANCER_LIT_INT_NETWORK	1.9208108	0	4.21E-05	0.015
SCHLOSSER_MYC_TARGETS_AND_SERUM_RESPONSE_DN	1.9177356	0	5.03E-05	0.018
GAL_LEUKEMIC_STEM_CELL_DN	1.9157475	0	5.85E-05	0.021
TOYOTA_TARGETS_OF_MIR34B_AND_MIR34C	1.914847	0	5.83E-05	0.021
WEST_ADRENOCORTICAL_TUMOR_UP	1.914315	0	5.80E-05	0.021
YU_BAP1_TARGETS	1.9132067	0	5.78E-05	0.021

REACTOME_RRNA_MODIFICATION_IN_THE_NUCLEUS_AND_CYTOSOL	1.9127208	0	5.76E-05	0.021
SIMBULAN_PARP1_TARGETS_DN	1.9117819	0	6.01E-05	0.022
ALCALAY_AML_BY_NPM1_LOCALIZATION_DN	1.9116814	0	5.99E-05	0.022
RIZ_ERYTHROID_DIFFERENTIATION	1.9111326	0	6.24E-05	0.023
DELPUECH_FOXO3_TARGETS_DN	1.9109129	0	6.21E-05	0.023
BENPORATH_ES_1	1.9102188	0	6.46E-05	0.024
SERVITJA_LIVER_HNF1A_TARGETS_UP	1.9083782	0	6.97E-05	0.026
ZHAN_MULTIPLE_MYELOMA_SUBGROUPS	1.9052405	0	6.94E-05	0.026
REACTOME_SUMOYLATION_OF_DNA_REPLICATION_PROTEINS	1.9031572	0	6.92E-05	0.026
REACTOME_DISORDERS_OF_TRANSMEMBRANE_TRANSPORTERS	1.8961599	0	9.54E-05	0.035
BHATTACHARYA_EMBRYONIC_STEM_CELL	1.8948563	0	9.51E-05	0.035
KEGG_PURINE_METABOLISM	1.8935556	0	1.03E-04	0.038
REACTOME_REGULATION_OF_RUNX3_EXPRESSION_AND_ACTIVITY	1.8927408	0	1.02E-04	0.038
WELCSH_BRCA1_TARGETS_DN	1.8906317	0	1.02E-04	0.038
WHITFIELD_CELL_CYCLE_G2_M	1.8899623	0	1.04E-04	0.039
KEGG_AMINOACYL_TRNA_BIOSYNTHESIS	1.8896333	0	1.04E-04	0.039
REACTOME_TRANSLESION_SYNTHESIS_BY_POLH	1.8884012	0	1.06E-04	0.04
REACTOME_REGULATION_OF_RAS_BY_GAPS	1.8879648	0	1.13E-04	0.043
JAEGER_METASTASIS_UP	1.8863615	0	1.13E-04	0.043

FERRANDO_HOX11_NEIGHBORS	1.885387	0	1.18E-04	0.045
REACTOME_INTERACTIONS_OF_REV_WITH_HOST_CELLULAR_PROTEINS	1.8787117	0	1.30E-04	0.049
REACTOME_G0_AND_EARLY_G1	1.8782036	0	1.29E-04	0.049
WHITFIELD_CELL_CYCLE_G1_S	1.8760438	0	1.44E-04	0.055
PETROVA_PROX1_TARGETS_UP	1.8744011	0	1.51E-04	0.058
LI_DCP2_BOUND_MRNA	1.8738283	0	1.56E-04	0.06
REACTOME_DEGRADATION_OF_AXIN	1.8737947	0	1.55E-04	0.06
REACTOME_POLO_LIKE_KINASE_MEDIATED_EVENTS	1.8731534	0	1.55E-04	0.06
REACTOME_REGULATION_OF_RUNX2_EXPRESSION_AND_ACTIVITY	1.8720307	0	1.57E-04	0.061
RAMASWAMY_METASTASIS_UP	1.8700333	0	1.78E-04	0.069
WINTER_HYPOXIA_UP	1.8670652	0	1.88E-04	0.073
FISCHER_G1_S_CELL_CYCLE	1.8667562	0	1.87E-04	0.073
ABRAMSON_INTERACT_WITH_AIRE	1.8659915	0	1.91E-04	0.074
REACTOME_REGULATION_OF_PTEN_STABILITY_AND_ACTIVITY	1.8607743	0	2.27E-04	0.087
REACTOME_DECTIN_1_MEDIATED_NONCANONICAL_NF_KB_SIGNALING	1.8586942	0	2.39E-04	0.091
BIDUS_METASTASIS_UP	1.8583413	0	2.40E-04	0.092
REACTOME_TRANSPORT_OF_MATURE_TRANSCRIPT_TO_CYTOPLASM	1.8577825	0	2.44E-04	0.094

REACTOME_TRANSCRIPTIONAL_REGULATION_BY_SMALL_RNAS	1.8577371	0	2.44E-04	0.094
SCIBETTA_KDM5B_TARGETS_DN	1.8573059	0	2.50E-04	0.097
KEGG_NUCLEOTIDE_EXCISION_REPAIR	1.8550637	0	2.54E-04	0.099
MARKEY_RB1_CHRONIC_LOF_UP	1.8537003	0	2.55E-04	0.1
SASAKI_ADULT_T_CELL_LEUKEMIA	1.8532574	0	2.57E-04	0.101
REACTOME_HEDGEHOG_ON_STATE	1.8529412	0	2.56E-04	0.101
REACTOME_NUCLEAR_PORE_COMPLEX_NPC_DISASSEMBLY	1.851537	0	2.70E-04	0.107
REACTOME_GAP_FILLING_DNA_REPAIR_SYNTHESIS_AND_LIGATION_IN_GG_NER	1.8508662	0	2.73E-04	0.109
REACTOME_GLUCOSE_METABOLISM	1.848348	0	2.96E-04	0.118
REACTOME_GLYCOLYSIS	1.844183	0	3.28E-04	0.13
IRITANI_MAD1_TARGETS_DN	1.8410518	0	3.57E-04	0.143
REACTOME_VIRAL_MESSENGER_RNA_SYNTHESIS	1.8407444	0	3.58E-04	0.144
LINDGREN_BLADDER_CANCER_CLUSTER_1_DN	1.8399115	0	3.59E-04	0.145
REACTOME_REGULATION_OF_TP53_ACTIVITY_THROUGH_PHOSPHORYLATION	1.8392131	0	3.63E-04	0.147
CAIRO_PML_TARGETS_BOUND_BY_MYC_UP	1.8387479	0	3.61E-04	0.147
STEIN_ESRRA_TARGETS_UP	1.8386195	0	3.60E-04	0.147
REACTOME_INTERCONVERSION_OF_NUCLEOTIDE_DI_AND_TRIPHOSPHATES	1.8371661	0.001269036	3.66E-04	0.15
MOOTHA_PGC	1.8332326	0	3.97E-04	0.164

KARAKAS_TGFB1_SIGNALING	1.8317298	0	4.09E-04	0.168
REACTOME_PYRUVATE_METABOLISM_AND_CITRIC_ACID_TCA_CYCLE	1.8296903	0	4.31E-04	0.175
GROSS_HYPOXIA_VIA_HIF1A_UP	1.8295425	0	4.29E-04	0.175
APPIERTO_RESPONSE_TO_FENRETINIDE_DN	1.829138	0	4.35E-04	0.177
PID_MYC_ACTIV_PATHWAY	1.8265599	0	4.54E-04	0.184
REACTOME_TRANSCRIPTION_COUPLED_NUCLEOTIDE_EXCISION_REPAIR_TC_NER	1.8250072	0	4.70E-04	0.19
JOHANSSON_GLIOMAGENESIS_BY_PDGFB_UP	1.8241004	0	4.80E-04	0.194
REACTOME_PCP_CE_PATHWAY	1.8177099	0	5.36E-04	0.215
MOOTHA_FFA_OXYDATION	1.81692	0	5.43E-04	0.219
XU_RESPONSE_TO_TRETINOIN_AND_NSC682994_DN	1.8160775	0	5.44E-04	0.22
IVANOVA_HEMATOPOIESIS_INTERMEDIATE_PROGENITOR	1.8122308	0	5.80E-04	0.232
KEGG_ONE_CARBON_POOL_BY_FOLATE	1.8112503	0	5.89E-04	0.236
SANSOM_APC_TARGETS_REQUIRE_MYC	1.809142	0	6.11E-04	0.244
REACTOME_CITRIC_ACID_CYCLE_TCA_CYCLE	1.8090429	0	6.09E-04	0.244
ZHONG_SECRETOME_OF_LUNG_CANCER_AND_FIBROBLAST	1.8087606	0	6.16E-04	0.247
BENPORATH_ES_2	1.8071458	0	6.43E-04	0.259
REACTOME_MRNA_CAPPING	1.8059963	0	6.58E-04	0.263
REACTOME_TRANSLESION_SYNTHESIS_BY_Y_FAMILY_DNA_POLYMERASES_BYPASSES_LESIONS_ON_DNA_TEMPLATE	1.8041166	0	6.80E-04	0.271

REACTOME_PROCESSING_OF_CAPPED_INTRON_CONTAINING_PRE_MRNA	1.8021319	0	7.14E-04	0.28
REACTOME_FATTY_ACYL_COA_BIOSYNTHESIS	1.8016361	0	7.16E-04	0.282
REACTOME_TRANSPORT_OF_THE_SLBP_DEPENDANT_MATURE_MRNA	1.8014843	0	7.14E-04	0.282
CAFFAREL_RESPONSE_TO_THC_24HR_5_DN	1.799474	0	7.38E-04	0.293
PELLICCIOTTA_HDAC_IN_ANTIGEN_PRESENTATION_DN	1.7991705	0	7.42E-04	0.295
GOLDRATH_HOMEOSTATIC_PROLIFERATION	1.79917	0	7.40E-04	0.295
CHEN_ETV5_TARGETS_TESTIS	1.7987163	0	7.48E-04	0.3
REACTOME_TRANSPORT_OF_MATURE_MRNAS_DERIVED_FROM_INTRONLESS_TRANSCRIPTS	1.7986495	0	7.46E-04	0.3
REACTOME_DUAL_INCISION_IN_GG_NER	1.7976185	0	7.62E-04	0.305
KEGG_OOCYTE_MEIOSIS	1.7973859	0	7.62E-04	0.306
REACTOME_CELLULAR_RESPONSE_TO_HYPOXIA	1.7971706	0	7.62E-04	0.307
REACTOME_GENE_SILENCING_BY_RNA	1.796867	0	7.64E-04	0.308
BURTON_ADIPOGENESIS_4	1.7963766	0	7.70E-04	0.312
IVANOVA_HEMATOPOIESIS_EARLY_PROGENITOR	1.7935168	0	8.26E-04	0.331
CAFFAREL_RESPONSE_TO_THC_DN	1.7933944	0	8.26E-04	0.332
REACTOME_TERMINATION_OF_TRANSLESION_DNA_SYNTHESIS	1.7930204	0.001264223	8.31E-04	0.334
REACTOME_SIGNALING_BY_NOTCH4	1.7923808	0	8.39E-04	0.337
REACTOME_GLOBAL_GENOME_NUCLEOTIDE_EXCISION_REPAIR	1.7921991	0	8.37E-04	0.337

_GG_NER				
REACTOME_NUCLEAR_IMPORT_OF_REV_PROTEIN	1.7914424	0	8.43E-04	0.339
PELLICCIOTTA_HDAC_IN_ANTIGEN_PRESENTATION_UP	1.790667	0.001146789	8.46E-04	0.341
WILCOX_RESPONSE_TO_PROGESTERONE_UP	1.7889124	0	8.91E-04	0.354
REACTOME_RHO_GTPASE_EFFECTORS	1.7873037	0	9.37E-04	0.372
REACTOME_TRANSLESION_SYNTHESIS_BY_POLK	1.7871504	0.002710027	9.36E-04	0.373
KEGG_ALZHEIMERS_DISEASE	1.783252	0	0.001012174	0.396
SUNG_METASTASIS_STROMA_DN	1.7787333	0	0.001091565	0.423
HONMA_DOCETAXEL_RESISTANCE	1.7753417	0	0.00115254	0.445
REACTOME_TRNA_MODIFICATION_IN_THE_NUCLEUS_AND_CYTOSOL	1.7745025	0	0.001157338	0.447
BURTON_ADIPOGENESIS_5	1.7728347	0	0.001191942	0.457
REACTOME_DETOXIFICATION_OF_REACTIVE_OXYGEN_SPECIES	1.772416	0	0.001194601	0.459
LASTOWSKA_NEUROBLASTOMA_COPY_NUMBER_UP	1.7705523	0	0.001232851	0.473
ZHONG_RESPONSE_TO_AZACITIDINE_AND_TSA_DN	1.768709	0	0.001261043	0.48
REACTOME_INTERACTIONS_OF_VPR_WITH_HOST_CELLULAR_PROTEINS	1.7683905	0	0.001261534	0.481
KIM_ALL_DISORDERS_DURATION_CORR_DN	1.7680881	0	0.001261994	0.483
HU_ANGIOGENESIS_DN	1.7668574	0	0.001291815	0.493
COLLER_MYC_TARGETS_UP	1.7665943	0	0.001288314	0.493
OLSSON_E2F3_TARGETS_DN	1.7658992	0	0.001302288	0.497

WONG_PROTEASOME_GENE_MODULE	1.7658522	0	0.001300736	0.498
GAZDA_DIAMOND_BLACKFAN_ANEMIA_PROGENITOR_DN	1.7634546	0	0.001355452	0.514
KEGG_CITRATE_CYCLE_TCA_CYCLE	1.762482	0	0.001367297	0.518
REACTOME_MEIOSIS	1.7619784	0	0.001369384	0.52
VANTVEER_BREAST_CANCER_POOR_PROGNOSIS	1.7603105	0	0.001406085	0.53
PRAMOONJAGO_SOX4_TARGETS_DN	1.758051	0	0.001476992	0.548
REACTOME_HEDGEHOG_OFF_STATE	1.7552583	0	0.001526551	0.564
BASSO_B_LYMPHOCYTE_NETWORK	1.7550131	0	0.001535813	0.567
KEGG_VALINE_LEUCINE_AND_ISOLEUCINE_DEGRADATION	1.7549738	0.001179245	0.001531761	0.567
BIOCARTA_MCM_PATHWAY	1.7541112	0	0.001556082	0.572
CAFFAREL_RESPONSE_TO_THC_24HR_5_UP	1.7517487	0	0.001625674	0.589
REACTOME_FORMATION_OF_THE_EARLY_ELONGATION_COMPLEX	1.7514207	0	0.001625148	0.59
REACTOME_UCH_PROTEINASES	1.7504739	0	0.001654756	0.598
ZHONG_SECRETOME_OF_LUNG_CANCER_AND_ENDOTHELIUM	1.7496305	0	0.001674834	0.602
REACTOME_TRANSCRIPTIONAL_REGULATION_BY_RUNX2	1.7495075	0	0.001672359	0.602
LEE_METASTASIS_AND_RNA_PROCESSING_UP	1.7482011	0	0.001703458	0.607
REACTOME_MITOCHONDRIAL_FATTY_ACID_BETA_OXIDATION	1.7471498	0	0.001738089	0.614
REACTOME_CONDENSATION_OF_PROPHASE_CHROMOSOMES	1.7469615	0	0.001744728	0.616
REACTOME_SUMOYLATION_OF_SUMOYLATION_PROTEINS	1.7463013	0	0.001768079	0.623
DAIRKEE_CANCER_PRONE_RESPONSE_BPA	1.74358	0	0.001855688	0.644

WHITFIELD_CELL_CYCLE_S	1.7430316	0	0.001871198	0.647
REACTOME_MITOTIC_PROPHASE	1.7425604	0	0.001886704	0.656
REACTOME_NUCLEOBASE_BIOSYNTHESIS	1.7423974	0.001342282	0.001892873	0.657
YAO_TEMPORAL_RESPONSE_TO_PROGESTERONE_CLUSTER_15	1.7414372	0	0.001922753	0.664
REACTOME_EXPORT_OF_VIRAL_RIBONUCLEOPROTEINS_FROM_NUCLEUS	1.7405778	0	0.001948881	0.674
REACTOME_HIV_LIFE_CYCLE	1.7401948	0	0.001960323	0.677
KEGG_SPLICEOSOME	1.7400458	0	0.001957182	0.678
REACTOME_DEFECTIVE_TPR_MAY_CONFER_SUSCEPTIBILITY_TOWARDS_THYROID_PAPILLARY_CARCINOMA_TPC	1.7365003	0	0.00208795	0.702
PID_E2F_PATHWAY	1.7353499	0	0.002122314	0.709
REACTOME_NUCLEOTIDE_EXCISION_REPAIR	1.7333847	0	0.002194519	0.719
KEGG_BASE_EXCISION_REPAIR	1.732458	0.002525253	0.002233991	0.725
HONRADO_BREAST_CANCER_BRCA1_VS_BRCA2	1.731011	0.002638523	0.00226426	0.733
PYEON_HPV_POSITIVE_TUMORS_UP	1.7308666	0	0.002264003	0.734
REACTOME_PIWI_INTERACTING_RNA_PIRNA_BIOGENESIS	1.7300875	0.00127551	0.002290485	0.74
SESTO_RESPONSE_TO_UV_C7	1.7290072	0	0.002341552	0.751
NATSUME_RESPONSE_TO_INTERFERON_BETA_DN	1.7279782	0	0.002387191	0.758
WANG_METASTASIS_OF_BREAST_CANCER_ESR1_UP	1.727479	0	0.002409626	0.762
TSENG_IRS1_TARGETS_UP	1.726736	0	0.002431973	0.765
ALONSO_METASTASIS_UP	1.7266886	0	0.002431335	0.766

REACTOME_DEGRADATION_OF_BETA_CATENIN_BY_THE_DESTRUCTION_COMPLEX	1.7265117	0	0.002428901	0.766
REACTOME_HOST_INTERACTIONS_WITH_INFLUENZA_FACTORS	1.7261477	0.001197605	0.002435254	0.767
JIANG_AGING_HYPOTHALAMUS_UP	1.7221211	0	0.002607612	0.791
REACTOME_METABOLISM_OF_FOLATE_AND_PTERINES	1.7219675	0.001360544	0.002616969	0.794
REACTOME_RNA_POLYMERASE_I_PROMOTER_ESCAPE	1.7216433	0	0.002631517	0.795
IWANAGA_E2F1_TARGETS_INDUCED_BY_SERUM	1.7205436	0	0.002696379	0.805
JAIN_NFKB_SIGNALING	1.7183406	0	0.002788686	0.814
GARY_CD5_TARGETS_DN	1.7178177	0	0.002816546	0.82
YAMAZAKI_TCEB3_TARGETS_DN	1.7174141	0	0.002832217	0.824
KEGG_AMINO_SUGAR_AND_NUCLEOTIDE_SUGAR_METABOLISM	1.7170846	0	0.002849459	0.826
REACTOME_ANTIGEN_PROCESSING_CROSS_PRESENTATION	1.7161047	0	0.002900976	0.828
BIOCARTA_G2_PATHWAY	1.7142457	0.00618047	0.002990024	0.836
KIM_MYC_AMPLIFICATION_TARGETS_UP	1.7139647	0	0.002994881	0.836
LI_WILMS_TUMOR_VS_FETAL_KIDNEY_2_UP	1.7137778	0.001259446	0.002992922	0.836
WILLIAMS_ESR1_TARGETS_UP	1.7130488	0	0.00302315	0.84
REACTOME_NUCLEAR_ENVELOPE_BREAKDOWN	1.7125559	0	0.003039774	0.841
REACTOME_DUAL_INCISION_IN_TC_NER	1.7122916	0	0.003042824	0.842
DORMOY_ELAVL1_TARGETS	1.7100211	0	0.003174007	0.852
TONKS_TARGETS_OF_RUNX1_RUNX1T1_FUSION_MONOCYTE_UP	1.7072334	0	0.003323066	0.863
REACTOME_INHIBITION_OF_THE_PROTEOLYTIC_ACTIVITY_OF_	1.7071499	0.002631579	0.003327022	0.865

APC_C_REQUIRED_FOR_THE_ONSET_OF_ANAPHASE_BY_MITOTIC_SPINDLE_CHECKPOINT_COMPONENTS				
XU_HGF_TARGETS_INDUCED_BY_AKT1_48HR_DN	1.7051865	0	0.003443227	0.877
BROWN_MYELOID_CELL_DEVELOPMENT_DN	1.7050356	0	0.003436925	0.878
REACTOME_TRISTETRAPROLIN_TTP_ZFP36_BINDS_AND_DESTABILIZES_MRNA	1.7017415	0.001377411	0.003628891	0.894
REACTOME_MAPK6_MAPK4_SIGNALING	1.7004294	0	0.003705452	0.899
REACTOME_BIOSYNTHESIS_OF_THE_N_GLYCAN_PRECURSOR_DOLICHOL_LIPID_LINKED_OLIGOSACCHARIDE_LLO_AND_TRANSFER_TO_A_NASCENT_PROTEIN	1.7002939	0	0.003703542	0.899
BORCZUK_MALIGNANT_MESOTHELIOMA_UP	1.699822	0	0.003716538	0.9
MOOTHA_TCA	1.6995132	0.003968254	0.003722859	0.901
REACTOME_RNA_POLYMERASE_II_TRANSCRIPTION_ELONGATION	1.6962006	0	0.003900577	0.91
REACTOME_ABORTIVE_ELONGATION_OF_HIV_1_TRANSCRIPT_IN_THE_ABSENCE_OF_TAT	1.6930425	0.001262626	0.004100254	0.918
PID_ATM_PATHWAY	1.6916867	0.00122399	0.004179402	0.923
KEGG_RNA_POLYMERASE	1.6902215	0.001290323	0.004274617	0.926
STEIN_ESRRA_TARGETS	1.6901202	0	0.004281232	0.926
REACTOME_DNA_METHYLATION	1.6893035	0.002512563	0.004335039	0.928
REACTOME_MRNA_SPLICING	1.6887845	0	0.004357809	0.93

KEGG_RNA_DEGRADATION	1.6865749	0.001180638	0.004502048	0.935
REACTOME_FORMATION_OF_HIV_ELONGATION_COMPLEX_IN_THE_ABSENCE_OF_HIV_TAT	1.6864723	0.00120919	0.004503265	0.935
LE_NEURONAL_DIFFERENTIATION_DN	1.6855619	0	0.004549677	0.937
MEINHOLD_OVARIAN_CANCER_LOW_GRADE_DN	1.6838309	0	0.004673321	0.943
THILLAINADESAN_ZNF217_TARGETS_UP	1.6813697	0	0.004839555	0.949
DAIRKEE_CANCER_PRONE_RESPONSE_BPA_E2	1.6797855	0.001086957	0.004968314	0.953
REACTOME_REGULATION_OF_HSF1_MEDIATED_HEAT_SHOCK_RESPONSE	1.6787193	0	0.005037208	0.956
SLEBOS_HEAD_AND_NECK_CANCER_WITH_HPV_UP	1.6784077	0	0.00504042	0.956
WANG_TUMOR_INVASIVENESS_UP	1.6782765	0	0.00503882	0.956
REACTOME_FORMATION_OF_ATP_BY_CHEMIOSMOTIC_COUPLING	1.6780392	0.008275862	0.005046797	0.956
KEGG_PROPANOATE_METABOLISM	1.6741171	0.001256281	0.005345253	0.962
REACTOME_TRANSCRIPTION_OF_E2F_TARGETS_UNDER_NEGATIVE_CONTROL_BY_DREAM_COMPLEX	1.6739978	0.001335114	0.005346125	0.962
KOINUMA_COLON_CANCER_MSI_UP	1.6735444	0.002781641	0.005380265	0.963
REACTOME_PROTEIN_LOCALIZATION	1.6732125	0	0.005403169	0.964
REACTOME_MRNA_SPLICING_MINOR_PATHWAY	1.6728883	0	0.005429057	0.964
NIKOLSKY_BREAST_CANCER_17Q21_Q25_AMPLICON	1.6714519	0	0.005564729	0.967
CHIARETTI_T_ALL_RELAPSE_PROGNOSIS	1.6704284	0.002684564	0.005638848	0.967

KIM_WT1_TARGETS_DN	1.6702172	0	0.005650078	0.968
REACTOME_RNA_POLYMERASE_II_PRE_TRANSCRIPTION_EVENTS	1.6688117	0.001096491	0.00578748	0.972
POOLA_INVASIVE_BREAST_CANCER_UP	1.6678268	0	0.005890077	0.976
REACTOME_PHOSPHORYLATION_OF_THE_APC_C	1.6673868	0.00136612	0.005910033	0.976
MOHANKUMAR_HOXA1_TARGETS_UP	1.6673075	0	0.005908182	0.976
BURTON_ADIPOGENESIS_6	1.665879	0	0.006036137	0.981
WANG_TARGETS_OF_MLL_CBP_FUSION_DN	1.6657581	0.001191895	0.006030902	0.981
UDAYAKUMAR_MED1_TARGETS_UP	1.6650679	0	0.006079555	0.982
MAYBURD_RESPONSE_TO_L663536_DN	1.6647465	0.001172333	0.006091176	0.982
REACTOME_MITOCHONDRIAL_CALCIUM_ION_TRANSPORT	1.6645195	0.005298013	0.006104277	0.983
HERNANDEZ_MITOTIC_ARREST_BY_DOCETAXEL_1_DN	1.662559	0	0.006282254	0.987
BOYAULT_LIVER_CANCER_SUBCLASS_G123_UP	1.6622444	0	0.006307124	0.987
REACTOME_MRNA_DECAY_BY_3_TO_5_EXORIBONUCLEASE	1.6618111	0.002721089	0.006356171	0.987
BOHN_PRIMARY_IMMUNODEFICIENCY_SYNDROM_UP	1.659806	0.001213592	0.006566134	0.988
KEGG_TYROSINE_METABOLISM	1.6585902	0	0.00666916	0.988
REACTOME_PURINE_CATABOLISM	1.6582942	0.004043127	0.006680849	0.989
GROSS_HYPOXIA_VIA_ELK3_UP	1.6577892	0	0.006721241	0.989
GEORGES_CELL_CYCLE_MIR192_TARGETS	1.6571968	0.002314815	0.006767428	0.99
REACTOME_TP53_REGULATES_TRANSCRIPTION_OF_DNA_REPAIR_GENES	1.6565536	0	0.006834519	0.99

REACTOME_APC_CDC20_MEDIATED_DEGRADATION_OF_NEK2A	1.6558677	0.001349528	0.006884779	0.991
SANA_RESPONSE_TO_IFNG_DN	1.6546974	0	0.00700367	0.991
REACTOME_BUTYRATE_RESPONSE_FACTOR_1_BRF1_BINDS_AND_DESTABILIZES_MRNA	1.6523647	0.00390117	0.007238561	0.992
REACTOME_TNFR2_NON_CANONICAL_NF_KB_PATHWAY	1.6512071	0	0.007350352	0.993
REACTOME_RRNA_PROCESSING	1.6501526	0	0.007463197	0.993
REACTOME_FGFR2_MUTANT_RECEPTOR_ACTIVATION	1.6501518	0.00125	0.007447809	0.993
WALLACE_JAK2_TARGETS_UP	1.649483	0.006451613	0.007513988	0.993
KRASNOSELSKAYA_ILF3_TARGETS_DN	1.6482657	0.002378121	0.007636173	0.993
KENNY_CTNNB1_TARGETS_UP	1.6473545	0	0.007704569	0.993
REACTOME_FGFR2_ALTERNATIVE_SPLICING	1.6451278	0.002522068	0.00791391	0.994
HILLION_HMGA1B_TARGETS	1.6446406	0	0.007968284	0.995
CHEN_HOXA5_TARGETS_9HR_DN	1.6439288	0.003658537	0.008039933	0.997
REACTOME_TRANSCRIPTIONAL_REGULATION_BY_E2F6	1.643252	0.001218027	0.008113001	0.997
CREIGHTON_AKT1_SIGNALING_VIA_MTOR_DN	1.6431553	0.002610966	0.008106785	0.997
REACTOME_CELLULAR_RESPONSE_TO_HEAT_STRESS	1.6424758	0	0.008163318	0.997
REACTOME_CELLULAR_RESPONSES_TO_STRESS	1.6407791	0	0.008347711	0.998
REACTOME_TRANSCRIPTION_OF_THE_HIV_GENOME	1.639478	0.001138952	0.008493439	0.998
ZHONG_SECRETOME_OF_LUNG_CANCER_AND_MACROPHAGE	1.6380944	0.001116072	0.008661673	0.998
COLINA_TARGETS_OF_4EBP1_AND_4EBP2	1.6357806	0	0.008964982	0.998
REACTOME_SIGNALING_BY_FGFR2_IIIA_TM	1.6355006	0.002621232	0.00900194	0.998

AIYAR_COBRA1_TARGETS_DN	1.631163	0.001261034	0.009580088	0.998
TURASHVILI_BREAST_DUCTAL_CARCINOMA_VS_LOBULAR_NORMAL_UP	1.6310252	0	0.009584004	0.998
REACTOME_SUMOYLATION_OF_UBIQUITINYLATION_PROTEINS	1.6307597	0.001201923	0.009606513	0.998
REACTOME_REPRODUCTION	1.630256	0.001075269	0.00965188	0.998
KEGG_PROTEIN_EXPORT	1.629872	0.003861004	0.009698371	0.999
REACTOME_METABOLISM_OF_PORPHYRINS	1.6293149	0.005486968	0.009761862	0.999
PODAR_RESPONSE_TO_ADAPHOSTIN_DN	1.6289097	0.005174644	0.00979817	0.999
CHIARADONNA_NEOPLASTIC_TRANSFORMATION_KRAS_UP	1.6286304	0	0.009824265	0.999
BRACHAT_RESPONSE_TO_CAMPTOTHECIN_DN	1.6277072	0.005966587	0.009933873	0.999
REACTOME_FORMATION_OF_TC_NER_PRE_INCISION_COMPLEX	1.6275657	0.00472255	0.009941277	0.999
REACTOME_SIGNALING_BY_HEDGEHOG	1.6273881	0	0.009945807	0.999
WALLACE_PROSTATE_CANCER_UP	1.62495	0.002610966	0.010320969	0.999
KORKOLA_TERATOMA	1.6238718	0.003554502	0.010459717	0.999
ELVIDGE_HYPOXIA_DN	1.6230105	0	0.010582591	0.999
KEGG_FATTY_ACID_METABOLISM	1.6229651	0.002403846	0.01057317	0.999
REACTOME_CONVERSION_FROM_APC_C:CDC20_TO_APC_C:CDH1_IN_LATE_ANAPHASE	1.6225756	0.001312336	0.010619825	0.999
ONDER_CDH1_TARGETS_1_DN	1.6217937	0	0.010710923	0.999
KEGG_PORPHYRIN_AND_CHLOROPHYLL_METABOLISM	1.6216413	0.006361323	0.01070134	0.999
REACTOME_KINESINS	1.6212567	0.002366864	0.010755773	0.999

SHAFFER_IRF4_TARGETS_IN_ACTIVATED_B_LYMPHOCYTE	1.6203222	0	0.010911337	0.999
BROWNE_HCMV_INFECTION_2HR_DN	1.6176118	0.00591716	0.011344519	0.999
CHAUHAN_RESPONSE_TO_METHOXYESTRADIOL_UP	1.6175896	0.004739337	0.011326888	0.999
REACTOME_FANCONI_ANEMIA_PATHWAY	1.6172138	0.003680982	0.011356189	0.999
LI_LUNG_CANCER	1.615857	0.001221001	0.011579629	0.999
REACTOME_ACTIVATION_OF_NF_KAPPAB_IN_B_CELLS	1.6139255	0.002288329	0.011907897	1
REACTOME_RRNA_PROCESSING_IN_THE_NUCLEUS_AND_CYTOSOL	1.613351	0	0.011993738	1
PID_AURORA_A_PATHWAY	1.6125673	0.002466091	0.012117342	1
JEON_SMAD6_TARGETS_DN	1.6120869	0.006493507	0.012200996	1
REACTOME_AURKA_ACTIVATION_BY_TPX2	1.611715	0	0.01223655	1
BIOCARTA_CELLCYCLE_PATHWAY	1.6113286	0.00656168	0.012270525	1
REACTOME_RNA_POLYMERASE_II_TRANSCRIPTION_PRE_INITIATION_AND_PROMOTER_OPENING	1.6110402	0.001218027	0.012305791	1
REACTOME_KSRP_KHSRP_BINDS_AND_DESTABILIZES_MRNA	1.6105094	0.002881844	0.012370748	1
LU_EZH2_TARGETS_UP	1.6104589	0	0.012357006	1
REACTOME_RNA_POLYMERASE_II_TRANSCRIPTION_TERMINATION	1.6103655	0.001149425	0.012347283	1
SAKAI_TUMOR_INFILTRATING_MONOCYTES_DN	1.6101795	0.001103753	0.012357869	1
RAMALHO_STEMNESS_UP	1.6098001	0	0.01242367	1
REACTOME_GLYOXYLATE_METABOLISM_AND_GLYCINE_DEGRA	1.607401	0.003731343	0.012807185	1

DATION				
YANG_BCL3_TARGETS_UP	1.6039029	0	0.013411818	1
KIM_TIAL1_TARGETS	1.6028342	0.007398274	0.0135916	1
NEMETH_INFLAMMATORY_RESPONSE_LPS_DN	1.5965607	0.005089059	0.014898213	1
TURASHVILI_BREAST_DUCTAL_CARCINOMA_VS_DUCTAL_NORMAL_UP	1.5929332	0.004914005	0.015664198	1
KEGG_PROGESTERONE_MEDIATED_OOCYTE_MATURATION	1.5910952	0	0.016029216	1
KATSANOU_ELAVL1_TARGETS_DN	1.5877529	0	0.016771652	1
REACTOME_METABOLISM_OF_AMINO_ACIDS_AND_DERIVATIVES	1.586917	0	0.016941063	1
SANSOM_APC_TARGETS	1.5858083	0	0.017194675	1
KARLSSON_TGFB1_TARGETS_UP	1.581903	0	0.018147686	1
CHICAS_RB1_TARGETS_SENESCENT	1.578149	0	0.019060453	1
ACOSTA_PROLIFERATION_INDEPENDENT_MYC_TARGETS_UP	1.5779568	0.002227172	0.019073067	1
TAKAO_RESPONSE_TO_UVB_RADIATION_UP	1.5772189	0	0.01922898	1
MULLIGAN_NTF3_SIGNALING_VIA_INSR_AND_IGF1R_UP	1.5771699	0.012804098	0.01920572	1
REACTOME_SYNTHESIS_OF_SUBSTRATES_IN_N_GLYCAN_BIOSYTHESIS	1.5743932	0.001137656	0.019936636	1
REACTOME_SYNTHESIS_OF_VERY_LONG_CHAIN_FATTY_ACYL_COAS	1.5689429	0.006435006	0.02143522	1
BILANGES_RAPAMYCIN_SENSITIVE_VIA_TSC1_AND_TSC2	1.567886	0.001141553	0.021691272	1

REACTOME_FATTY_ACID_METABOLISM	1.5648302	0	0.022572346	1
KAYO_CALORIE_RESTRICTION_MUSCLE_DN	1.5646363	0.003428571	0.022574507	1
BIOCARTA_MPR_PATHWAY	1.5645049	0.010596027	0.022572765	1
TONG_INTERACT_WITH_PTTG1	1.5643901	0.004694836	0.022569776	1
SPIELMAN_LYMPHOBLAST_EUROPEAN_VS_ASIAN_UP	1.5641259	0	0.022618633	1
SMID_BREAST_CANCER_RELAPSE_IN_BRAIN_UP	1.5634288	0.007556675	0.022787213	1
KOKKINAKIS_METHIONINE_DEPRIVATION_96HR_DN	1.5633143	0.002252252	0.022770908	1
REACTOME_SLC_TRANSPORTER_DISORDERS	1.5621676	0.001094092	0.023087395	1
STEIN_ESR1_TARGETS	1.5599678	0.002159827	0.023722198	1
CUI_GLUCOSE_DEPRIVATION	1.5594717	0.003488372	0.023815742	1
REACTOME_GLUCONEOGENESIS	1.559362	0.008782936	0.023808029	1
JACKSON_DNMT1_TARGETS_DN	1.5589828	0.019582245	0.023907544	1
PUIFFE_INVASION_INHIBITED_BY_ASCITES_UP	1.5583682	0.002267574	0.024052596	1
REACTOME_ANTIVIRAL_MECHANISM_BY_IFN_STIMULATED_GENES	1.5582114	0.001122335	0.024055926	1
ELVIDGE_HYPOXIA_BY_DMOG_DN	1.5579777	0.003468208	0.024070635	1
VANTVEER_BREAST_CANCER_ESR1_DN	1.5575016	0	0.024169046	1
CHEN_LUNG_CANCER_SURVIVAL	1.5567504	0.007884363	0.024373425	1
REACTOME_RNA_POLYMERASE_I_TRANSCRIPTION_TERMINATION	1.5547142	0.008905852	0.025035482	1
REACTOME_INFECTIOUS_DISEASE	1.5540743	0	0.025181953	1

JIANG_VHL_TARGETS	1.5509514	0.001098901	0.026202809	1
NIKOLSKY_BREAST_CANCER_16P13_AMPLICON	1.5509222	0	0.026169658	1
LI_AMPLIFIED_IN_LUNG_CANCER	1.5507361	0	0.026179207	1
REACTOME_PRC2_METHYLATES_HISTONES_AND_DNA	1.5501846	0.003663004	0.026331512	1
REACTOME_REGULATION_OF_PLK1_ACTIVITY_AT_G2_M_TRANSITION	1.5493778	0.001101322	0.026574725	1
REACTOME_TRANSCRIPTIONAL_REGULATION_BY_RUNX3	1.5486196	0	0.026783291	1
JIANG_HYPOXIA_CANCER	1.5485997	0.004576659	0.026740713	1
MATTIOLI_MGUS_VS_PCL	1.5458068	0.001082251	0.02767866	1
KEGG_N_GLYCAN_BIOSYNTHESIS	1.5448799	0.003649635	0.02795244	1
PAL_PRMT5_TARGETS_DN	1.5443556	0.007772021	0.02812623	1
REACTOME_MTORC1_MEDIATED_SIGNALLING	1.5442799	0.014248705	0.028107556	1
REACTOME_NEGATIVE_EPIGENETIC_REGULATION_OF_RRNA_EXPRESSION	1.5429674	0.007918553	0.028560769	1
KEGG_PENTOSE_PHOSPHATE_PATHWAY	1.5429273	0.017971758	0.028529083	1
REACTOME_NEDDYLATION	1.5411421	0	0.029125517	1
CHUNG_BLISTER_CYTOTOXICITY_UP	1.5395461	0.001055966	0.029711422	1
REACTOME_ATF4_ACTIVATES_GENES_IN_RESPONSE_TO_ENDOPLASMIC_RETICULUM_STRESS	1.5392908	0.006393862	0.029761402	1
REACTOME_APC_C:CDC20_MEDIATED_DEGRADATION_OF_CYCLIN_B	1.5383754	0.015978696	0.030053822	1

RIGGI_EWING_SARCOMA_PROGENITOR_DN	1.5381949	0	0.03007615	1
REACTOME_TRANSCRIPTIONAL_REGULATION_BY_TP53	1.5369029	0	0.030496307	1
ZHAN_VARIABLE_EARLY_DIFFERENTIATION_GENES_DN	1.5367875	0.017994858	0.030492295	1
REACTOME_HIV_ELONGATION_ARREST_AND_RECOVERY	1.535699	0.006075334	0.030859321	1
BENPORATH_MYC_TARGETS_WITH_EBOX	1.5343515	0	0.031320777	1
PEART_HDAC_PROLIFERATION_CLUSTER_UP	1.5269278	0.004602992	0.03428316	1
REACTOME_BASE_EXCISION_REPAIR_AP_SITE_FORMATION	1.5268358	0.009638554	0.034259435	1
RAY_TUMORIGENESIS_BY_ERBB2_CDC25A_UP	1.526095	0	0.03451974	1
BYSTRYKH_HEMATOPOIESIS_STEM_CELL_QTL_CIS	1.5253506	0.001083424	0.034765773	1
YORDY_RECIPROCAL_REGULATION_BY_ETS1_AND_SP100_UP	1.5243908	0.015768725	0.03511459	1
KAAB_HEART_ATRIUM_VS_VENTRICLE_DN	1.5226369	0	0.03584566	1
REACTOME_REGULATION_OF_TP53_ACTIVITY	1.5223675	0.002053388	0.03591071	1
REACTOME_SUMOYLATION_OF_RNA_BINDING_PROTEINS	1.5220366	0.007151371	0.03601271	1
TOMIDA_METASTASIS_UP	1.5219156	0.01369863	0.0360019	1
REACTOME_CELLULAR_RESPONSES_TO_EXTERNAL_STIMULI	1.5217842	0	0.035988867	1
CREIGHTON_ENDOCRINE_THERAPY_RESISTANCE_1	1.5208768	0	0.036319114	1
THUM_MIR21_TARGETS_HEART_DISEASE_UP	1.519501	0.017832648	0.0368627	1
MATZUK_MEIOTIC_AND_DNA_REPAIR	1.5165398	0.007371008	0.03817441	1
REACTOME_TP53_REGULATES_TRANSCRIPTION_OF_GENES_INVOLVED_IN_G2_CELL_CYCLE_ARREST	1.515321	0.017105263	0.038666695	1
HEIDENBLAD_AMPLICON_8Q24_UP	1.5138958	0.015853658	0.039239258	1

REACTOME_PROGRAMMED_CELL_DEATH	1.5132763	0	0.039476383	1
KAAB_FAILED_HEART_ATRIUM_DN	1.5130935	0.002083333	0.039493024	1
REACTOME_NUCLEOBASE_CATABOLISM	1.5128013	0.015795868	0.03957444	1
KEGG_BUTANOATE_METABOLISM	1.5123893	0.018518519	0.03969572	1
REACTOME_RNA_POLYMERASE_I_TRANSCRIPTION	1.5123636	0.005624297	0.039643932	1
REACTOME_RNA_POLYMERASE_III_CHAIN_ELONGATION	1.5118548	0.018918918	0.03982322	1
FARMER_BREAST_CANCER_CLUSTER_5	1.5118324	0.0198939	0.039765503	1
MODY_HIPPOCAMPUS_PRENATAL	1.5100858	0.013431014	0.040560063	1
NADLER_OBESITY_DN	1.5080761	0.016166281	0.041441925	1
KAYO_AGING_MUSCLE_DN	1.5050995	0.001070664	0.042818416	1
REACTOME_TRANSCRIPTION_OF_E2F_TARGETS_UNDER_NEGATIVE_CONTROL_BY_P107_RBL1_AND_P130_RBL2_IN_COMPLEX_WITH_HDAC1	1.5037423	0.02631579	0.043439083	1
REACTOME_PROCESSING_OF_SMDT1	1.499365	0.027285129	0.04572911	1
MONNIER_POSTRADIATION_TUMOR_ESCAPE_UP	1.499316	0	0.04567744	1
REACTOME_RMTS_METHYLATE_HISTONE_ARGININES	1.4991145	0.015169195	0.045717508	1
REACTOME_RNA_POLYMERASE_III_TRANSCRIPTION_TERMINATION	1.49911	0.023622047	0.04564645	1
IVANOVA_HEMATOPOIESIS_LATE_PROGENITOR	1.4989604	0	0.04564137	1
SANSOM_APC_MYC_TARGETS	1.4958225	0	0.047212224	1
SANSOM_APC_TARGETS_UP	1.4949116	0	0.04759922	1

REACTOME_NONHOMOLOGOUS_END_JOINING_NHEJ	1.4941967	0.014218009	0.047951598	1
LEE_CALORIE_RESTRICTION_NEOCORTEX_DN	1.4930867	0.01010101	0.048508357	1
REACTOME_COOPERATION_OF_PREFOLDIN_AND_TRIC_CCT_IN_ACTIN_AND_TUBULIN_FOLDING	1.4928902	0.016476553	0.04855486	1
REACTOME_DEADENYLATION_DEPENDENT_MRNA_DECAY	1.4924425	0.018244013	0.048739556	1
REACTOME_CENTROSOME_MATURATION	1.4917263	0.006711409	0.04904699	1
LUI_THYROID_CANCER_CLUSTER_3	1.4915998	0.017971758	0.049041122	1
POMEROY_MEDULLOBLASTOMA_PROGNOSIS_DN	1.4911838	0.018359853	0.04919459	1
GARGALOVIC_RESPONSE_TO_OXIDIZED_PHOSPHOLIPIDS_RED_UP	1.4907231	0.020491803	0.049407654	1
BIOCARTA_G1_PATHWAY	1.4860595	0.020330368	0.05200451	1
REACTOME_PREFOLDIN_MEDIATED_TRANSFER_OF_SUBSTRATE_TO_CCT_TRIC	1.4838407	0.026649747	0.05327025	1
REACTOME_SIGNALING_BY_RHO_GTPASES	1.4830707	0	0.05365933	1
WENG_POR_TARGETS_LIVER_UP	1.4830624	0.024600247	0.053583127	1
YEGNASUBRAMANIAN_PROSTATE_CANCER	1.4821281	0.004390779	0.05406813	1
KUNINGER_IGF1_VS_PDGFB_TARGETS_DN	1.4820642	0.01703163	0.054023024	1
KEGG_ALANINE_ASPARTATE_AND_GLUTAMATE_METABOLISM	1.4812955	0.016149068	0.054390207	1
DAIRKEE_CANCER_PRONE_RESPONSE_E2	1.4807607	0.025445292	0.054639716	1
NIKOLSKY_BREAST_CANCER_8Q23_Q24_AMPLICON	1.4806496	0.002105263	0.054633174	1
REACTOME_DNA_DAMAGE_RECOGNITION_IN_GG_NER	1.4798951	0.025094103	0.05501574	1

DITTMER_PTHLH_TARGETS_UP	1.4798329	0.004352557	0.054973997	1
REACTOME_DNA_DAMAGE_TELOMERE_STRESS_INDUCED_SENESCENCE	1.4793931	0.009569378	0.055146422	1
KEGG_GLYOXYLATE_AND_DICARBOXYLATE_METABOLISM	1.4789104	0.02486911	0.055372693	1
REACTOME_TP53_REGULATES_TRANSCRIPTION_OF_CELL_CYCLE_GENES	1.4781762	0.01988304	0.055748474	1
LEE_TARGETS_OF_PTCH1_AND_SUFU_UP	1.478007	0.017814728	0.055752322	1
MACLACHLAN_BRCA1_TARGETS_DN	1.4774582	0.035422344	0.056054283	1
SMIRNOV_RESPONSE_TO_IR_6HR_DN	1.4772017	0.003171247	0.056139637	1
REACTOME_SUMOYLATION_OF_DNA_DAMAGE_RESPONSE_AND_REPAIR_PROTEINS	1.477095	0.015730336	0.056115292	1
ZHAN_MULTIPLE_MYELOMA_CD2_DN	1.4765486	0.020359281	0.056356918	1
KEGG_PEROXISOME	1.4762957	0.011135858	0.05645688	1
ANDERSEN_CHOLANGIOCARCINOMA_CLASS2	1.4748371	0.002076843	0.057296462	1
KEGG_PYRUVATE_METABOLISM	1.4733461	0.026796589	0.058161095	1
STEIN_ESRRA_TARGETS_RESPONSIVE_TO_ESTROGEN_UP	1.4725239	0.02625	0.058595587	1
SESTO_RESPONSE_TO_UV_C6	1.4715475	0.02366127	0.059137993	1
REACTOME_DOWNSTREAM_SIGNALING_EVENTS_OF_B_CELL_RECEPTOR_BCR	1.4713321	0.006637168	0.059188176	1
JIANG_AGING_CEREBRAL_CORTEX_UP	1.4696714	0.022836538	0.060232636	1
REACTOME_PEROXISOMAL_LIPID_METABOLISM	1.4680831	0.025542784	0.0611534	1

REACTOME_SIGNALING_BY_NOTCH	1.466041	0.001027749	0.062424347	1
LIEN_BREAST_CARCINOMA_METAPLASTIC_VS_DUCTAL_UP	1.4647259	0.016574586	0.06323196	1
FARMER_BREAST_CANCER_APOCRINE_VS_BASAL	1.4634118	0	0.06407582	1
REACTOME_FCERI_MEDIATED_NF_KB_ACTIVATION	1.4622335	0.006550218	0.06485651	1
REACTOME_BETA_CATENIN_INDEPENDENT_WNT_SIGNALING	1.4621135	0.003181336	0.0648359	1
YIH_RESPONSE_TO_ARSENITE_C3	1.4620595	0.03787879	0.06476785	1
MARTINEZ_RESPONSE_TO_TRABECTEDIN_DN	1.4615114	0	0.06503308	1
CORRE_MULTIPLE_MYELOMA_DN	1.4602858	0.020023556	0.06583888	1
REACTOME_PERK_REGULATES_GENE_EXPRESSION	1.4580514	0.024660913	0.06733699	1
REACTOME_DISEASES_ASSOCIATED_WITH_N_GLYCOSYLATION_OF_PROTEINS	1.4549925	0.047169812	0.06939353	1
REACTOME_DEPURINATION	1.4546232	0.02117061	0.069584936	1
DEMAGALHAES_AGING_DN	1.4523764	0.058432937	0.07117745	1
HILLION_HMGA1_TARGETS	1.4514371	0.012222222	0.07177065	1
KEGG_TERPENOID_BACKBONE_BIOSYNTHESIS	1.4509395	0.03342246	0.072088905	1
WEBER_METHYLATED_IN_COLON_CANCER	1.4506309	0.038926173	0.07226873	1
ENK_UV_RESPONSE_EPIDERMIS_UP	1.4501469	0	0.072536275	1
PURBEY_TARGETS_OF_CTBP1_AND_SATB1_DN	1.4492091	0.001044932	0.073156886	1
KORKOLA_YOLK_SAC_TUMOR_UP	1.4490993	0.04845222	0.07312341	1
REACTOME_RNA_POLYMERASE_III_TRANSCRIPTION_INITIATION_FROM_TYPE_1_PROMOTER	1.4489716	0.044871796	0.07312609	1

GOLUB_ALL_VS_AML_UP	1.4475582	0.033942558	0.074104965	1
HWANG_PROSTATE_CANCER_MARKERS	1.4472601	0.036082473	0.07422229	1
YANG_BREAST_CANCER_ESR1_LASER_DN	1.4472394	0.028901733	0.074127324	1
REACTOME_STING_MEDIATED_INDUCTION_OF_HOST_IMMUNE_RESPONSES	1.4468303	0.044	0.07435817	1
KEGG_PHENYLALANINE_METABOLISM	1.4463929	0.038873993	0.074575625	1
REACTOME_SUMOYLATION_OF_CHROMATIN_ORGANIZATION_PROTEINS	1.4456564	0.021764033	0.075100906	1
KEGG_GLYCINE_SERINE_AND_THREONINE_METABOLISM	1.4433929	0.027883397	0.07671393	1
WANG_SMARCE1_TARGETS_DN	1.442483	0.001003009	0.07736633	1
REACTOME_INTERLEUKIN_1_SIGNALING	1.4415183	0.010822511	0.07804625	1
RIZ_ERYTHROID_DIFFERENTIATION_HBZ	1.440718	0.030674847	0.07857489	1
REACTOME_COPI_DEPENDENT_GOLGI_TO_ER_RETROGRADE_TRAFFIC	1.4406258	0.010952903	0.07855396	1
GRADE_COLON_VS_RECTAL_CANCER_UP	1.4402617	0.03213844	0.07875673	1
VANTVEER_BREAST_CANCER_BRCA1_UP	1.4402412	0.02997602	0.078653455	1
WU_HBX_TARGETS_2_UP	1.4375743	0.053108808	0.0807579	1
VANHARANTA_UTERINE_FIBROID_WITH_7Q_DELETION_UP	1.436989	0.01918736	0.08110273	1
REACTOME_POSITIVE_EPIGENETIC_REGULATION_OF_RRNA_EXPRESSION	1.4346985	0.011402508	0.082941994	1
KEGG_TRYPTOPHAN_METABOLISM	1.4339991	0.02955665	0.08342525	1

YOKOE_CANCER_TESTIS_ANTIGENS	1.4334464	0.04071247	0.08381859	1
REACTOME_NEURODEGENERATIVE_DISEASES	1.4334413	0.037711315	0.08370383	1
BAKKER_FOXO3_TARGETS_DN	1.4325367	0.003112033	0.084382676	1
REACTOME_MITOCHONDRIAL_TRNA_AMINOACYLATION	1.4324054	0.040843215	0.08438562	1
NAM_FXYD5_TARGETS_DN	1.4322685	0.06675749	0.08439261	1
PYEON_CANCER_HEAD_AND_NECK_VS_CERVICAL_UP	1.4317893	0	0.08467621	1
GAJATE_RESPONSE_TO_TRABECTEDIN_DN	1.4316132	0.044619422	0.0847248	1
MELLMAN_TUT1_TARGETS_UP	1.4310083	0.044619422	0.08514522	1
BENPORATH_ES_CORE_NINE_CORRELATED	1.4308362	0.006622517	0.08516839	1
REACTOME_SENESCENCE_ASSOCIATED_SECRETORY_PHENOTYPE_SASP	1.4300975	0.016018307	0.08568977	1
HOUSTIS_ROS	1.4296106	0.037926674	0.08599578	1
REACTOME_ERCC6_CSB_AND_EHMT2_G9A_POSITIVELY_REGULATE_RRNA_EXPRESSION	1.4293945	0.027577939	0.086050324	1
GOTZMANN_EPITHELIAL_TO_MESENCHYMAL_TRANSITION_DN	1.428526	0.00204918	0.08669499	1
TOOKER_GEMCITABINE_RESISTANCE_DN	1.4279956	0.00955414	0.08702287	1
ZHAN_MULTIPLE_MYELOMA_UP	1.4255408	0.027027028	0.089085616	1
SCHLOSSER_MYC_AND_SERUM_RESPONSE_SYNERGY	1.4254788	0.04136253	0.089004084	1
REACTOME_DNA_DOUBLE_STRAND_BREAK_RESPONSE	1.4253138	0.022196261	0.089027666	1
GUO_HEX_TARGETS_DN	1.4252279	0.01793722	0.08899271	1
REACTOME_TCF_DEPENDENT_SIGNALING_IN_RESPONSE_TO_W	1.4249144	0.001039501	0.08915807	1

NT				
MORI_SMALL_PRE_BII_LYMPHOCYTE_DN	1.4231329	0.022573363	0.090616666	1
VECCHI_GASTRIC_CANCER_ADVANCED_VS_EARLY_DN	1.4222928	0.005399568	0.091263786	1
REACTOME_PYRUVATE_METABOLISM	1.4219459	0.041772153	0.09145034	1
WEIGEL_OXIDATIVE_STRESS_BY_TBH_AND_H2O2	1.4212892	0.04779874	0.09192574	1
MCMURRAY_TP53_HRAS_COOPERATION_RESPONSE_UP	1.4196438	0.04768041	0.09340155	1
REACTOME_GENE_AND_PROTEIN_EXPRESSION_BY_JAK_STAT_SIGNALING_AFTER_INTERLEUKIN_12_STIMULATION	1.4184625	0.04040404	0.094407156	1
RUAN_RESPONSE_TO_TROGLITAZONE_DN	1.417013	0.0665779	0.09566508	1
RIZ_ERYTHROID_DIFFERENTIATION_CCNE1	1.4168986	0.03897686	0.095631436	1
WENG_POR_TARGETS_GLOBAL_UP	1.4164878	0.069986545	0.095885865	1
OUELLET_CULTURED_OVARIAN_CANCER_INVASIVE_VS_LMP_UP	1.4161855	0.032657657	0.09605239	1
TANAKA_METHYLATED_IN_ESOPHAGEAL_CARCINOMA	1.4151005	0.015250545	0.09696175	1
VANOEVELEN_MYOGENESIS_SIN3A_TARGETS	1.4135365	0.001025641	0.098357804	1
REACTOME_DISEASES_ASSOCIATED_WITH_GLYCOSYLATION_PRECURSOR_BIOSYNTHESIS	1.4131423	0.05	0.09860819	1
KANNAN_TP53_TARGETS_DN	1.4127736	0.055181697	0.0988292	1
BYSTRYKH_HEMATOPOIESIS_STEM_CELL_AND_BRAIN_QTL_CIS	1.411825	0.019428572	0.09964092	1
KAMIKUBO_MYELOID_CEBPA_NETWORK	1.4116191	0.050931677	0.099736154	1
KEGG_DRUG_METABOLISM_OTHER_ENZYMES	1.4114912	0.045622688	0.09971122	1
REACTOME_METABOLISM_OF_CARBOHYDRATES	1.4109875	0	0.10007071	1

DAZARD_RESPONSE_TO_UV_SCC_UP	1.410353	0.015267176	0.1005539	1
REACTOME_RNA_POLYMERASE_II_TRANSCRIBES_SNRNA_GENES	1.4098471	0.025669644	0.10096333	1
REACTOME_CLASS_I_PEROXISOMAL_MEMBRANE_PROTEIN_IMPORT	1.4095124	0.04611331	0.10113512	1
NIKOLSKY_BREAST_CANCER_12Q24_AMPLICON	1.4094937	0.055934515	0.10101273	1
WANG_ADIPOGENIC_GENES_REPRESSED_BY_SIRT1	1.4092413	0.042875156	0.10110707	1
TARTE_PLASMA_CELL_VS_B_LYMPHOCYTE_UP	1.408907	0.018202502	0.10131285	1
AGUIRRE_PANCREATIC_CANCER_COPY_NUMBER_UP	1.4087484	0	0.10135311	1
REACTOME_PTEN_REGULATION	1.4084855	0.006256517	0.10146968	1
REACTOME_HSF1_ACTIVATION	1.4083171	0.05216285	0.10150178	1
WEST_ADRENOCORTICAL_CARCINOMA_VS_ADENOMA_UP	1.4063891	0.060959794	0.10339091	1
GUTIERREZ_MULTIPLE_MYELOMA_UP	1.403002	0.05147059	0.10677353	1
LEE_LIVER_CANCER_MYC_UP	1.4026165	0.032902468	0.10702814	1
DACOSTA_UV_RESPONSE_VIA_ERCC3_TTD_UP	1.4020089	0.027939465	0.10754723	1
REACTOME_SULFUR_AMINO_ACID_METABOLISM	1.4012543	0.049555272	0.10817839	1
BURTON_ADIPOGENESIS_12	1.3992344	0.057788946	0.11006532	1
REACTOME_MICRORNA_MIRNA_BIOGENESIS	1.3989497	0.062261753	0.11020456	1
ZWANG_EGF_PERSISTENTLY_UP	1.3988448	0.04534005	0.11015946	1
REACTOME_RECRUITMENT_OF_NUMA_TO_MITOTIC_CENTROSOMES	1.3984159	0.015118791	0.11050606	1

MCBRYAN_PUBERTAL_BREAST_6_7WK_DN	1.3983619	0.02663707	0.11042817	1
HUANG_GATA2_TARGETS_DN	1.3977509	0.02860286	0.110947534	1
PID_SYNDECAN_1_PATHWAY	1.3969369	0.04074074	0.111640684	1
VANDESLUIS_COMMD1_TARGETS_GROUP_3_UP	1.3962528	0.020293122	0.11225778	1
HSIAO_HOUSEKEEPING_GENES	1.3956329	0	0.11279548	1
DOANE_BREAST_CANCER_ESR1_DN	1.395047	0.04676259	0.1132842	1
KEGG_GLYCOLYSIS_GLUCONEOGENESIS	1.3950348	0.03291714	0.1131501	1
BIOCARTA_ARF_PATHWAY	1.3944	0.07629428	0.113673255	1
REACTOME_ACTIVATION_OF_HOX_GENES_DURING_DIFFERENTIATION	1.3930602	0.023001095	0.11506751	1
RUAN_RESPONSE_TO_TNF_TROGLITAZONE_DN	1.3929216	0.040048543	0.11506102	1
JIANG_HYPOXIA_VIA_VHL	1.3923252	0.06518905	0.115592256	1
REACTOME_METABOLISM_OF_COFACTORS	1.392091	0.06949807	0.11569536	1
REACTOME_REGULATION_OF_EXPRESSION_OF_SLITS_AND_ROBOS	1.391172	0.005235602	0.11655884	1
COLLIS_PRKDC_REGULATORS	1.3906598	0.07783641	0.11698955	1
REACTOME_SIRT1_NEGATIVELY_REGULATES_RRNA_EXPRESSION	1.3902982	0.049555272	0.117261335	1
REACTOME_G1_PHASE	1.3901697	0.055555556	0.117261484	1
AMIT_SERUM_RESPONSE_480_MCF10A	1.3898154	0.048346058	0.11749946	1
LIANG_HEMATOPOIESIS_STEM_CELL_NUMBER_SMALL_VS_HUG	1.3896606	0.03677343	0.11751609	1

E_UP				
HIRSCH_CELLULAR_TRANSFORMATION_SIGNATURE_DN	1.3896312	0.021598272	0.117409386	1
REACTOME_MRNA_DECAY_BY_5_TO_3_EXORIBONUCLEASE	1.3894544	0.06887417	0.11746437	1
KEGG_CYSTEINE_AND_METHIONINE_METABOLISM	1.3892018	0.052955665	0.11757334	1
SEMENZA_HIF1_TARGETS	1.3873954	0.04400978	0.11940848	1
PROVENZANI_METASTASIS_UP	1.3869172	0.006160164	0.11976634	1
MARZEC_IL2_SIGNALING_UP	1.3849163	0.012944984	0.1218866	1
GROSS_HIF1A_TARGETS_DN	1.3843333	0.06887417	0.12238398	1
REACTOME_CHOLESTEROL_BIOSYNTHESIS	1.3839241	0.054263566	0.122672714	1
DEURIG_T_CELL_PROLYMPHOCYTIC_LEUKEMIA_UP	1.3827342	0.001008065	0.12391663	1
KEGG_HISTIDINE_METABOLISM	1.3825774	0.061381076	0.12393698	1
REACTOME_ACTIVATED_PKN1_STIMULATES_TRANSCRIPTION_OF_AR_ANDROGEN_RECEPTOR_REGULATED_GENES_KLK2_AND_KLK3	1.3821367	0.06163522	0.124282874	1
DURCHDEWALD_SKIN_CARCINOGENESIS_UP	1.3804177	0.031076582	0.12606192	1
LUI_TARGETS_OF_PAX8_PPARG_FUSION	1.3800279	0.07644883	0.12635343	1
REACTOME_IRON_UPTAKE_AND_TRANSPORT	1.3768728	0.04806565	0.1298527	1
OISHI_CHOLANGIOMA_STEM_CELL_LIKE_UP	1.3768666	0.001009082	0.12969828	1
ELVIDGE_HIF1A_TARGETS_UP	1.3756737	0.03243848	0.13093132	1
REACTOME_PROCESSING_OF_CAPPED_INTRONLESS_PRE_MRNA	1.3754711	0.0524968	0.1310239	1
REACTOME_COOPERATION_OF_PDCL_PHLP1_AND_TRIC_CCT_IN	1.3753669	0.0495283	0.1309809	1

_G_PROTEIN_BETA_FOLDING				
REACTOME_MTOR_SIGNALLING	1.3743448	0.04534314	0.13203236	1
REACTOME_RNA_POLYMERASE_I_TRANSCRIPTION_INITIATION	1.3743188	0.053117782	0.13188984	1
GROSS_HYPOXIA_VIA_ELK3_ONLY_DN	1.3735358	0.049219687	0.13261159	1
OHM_METHYLATED_IN_ADULT_CANCERS	1.3730434	0.06709678	0.1330177	1
BILD_MYC_ONCOGENIC_SIGNATURE	1.3718766	0.004153687	0.13432688	1
APRELIKOVA_BRCA1_TARGETS	1.3702681	0.051869724	0.13610324	1
NUNODA_RESPONSE_TO_DASATINIB_IMATINIB_UP	1.3698543	0.07026349	0.1364548	1
COLDREN_GEFITINIB_RESISTANCE_UP	1.369767	0.02183406	0.13640991	1
KEGG_VIBRIO_CHOLERAE_INFECTION	1.3697547	0.047180668	0.13625684	1
DEN_INTERACT_WITH_LCA5	1.3682569	0.075351216	0.13793524	1
SMITH_LIVER_CANCER	1.3674405	0.056009334	0.13881443	1
WHITEHURST_PACLITAXEL_SENSITIVITY	1.3670466	0.07371008	0.1391461	1
SEIDEN_MET_SIGNALING	1.36658	0.08322497	0.13955787	1
TURASHVILI_BREAST_LOBULAR_CARCINOMA_VS_LOBULAR_NORMAL_DN	1.3664843	0.037628278	0.13951392	1
YAO_TEMPORAL_RESPONSE_TO_PROGESTERONE_CLUSTER_8	1.366343	0.046403714	0.13950965	1
MODY_HIPPOCAMPUS_NEONATAL	1.3659332	0.066332914	0.13986571	1
BOUDOUKHA_BOUND_BY_IGF2BP2	1.3655392	0.019438446	0.14017762	1
RICKMAN_METASTASIS_UP	1.3653462	0.001008065	0.14023863	1
ZHAN_EARLY_DIFFERENTIATION_GENES_DN	1.3651874	0.057623047	0.14025946	1

MORI_PLASMA_CELL_UP	1.3637174	0.053550642	0.14195791	1
REACTOME_BRANCHED_CHAIN_AMINO_ACID_CATABOLISM	1.3627104	0.075718015	0.14312574	1
REACTOME_INTERLEUKIN_1_FAMILY_SIGNALING	1.3621836	0.017021276	0.14363341	1
KEGG_GALACTOSE_METABOLISM	1.361748	0.082914576	0.14401644	1
REACTOME_DOWNSTREAM_TCR_SIGNALING	1.3606094	0.028571429	0.1453567	1
BOYLAN_MULTIPLE_MYELOMA_C_D_UP	1.3604661	0.014418126	0.14539582	1
PID_MYC_PATHWAY	1.3596027	0.072916664	0.1463123	1
ZAMORA_NOS2_TARGETS_DN	1.3593155	0.03414097	0.14650889	1
LEE_LIVER_CANCER_E2F1_DN	1.3585389	0.05373832	0.14728512	1
MCBRYAN_PUBERTAL_BREAST_4_5WK_DN	1.3584474	0.007186858	0.1472195	1
SMITH_TERT_TARGETS_UP	1.3575696	0.01875	0.14819734	1
REACTOME_FORMATION_OF_INCISION_COMPLEX_IN_GG_NER	1.3560565	0.07305389	0.14998014	1
KEGG_OTHER_GLYCAN_DEGRADATION	1.3550801	0.10094213	0.15108618	1
REACTOME_UB_SPECIFIC_PROCESSING_PROTEASES	1.354876	0.015527951	0.15116978	1
BOYAULT_LIVER_CANCER_SUBCLASS_G123_DN	1.3544773	0.056516726	0.1515343	1
REACTOME_CLEC7A_DECTIN_1_SIGNALING	1.3544014	0.030270271	0.15144561	1
REACTOME_RNA_POLYMERASE_III_TRANSCRIPTION	1.3523592	0.05910736	0.15403004	1
HASLINGER_B_CLL_WITH_CHROMOSOME_12_TRISOMY	1.3513197	0.07105943	0.15526536	1
ZHAN_V1_LATE_DIFFERENTIATION_GENES_DN	1.3512173	0.10135135	0.15523435	1
REACTOME_HYALURONAN_METABOLISM	1.3510911	0.111850865	0.15522777	1
HAHTOLA_SEZARY_SYNDROM_UP	1.3506973	0.045454547	0.15558209	1

LANDIS_ERBB2_BREAST_TUMORS_324_UP	1.3502722	0.01049318	0.155947	1
KEGG_GLUTATHIONE_METABOLISM	1.349413	0.06634499	0.15691513	1
REACTOME_EPIGENETIC_REGULATION_OF_GENE_EXPRESSION	1.3489641	0.02459893	0.15733805	1
FLOTHO_PEDIATRIC_ALL_THERAPY_RESPONSE_DN	1.3480033	0.08312342	0.15847738	1
JAZAERI_BREAST_CANCER_BRCA1_VS_BRCA2_UP	1.3475956	0.070743404	0.15884563	1
CAIRO_HEPATOBLASTOMA_UP	1.3471214	0.007106599	0.1593036	1
NOUZOVA_TRETINOIN_AND_H4_ACETYLATION	1.3468117	0.021097047	0.15950619	1
WOO_LIVER_CANCER_RECURRENCE_DN	1.3467219	0.054114994	0.15944627	1
LEE_CALORIE_RESTRICTION_MUSCLE_UP	1.3449179	0.08262455	0.16182376	1
KAAB_FAILED_HEART_VENTRICLE_DN	1.344792	0.06666667	0.16182217	1
FERNANDEZ_BOUND_BY_MYC	1.3447691	0.015625	0.1616679	1
CHIN_BREAST_CANCER_COPY_NUMBER_UP	1.343515	0.08481013	0.16323102	1
SCHLOSSER_SERUM_RESPONSE_AUGMENTED_BY_MYC	1.3431275	0.029978586	0.16356665	1
REACTOME_GOLGI_TO_ER_RETROGRADE_TRANSPORT	1.3421707	0.018907564	0.16472636	1
HAHTOLA_CTCL_CUTANEOUS	1.3421094	0.08847185	0.16462322	1
BOYLAN_MULTIPLE_MYELOMA_C_CLUSTER_UP	1.3409076	0.05946602	0.16615205	1
RUAN_RESPONSE_TO_TNF_DN	1.3407872	0.04793757	0.166125	1
WEIGEL_OXIDATIVE_STRESS_RESPONSE	1.3396018	0.08723135	0.167626	1
MOREIRA_RESPONSE_TO_TSA_UP	1.3380306	0.089420654	0.16968903	1
KEGG_GLYCOSYLPHOSPHATIDYLINOSITOL_GPI_ANCHOR_BIOSYNTHESIS	1.3375747	0.1042471	0.17012553	1

REACTOME_TP53_REGULATES_METABOLIC_GENES	1.3365301	0.051591657	0.17145379	1
REACTOME_FACTORS_INVOLVED_IN_MEGAKARYOCYTE_DEVELOPMENT_AND_PLATELET_PRODUCTION	1.336027	0.02739726	0.17198746	1
SYED_ESTRADIOL_RESPONSE	1.3355153	0.09549072	0.17250445	1
MAGRANGEAS_MULTIPLE_MYELOMA_IGG_VS_IGA_DN	1.3354398	0.08962868	0.17240772	1
BLALOCK_ALZHEIMERS_DISEASE_INCIPIENT_DN	1.3340906	0.020682523	0.17413902	1
XU_GH1_AUTOCRINE_TARGETS_UP	1.3323423	0.014447885	0.17645699	1
REACTOME_INFLUENZA_INFECTION	1.3309919	0.033862434	0.17832819	1
TERAMOTO_OPN_TARGETS_CLUSTER_6	1.3303236	0.0859375	0.17912355	1
XU_CREBBP_TARGETS_UP	1.3284104	0.116036505	0.18181959	1
REACTOME_ADP_SIGNALLING_THROUGH_P2Y_PURINOCEPTOR_12	1.328268	0.109643325	0.1818275	1
MATZUK_SPERMATOCYTE	1.3280247	0.049944505	0.18198209	1
PARK_HSC_AND_MULTIPOTENT_PROGENITORS	1.3269379	0.081145585	0.18341105	1
REACTOME_MHC_CLASS_II_ANTIGEN_PRESENTATION	1.3266926	0.037796978	0.18358879	1
REACTOME_TRANSFERRIN_ENDOCYTOSIS_AND_RECYCLING	1.3249028	0.09564164	0.1861148	1
VANDESLUIS_COMMD1_TARGETS_GROUP_4_DN	1.3239429	0.12955466	0.18735678	1
SHIPP_DLBCL_CURED_VS_FATAL_DN	1.3237425	0.08716707	0.18745247	1
LEE_AGING_MUSCLE_DN	1.3229607	0.09012346	0.18842146	1
KORKOLA_EMBRYONAL_CARCINOMA_UP	1.3226817	0.07080746	0.18867281	1
BORLAK_LIVER_CANCER_EGF_UP	1.3219784	0.059293043	0.18955898	1

WIERENGA_PML_INTERACTOME	1.3208187	0.09405941	0.19116324	1
SHEPARD_CRUSH_AND_BURN_MUTANT_UP	1.3197651	0.01336074	0.19257268	1
MARTORIATI_MDM4_TARGETS_FETAL_LIVER_UP	1.3196653	0.012282497	0.19251597	1
REACTOME_SIALIC_ACID_METABOLISM	1.318813	0.09727626	0.19366345	1
CAIRO_HEPATOBLASTOMA_POOR_SURVIVAL	1.3181251	0.11081081	0.19450714	1
LIAO_METASTASIS	1.3169417	0.001003009	0.19619206	1
WEIGEL_OXIDATIVE_STRESS_BY_HNE_AND_H2O2	1.3169125	0.08262455	0.19601376	1
REACTOME_RHO_GTPASES_ACTIVATE_PKNS	1.3166239	0.07403189	0.19621061	1
CHENG_IMPRINTED_BY_ESTRADIOL	1.3157297	0.054884743	0.19736531	1
LEIN_LOCALIZED_TO_PROXIMAL_DENDRITES	1.3152407	0.08856089	0.19795379	1
FARMER_BREAST_CANCER_BASAL_VS_LULMINAL	1.3148491	0.002022245	0.19835101	1
ELVIDGE_HIF1A_AND_HIF2A_TARGETS_UP	1.3148422	0.088709675	0.19813761	1
MATSUDA_NATURAL_KILLER_DIFFERENTIATION	1.3148178	0.001001001	0.19795254	1
FONTAINE_FOLLICULAR_THYROID_ADENOMA_DN	1.3146565	0.06666667	0.19797891	1
REACTOME_RNA_POLYMERASE_III_TRANSCRIPTION_INITIATION_FROM_TYPE_3_PROMOTER	1.3140167	0.1126408	0.19877516	1
REACTOME_SIGNALING_BY_FGFR2_IN_DISEASE	1.3124772	0.08888889	0.20111252	1
ZHAN_MULTIPLE_MYELOMA_CD1_VS_CD2_UP	1.3123666	0.06682028	0.20108609	1
FAELT_B_CLL_WITH_VH3_21_UP	1.3120985	0.09540636	0.2013302	1
LEE_LIVER_CANCER_CIPROFIBRATE_UP	1.3116838	0.07932961	0.20176327	1
SMITH_TERT_TARGETS_DN	1.3116206	0.06394708	0.20163079	1

LAMB_CCND1_TARGETS	1.3110963	0.1255116	0.20224962	1
REACTOME_DEFECTS_IN_VITAMIN_AND_COFACTOR_METABOLISM	1.310795	0.112840466	0.20252997	1
WANG_RESPONSE_TO_BEXAROTENE_UP	1.3105707	0.086419754	0.20266797	1
REACTOME_ASPARAGINE_N_LINKED_GLYCOSYLATION	1.310569	0.007042253	0.20244618	1
MACLACHLAN_BRCA1_TARGETS_UP	1.3095354	0.12763157	0.20391127	1
LUI_THYROID_CANCER_PAX8_PPARG_DN	1.3094763	0.10071942	0.20380053	1
WELCH_GATA1_TARGETS	1.30925	0.11932555	0.20397224	1
REACTOME_FORMATION_OF_THE_BETA_CATENIN:TCF_TRANSACTIVATING_COMPLEX	1.3091805	0.092289716	0.20386817	1
APPEL_IMATINIB_RESPONSE	1.3090895	0.10406091	0.20378609	1
LOCKWOOD_AMPLIFIED_IN_LUNG_CANCER	1.3078815	0.017525773	0.2055952	1
REACTOME_SUMOYLATION	1.3078482	0.026288118	0.20543286	1
REACTOME_METABOLISM_OF_WATER_SOLUBLE_VITAMINS_AND_COFACTORS	1.3056672	0.04812834	0.2088429	1
YAO_TEMPORAL_RESPONSE_TO_PROGESTERONE_CLUSTER_4	1.3053147	0.1302578	0.20916937	1
NIKOLSKY_BREAST_CANCER_7P22_AMPLICON	1.3051429	0.10827251	0.20922105	1
PID_TELOMERASE_PATHWAY	1.3047022	0.06494961	0.20972607	1
NAKAMURA_ADIPOGENESIS_LATE_DN	1.3023514	0.10436893	0.21351977	1
DARWICHE_PAPILLOMA_RISK_LOW_UP	1.3021312	0.03125	0.21364689	1
NIKOLSKY_BREAST_CANCER_17Q11_Q21_AMPLICON	1.3002589	0.049409237	0.21664459	1

FOSTER_KDM1A_TARGETS_DN	1.3001764	0.026831785	0.21654847	1
KANG_AR_TARGETS_UP	1.2990447	0.1316129	0.21820796	1
POMEROY_MEDULLOBLASTOMA_DESMOPLASIC_VS_CLASSIC_UP	1.2982173	0.081986144	0.21945672	1
NELSON_RESPONSE_TO_ANDROGEN_DN	1.2981896	0.13580246	0.21926287	1
GUENTHER_GROWTH_SPHERICAL_VS_ADHERENT_UP	1.298168	0.12980132	0.21906152	1
REACTOME_TRANSCRIPTIONAL_REGULATION_OF_GRANULOPOIESIS	1.2970418	0.09396752	0.22075634	1
KEGG_STEROID_BIOSYNTHESIS	1.2964628	0.13066667	0.22154024	1
SAKAI_CHRONIC_HEPATITIS_VS_LIVER_CANCER_UP	1.2963506	0.0676275	0.22150122	1
REACTOME_METABOLISM_OF_VITAMINS_AND_COFACTORS	1.2959033	0.02371134	0.22201078	1
WOOD_EBV_EBNA1_TARGETS_UP	1.295639	0.056277055	0.22223808	1
LANDIS_ERBB2_BREAST_PRENEOPLASTIC_UP	1.2954787	0.1380697	0.2222838	1
LIU_COMMON_CANCER_GENES	1.2943952	0.10116279	0.22389337	1
WELCSH_BRCA1_TARGETS_UP	1.2937297	0.031729784	0.22484006	1
STAMBOLSKY_BOUND_BY_MUTATED_TP53	1.2934538	0.123324394	0.22508834	1
RAMPON_ENRICHED_LEARNING_ENVIRONMENT_LATE_UP	1.2932392	0.1368421	0.22524208	1
KRIEG_KDM3A_TARGETS_NOT_HYPOXIA	1.2926023	0.03409091	0.22613908	1
LAIHO_COLORECTAL_CANCER_SERRATED_UP	1.2922785	0.043991417	0.22641478	1
SHETH_LIVER_CANCER_VS_TXNIP_LOSS_PAM4	1.2918358	0.015197569	0.22697605	1
REACTOME_FORMATION_OF_TUBULIN_FOLDING_INTERMEDIAT	1.2900872	0.12565444	0.22990441	1

ES_BY_CCT_TRIC				
BIOCARTA_ERAD_PATHWAY	1.2894205	0.12214765	0.23090002	1
VILLANUEVA_LIVER_CANCER_KRT19_DN	1.288975	0.08661418	0.23142344	1
REACTOME_SCAVENGING_BY_CLASS_A_RECEPTORS	1.2887498	0.13084112	0.2315963	1
KEGG_BETA_ALANINE_METABOLISM	1.2864007	0.140625	0.23562522	1
MARIADASON_RESPONSE_TO_CURCUMIN_SULINDAC_5	1.2860522	0.1387808	0.2359792	1
MARCINIAK_ER_STRESS_RESPONSE_VIA_CHOP	1.2853428	0.12919897	0.23703738	1
ABE_VEGFA_TARGETS	1.2851892	0.14401077	0.2370694	1
TOMLINS_PROSTATE_CANCER_UP	1.2844254	0.113553114	0.23831613	1
TAYLOR_METHYLATED_IN_ACUTE_LYMPHOBLASTIC_LEUKEMIA	1.2840625	0.081018515	0.23874222	1
WAKABAYASHI_ADIPOGENESIS_PPARG_BOUND_36HR	1.2837846	0.12562189	0.23898555	1
ACEVEDO_LIVER_CANCER_WITH_H3K9ME3_DN	1.2837045	0.0636663	0.23886772	1
DACOSTA_UV_RESPONSE_VIA_ERCC3_UP	1.2836959	0.01711984	0.23862101	1
REACTOME_ANTIGEN_PROCESSING:_UBIQUITINATION_PROTEASOME_DEGRADATION	1.2811526	0.013091642	0.24310295	1
KEGG_BASAL_TRANSCRIPTION_FACTORS	1.2803622	0.11111111	0.24439366	1
KIM_WT1_TARGETS_12HR_DN	1.280332	0.025614753	0.24417548	1
MMS_MOUSE_LYMPH_HIGH_4HRS_UP	1.2792927	0.0996264	0.24598892	1
ENK_UV_RESPONSE_KERATINOCYTE_DN	1.2787288	0.005005005	0.2468248	1
KYNG_RESPONSE_TO_H2O2_VIA_ERCC6_DN	1.278583	0.11030303	0.24683955	1
JAZAG_TGFB1_SIGNALING_UP	1.277585	0.066521265	0.24848625	1

BIOCARTA_NO1_PATHWAY	1.2773719	0.13520408	0.24861906	1
RIZKI_TUMOR_INVASIVENESS_3D_DN	1.2772452	0.034517765	0.2485756	1
***p53*$^{-/-}$ V-Fus CD4 naïve T cells vs WT CD4 naïve T cells at non-tumor bearing status**	**NES**	**NOM p-val**	**FDR q-val**	**FWER p-val**
BROWNE_INTERFERON_RESPONSIVE_GENES	2.721451	0	0	0
BOSCO_INTERFERON_INDUCED_ANTIVIRAL_MODULE	2.6463692	0	0	0
SANA_RESPONSE_TO_IFNG_UP	2.6163497	0	0	0
HECKER_IFNB1_TARGETS	2.607474	0	0	0
ICHIBA_GRAFT_VERSUS_HOST_DISEASE_D7_UP	2.5636215	0	0	0
BENNETT_SYSTEMIC_LUPUS_ERYTHEMATOSUS	2.5298376	0	0	0
MOSERLE_IFNA_RESPONSE	2.527623	0	0	0
BOYLAN_MULTIPLE_MYELOMA_PCA1_UP	2.4860706	0	0	0
MARKEY_RB1_ACUTE_LOF_DN	2.4685166	0	0	0
REACTOME_INTERFERON_ALPHA_BETA_SIGNALING	2.4519846	0	0	0
TAKEDA_TARGETS_OF_NUP98_HOXA9_FUSION_3D_UP	2.4372962	0	0	0
GOLDRATH_ANTIGEN_RESPONSE	2.4048588	0	0	0
WUNDER_INFLAMMATORY_RESPONSE_AND_CHOLESTEROL_UP	2.3588724	0	0	0
GAVIN_FOXP3_TARGETS_CLUSTER_P6	2.3531559	0	0	0
REACTOME_INTERFERON_GAMMA_SIGNALING	2.3422148	0	0	0
KIM_GLIS2_TARGETS_UP	2.33705	0	0	0
KRASNOSELSKAYA_ILF3_TARGETS_UP	2.3227305	0	0	0

LIAN_LIPA_TARGETS_6M	2.3086917	0	0	0
UROSEVIC_RESPONSE_TO_IMIQUIMOD	2.2983854	0	0	0
GRAESSMANN_RESPONSE_TO_MC_AND_SERUM_DEPRIVATION_UP	2.275479	0	4.41E-05	0.001
KLEIN_PRIMARY_EFFUSION_LYMPHOMA_DN	2.2594383	0	4.20E-05	0.001
TAKEDA_TARGETS_OF_NUP98_HOXA9_FUSION_16D_UP	2.2589498	0	4.01E-05	0.001
HOFFMANN_SMALL_PRE_BII_TO_IMMATURE_B_LYMPHOCYTE_UP	2.2575	0	3.84E-05	0.001
LIAN_LIPA_TARGETS_3M	2.254935	0	3.68E-05	0.001
FARMER_BREAST_CANCER_CLUSTER_1	2.2282734	0	7.02E-05	0.002
MCLACHLAN_DENTAL_CARIES_UP	2.2266681	0	6.75E-05	0.002
LIU_VAV3_PROSTATE_CARCINOGENESIS_UP	2.2164314	0	1.93E-04	0.006
ZHANG_INTERFERON_RESPONSE	2.177546	0	2.77E-04	0.009
YAN_ESCAPE_FROM_ANOIKIS	2.1771367	0	2.68E-04	0.009
TAKEDA_TARGETS_OF_NUP98_HOXA9_FUSION_10D_UP	2.1754768	0	2.59E-04	0.009
EINAV_INTERFERON_SIGNATURE_IN_CANCER	2.1688135	0	3.05E-04	0.011
MAEKAWA_ATF2_TARGETS	2.1570828	0	3.76E-04	0.014
DAUER_STAT3_TARGETS_DN	2.151782	0	3.91E-04	0.015
WIELAND_UP_BY_HBV_INFECTION	2.1516752	0	3.79E-04	0.015
MORI_LARGE_PRE_BII_LYMPHOCYTE_DN	2.146309	0	3.93E-04	0.016
LIANG_SILENCED_BY_METHYLATION_2	2.1431558	0	4.30E-04	0.018

BAUS_TFF2_TARGETS_UP	2.1304638	0	5.11E-04	0.022
CADWELL_ATG16L1_TARGETS_UP	2.12703	0	5.66E-04	0.025
PLASARI_TGFB1_TARGETS_10HR_DN	2.1075313	0	8.83E-04	0.04
REACTOME_INTERFERON_SIGNALING	2.0933769	0	0.001120407	0.052
TAKEDA_TARGETS_OF_NUP98_HOXA9_FUSION_8D_UP	2.08158	0	0.001323427	0.063
MORI_IMMATURE_B_LYMPHOCYTE_UP	2.0781353	0	0.001333039	0.065
SHIN_B_CELL_LYMPHOMA_CLUSTER_9	2.061712	0	0.00173931	0.084
ZHANG_ANTIVIRAL_RESPONSE_TO_RIBAVIRIN_UP	2.0543427	0	0.001758068	0.087
BOSCO_TH1_CYTOTOXIC_MODULE	2.0501611	0	0.001890884	0.095
KEGG_TYPE_I_DIABETES_MELLITUS	2.0497863	0	0.001887006	0.097
VANASSE_BCL2_TARGETS_DN	2.0203419	0	0.003020487	0.153
JECHLINGER_EPITHELIAL_TO_MESENCHYMAL_TRANSITION_UP	2.0180414	0	0.003029637	0.156
HELLER_SILENCED_BY_METHYLATION_UP	2.0096393	0	0.003371075	0.178
BOYLAN_MULTIPLE_MYELOMA_D_DN	2.0049827	0	0.003666129	0.191
ICHIBA_GRAFT_VERSUS_HOST_DISEASE_35D_UP	2.001431	0	0.003850458	0.204
CROONQUIST_NRAS_SIGNALING_UP	1.9870669	0	0.004736831	0.25
ZHAN_MULTIPLE_MYELOMA_LB_DN	1.9817283	0	0.004906705	0.261
ZHAN_MULTIPLE_MYELOMA_PR_UP	1.9805466	0	0.00487902	0.263
FLORIO_NEOCORTEX_BASAL_RADIAL_GLIA_DN	1.96596	0	0.00609451	0.32
GAURNIER_PSMD4_TARGETS	1.9623002	0	0.006367714	0.339
GAVIN_IL2_RESPONSIVE_FOXP3_TARGETS_UP	1.9606321	0	0.006406881	0.347

STEARMAN_TUMOR_FIELD_EFFECT_UP	1.9600813	0.003944773	0.0063858	0.351
GAVIN_PDE3B_TARGETS	1.9579961	0.001953125	0.006410098	0.353
NAKAYAMA_SOFT_TISSUE_TUMORS_PCA1_UP	1.9570189	0	0.006405331	0.358
APPEL_IMATINIB_RESPONSE	1.954013	0	0.006737313	0.375
GAVIN_FOXP3_TARGETS_CLUSTER_T4	1.9490043	0	0.007253366	0.407
STAMBOLSKY_TARGETS_OF_MUTATED_TP53_DN	1.9383173	0	0.007984743	0.439
KLEIN_TARGETS_OF_BCR_ABL1_FUSION	1.9365014	0	0.008141121	0.452
REACTOME_OLFACTORY_SIGNALING_PATHWAY	1.9354873	0	0.008082676	0.455
KEGG_ALLOGRAFT_REJECTION	1.9287807	0.001937985	0.008716852	0.486
RUAN_RESPONSE_TO_TNF_TROGLITAZONE_UP	1.9238755	0.00204499	0.009216231	0.504
SANA_TNF_SIGNALING_UP	1.9169403	0	0.00991653	0.542
POOLA_INVASIVE_BREAST_CANCER_UP	1.9088033	0	0.011008031	0.581
WALLACE_PROSTATE_CANCER_RACE_UP	1.9029245	0	0.011566062	0.605
KIM_LRRC3B_TARGETS	1.8999126	0.002	0.011865896	0.618
KEGG_GRAFT_VERSUS_HOST_DISEASE	1.8976804	0.003831418	0.012059054	0.629
REACTOME_TNFS_BIND_THEIR_PHYSIOLOGICAL_RECEPTORS	1.8975279	0	0.01190593	0.629
HOLLERN_SOLID_NODULAR_BREAST_TUMOR_DN	1.896008	0	0.012057982	0.641
REACTOME_ANTIMICROBIAL_PEPTIDES	1.8938165	0.001968504	0.012172398	0.652
FURUKAWA_DUSP6_TARGETS_PCI35_UP	1.8936082	0	0.012045963	0.652
WILENSKY_RESPONSE_TO_DARAPLADIB	1.8860397	0	0.013143505	0.688
GAUSSMANN_MLL_AF4_FUSION_TARGETS_B_UP	1.8827441	0	0.013549948	0.704

KAMIKUBO_MYELOID_CEBPA_NETWORK	1.8696866	0	0.015945217	0.758
REACTOME_IMMUNOREGULATORY_INTERACTIONS_BETWEEN_A_LYMPHOID_AND_A_NON_LYMPHOID_CELL	1.8690003	0	0.015842495	0.759
ZHENG_IL22_SIGNALING_UP	1.8582451	0	0.018019266	0.807
MIKKELSEN_IPS_WITH_HCP_H3K27ME3	1.8538721	0.002070393	0.018829966	0.824
RADAEVA_RESPONSE_TO_IFNA1_UP	1.851335	0	0.019234892	0.833
KEGG_AUTOIMMUNE_THYROID_DISEASE	1.8445666	0	0.020644365	0.855
DER_IFN_ALPHA_RESPONSE_UP	1.8422979	0	0.021070015	0.865
GAVIN_FOXP3_TARGETS_CLUSTER_P3	1.8385504	0	0.021593792	0.875
BOYLAN_MULTIPLE_MYELOMA_C_D_DN	1.8374437	0	0.021543806	0.879
GRAHAM_CML_QUIESCENT_VS_NORMAL_QUIESCENT_DN	1.8282762	0.001930502	0.023599274	0.908
BASSO_CD40_SIGNALING_UP	1.8275243	0	0.023507556	0.908
QI_PLASMACYTOMA_UP	1.8269231	0	0.023370648	0.909
KANG_DOXORUBICIN_RESISTANCE_UP	1.8256017	0	0.023482537	0.913
BERTUCCI_MEDULLARY_VS_DUCTAL_BREAST_CANCER_UP	1.8248806	0	0.023432463	0.918
KUROZUMI_RESPONSE_TO_ONCOCYTIC_VIRUS	1.8241271	0	0.023477834	0.92
HAHTOLA_SEZARY_SYNDROM_DN	1.8221586	0.00390625	0.023804126	0.928
BOYLAN_MULTIPLE_MYELOMA_PCA3_DN	1.8200532	0.001934236	0.024035577	0.93
LEE_LIVER_CANCER_MYC_E2F1_UP	1.8196653	0.004149378	0.023883408	0.93
GREENBAUM_E2A_TARGETS_DN	1.8131071	0.003952569	0.025183799	0.943
LI_WILMS_TUMOR_ANAPLASTIC_UP	1.8105294	0.006	0.025700813	0.948

GENTLES_LEUKEMIC_STEM_CELL_UP	1.8046745	0.00189394	0.027139137	0.958
SEITZ_NEOPLASTIC_TRANSFORMATION_BY_8P_DELETION_UP	1.8039767	0.00203252	0.027090387	0.961
KEGG_ANTIGEN_PROCESSING_AND_PRESENTATION	1.8023436	0.001964637	0.027241101	0.964
COLINA_TARGETS_OF_4EBP1_AND_4EBP2	1.7966243	0	0.028652849	0.971
PID_IL27_PATHWAY	1.7962662	0.003802281	0.02843315	0.971
KEGG_CYTOKINE_CYTOKINE_RECEPTOR_INTERACTION	1.7942992	0	0.028771851	0.974
VILIMAS_NOTCH1_TARGETS_DN	1.793791	0.00203252	0.028679274	0.975
TARTE_PLASMA_CELL_VS_B_LYMPHOCYTE_DN	1.7928523	0	0.02867647	0.976
VERRECCHIA_RESPONSE_TO_TGFB1_C1	1.7920362	0.007662835	0.028650217	0.978
KIM_ALL_DISORDERS_CALB1_CORR_DN	1.7880522	0.001976285	0.029489856	0.982
PID_IL23_PATHWAY	1.7833557	0	0.030553319	0.984
DER_IFN_BETA_RESPONSE_UP	1.7722557	0.001926782	0.034055635	0.988
KEGG_ASTHMA	1.770625	0.008016032	0.034315016	0.988
NAKAJIMA_MAST_CELL	1.7615378	0.008097166	0.03729582	0.993
YU_MYC_TARGETS_DN	1.7608477	0	0.037326075	0.993
SHARMA_PILOCYTIC_ASTROCYTOMA_LOCATION_UP	1.7581947	0.00408998	0.038011245	0.993
ABBUD_LIF_SIGNALING_1_DN	1.7525579	0.005836576	0.040072266	0.995
WORSCHECH_TUMOR_REJECTION_UP	1.7505296	0	0.040600993	0.995
KIM_MYC_AMPLIFICATION_TARGETS_DN	1.7495356	0	0.040629584	0.997
ALTEMEIER_RESPONSE_TO_LPS_WITH_MECHANICAL_VENTILATION	1.7469877	0	0.041330386	0.998

DER_IFN_GAMMA_RESPONSE_UP	1.7391404	0.001919386	0.044542283	0.999
NOJIMA_SFRP2_TARGETS_DN	1.738827	0.005780347	0.044292804	0.999
SAMOLS_TARGETS_OF_KHSV_MIRNAS_DN	1.7256515	0.001919386	0.050000813	1
GOLDRATH_IMMUNE_MEMORY	1.7251215	0.002004008	0.049837235	1
GAL_LEUKEMIC_STEM_CELL_DN	1.720317	0	0.05205291	1
BOYAULT_LIVER_CANCER_SUBCLASS_G5_DN	1.7191123	0.002	0.0522991	1
CHIANG_LIVER_CANCER_SUBCLASS_INTERFERON_UP	1.7183875	0.011673152	0.052300792	1
HANN_RESISTANCE_TO_BCL2_INHIBITOR_UP	1.7182022	0.01004016	0.051960897	1
MORI_MATURE_B_LYMPHOCYTE_UP	1.7153314	0.002008032	0.053219497	1
RASHI_RESPONSE_TO_IONIZING_RADIATION_6	1.7004489	0	0.060491193	1
ZHAN_MULTIPLE_MYELOMA_DN	1.6950217	0.004040404	0.063040465	1
RODWELL_AGING_KIDNEY_UP	1.6937995	0	0.06327082	1
KEGG_CELL_ADHESION_MOLECULES_CAMS	1.693147	0.001941748	0.063109756	1
MORI_PLASMA_CELL_DN	1.6894119	0.003960396	0.0647592	1
WANG_NFKB_TARGETS	1.687932	0.016260162	0.06520437	1
ROSTY_CERVICAL_CANCER_PROLIFERATION_CLUSTER	1.6826415	0	0.0679281	1
REACTOME_INTERLEUKIN_10_SIGNALING	1.6819372	0.011976048	0.06789207	1
ROSS_AML_WITH_MLL_FUSIONS	1.6802971	0	0.06845994	1
GRAHAM_CML_DIVIDING_VS_NORMAL_QUIESCENT_UP	1.677752	0	0.06938136	1
FLORIO_NEOCORTEX_BASAL_RADIAL_GLIA_UP	1.6765192	0	0.0697459	1
ZHAN_MULTIPLE_MYELOMA_CD2_UP	1.673815	0.008368201	0.0710157	1

NAKAYAMA_SOFT_TISSUE_TUMORS_PCA2_UP	1.6726347	0.001901141	0.0712974	1
LEE_AGING_CEREBELLUM_UP	1.6724845	0.00407332	0.070828505	1
SCIAN_CELL_CYCLE_TARGETS_OF_TP53_AND_TP73_DN	1.6717665	0.009803922	0.070814	1
MEISSNER_BRAIN_HCP_WITH_H3K27ME3	1.6701419	0	0.071504	1
REACTOME_DISEASES_OF_IMMUNE_SYSTEM	1.669293	0.011450382	0.071546346	1
LI_INDUCED_T_TO_NATURAL_KILLER_UP	1.6688527	0	0.07138012	1
ONO_AML1_TARGETS_DN	1.6686071	0.005859375	0.071056135	1
JISON_SICKLE_CELL_DISEASE_UP	1.6663535	0	0.072054215	1
GRAHAM_CML_DIVIDING_VS_NORMAL_QUIESCENT_DN	1.6655172	0	0.07215565	1
FARMER_BREAST_CANCER_CLUSTER_2	1.6620158	0.007920792	0.07407018	1
VALK_AML_CLUSTER_5	1.6574414	0.015779093	0.076718666	1
YANG_BCL3_TARGETS_UP	1.6560555	0	0.07716853	1
KEGG_COMPLEMENT_AND_COAGULATION_CASCADES	1.6496891	0.001879699	0.08113549	1
HUPER_BREAST_BASAL_VS_LUMINAL_DN	1.6485649	0.011764706	0.08136986	1
SCHUETZ_BREAST_CANCER_DUCTAL_INVASIVE_UP	1.6445125	0	0.08368504	1
KRIEG_KDM3A_TARGETS_NOT_HYPOXIA	1.6417382	0	0.08520577	1
KEGG_INTESTINAL_IMMUNE_NETWORK_FOR_IGA_PRODUCTION	1.639997	0.01754386	0.08591804	1
BIOCARTA_TH1TH2_PATHWAY	1.6393495	0.015936255	0.085886866	1
SHEPARD_BMYB_TARGETS	1.6384519	0.012244898	0.086019725	1
REACTOME_ANTIGEN_ACTIVATES_B_CELL_RECEPTOR_BCR_LEADING_TO_GENERATION_OF_SECOND_MESSENGERS	1.638233	0.011976048	0.0856472	1

GAVIN_FOXP3_TARGETS_CLUSTER_P4	1.6370009	0	0.08600623	1
ALCALAY_AML_BY_NPM1_LOCALIZATION_DN	1.6369673	0	0.085477434	1
ISHIDA_E2F_TARGETS	1.6303155	0.001876173	0.089954205	1
CHIANG_LIVER_CANCER_SUBCLASS_PROLIFERATION_UP	1.6273018	0	0.091710195	1
FOSTER_KDM1A_TARGETS_UP	1.6247002	0	0.093125	1
LEE_TARGETS_OF_PTCH1_AND_SUFU_UP	1.6216371	0.006276151	0.09516476	1
FONTAINE_THYROID_TUMOR_UNCERTAIN_MALIGNANCY_DN	1.6207069	0.0186722	0.09538069	1
KAAB_FAILED_HEART_VENTRICLE_DN	1.6205975	0.010060363	0.09489728	1
WANG_RESPONSE_TO_GSK3_INHIBITOR_SB216763_UP	1.6188102	0	0.095715135	1
WORSCHECH_TUMOR_EVASION_AND_TOLEROGENICITY_UP	1.6172116	0.019762846	0.096441716	1
MATSUDA_NATURAL_KILLER_DIFFERENTIATION	1.6150467	0	0.09755749	1
REACTOME_INTERLEUKIN_20_FAMILY_SIGNALING	1.6148942	0.034	0.09714845	1
LINDSTEDT_DENDRITIC_CELL_MATURATION_D	1.6112365	0.009746589	0.09980373	1
TAVOR_CEBPA_TARGETS_DN	1.6104733	0.02244898	0.099899255	1
GARGALOVIC_RESPONSE_TO_OXIDIZED_PHOSPHOLIPIDS_PINK_DN	1.610015	0.013307985	0.099682294	1
PICCALUGA_ANGIOIMMUNOBLASTIC_LYMPHOMA_UP	1.6054101	0	0.10275926	1
REACTOME_INTERLEUKIN_2_FAMILY_SIGNALING	1.6038246	0.01171875	0.10346831	1
ZHONG_SECRETOME_OF_LUNG_CANCER_AND_ENDOTHELIUM	1.6029936	0.013888889	0.10358763	1
KONDO_PROSTATE_CANCER_WITH_H3K27ME3	1.6013297	0.005639098	0.10455093	1
KEGG_PRIMARY_IMMUNODEFICIENCY	1.5968322	0.025242718	0.108046725	1

HUTTMANN_B_CLL_POOR_SURVIVAL_DN	1.5943121	0.007984032	0.1095974	1
REACTOME_INCRETIN_SYNTHESIS_SECRETION_AND_INACTIVATION	1.5928118	0.019569471	0.110343456	1
SENGUPTA_NASOPHARYNGEAL_CARCINOMA_UP	1.5923461	0	0.110186756	1
LEE_EARLY_T_LYMPHOCYTE_UP	1.5903956	0.004310345	0.11146595	1
GRAESSMANN_APOPTOSIS_BY_SERUM_DEPRIVATION_UP	1.5900137	0	0.1111094	1
SMID_BREAST_CANCER_NORMAL_LIKE_UP	1.5868336	0	0.11347031	1
LY_AGING_MIDDLE_DN	1.5868328	0.026119404	0.112860255	1
CASTELLANO_NRAS_TARGETS_UP	1.5833777	0.005780347	0.11552922	1
HAHTOLA_SEZARY_SYNDROM_UP	1.5804491	0.004158004	0.11770305	1
SASAKI_ADULT_T_CELL_LEUKEMIA	1.579179	0	0.11832734	1
BIOCARTA_IGF1MTOR_PATHWAY	1.5749254	0.01778656	0.12196519	1
HOWLIN_CITED1_TARGETS_2_DN	1.572457	0.03373016	0.12387486	1
LINDSTEDT_DENDRITIC_CELL_MATURATION_A	1.5712417	0.013972056	0.124545634	1
PID_IL12_2PATHWAY	1.569984	0.00729927	0.12518045	1
HOFFMANN_LARGE_TO_SMALL_PRE_BII_LYMPHOCYTE_UP	1.5668211	0.001960784	0.12786216	1
KEGG_RIG_I_LIKE_RECEPTOR_SIGNALING_PATHWAY	1.5640893	0.005870841	0.1300404	1
REACTOME_DECTIN_2_FAMILY	1.5635228	0.024482109	0.12992121	1
KUMAR_TARGETS_OF_MLL_AF9_FUSION	1.5629566	0	0.12985675	1
SOTIRIOU_BREAST_CANCER_GRADE_1_VS_3_UP	1.5611299	0.003944773	0.1310197	1
YAO_TEMPORAL_RESPONSE_TO_PROGESTERONE_CLUSTER_15	1.5610355	0.01980198	0.13048299	1

XU_AKT1_TARGETS_6HR	1.5605088	0.02173913	0.13036399	1
KUROZUMI_RESPONSE_TO_ONCOCYTIC_VIRUS_AND_CYCLIC_RGD	1.5603769	0.0295858	0.12984827	1
SHIN_B_CELL_LYMPHOMA_CLUSTER_5	1.5593513	0.03807615	0.13033222	1
VERHAAK_AML_WITH_NPM1_MUTATED_UP	1.5573971	0.00407332	0.1319256	1
REACTOME_LAMININ_INTERACTIONS	1.5561074	0.018552875	0.13255773	1
DEMAGALHAES_AGING_UP	1.554513	0.027139874	0.1335861	1
VERHAAK_GLIOBLASTOMA_MESENCHYMAL	1.5534968	0	0.1339256	1
ZHOU_CELL_CYCLE_GENES_IN_IR_RESPONSE_24HR	1.5525407	0.001926782	0.13431393	1
REACTOME_ANTIGEN_PROCESSING_CROSS_PRESENTATION	1.5515186	0.003976143	0.13472275	1
DIAZ_CHRONIC_MEYLOGENOUS_LEUKEMIA_DN	1.551082	0.002004008	0.13451906	1
SHIN_B_CELL_LYMPHOMA_CLUSTER_7	1.5492789	0.030075189	0.13581428	1
REACTOME_PEPTIDE_LIGAND_BINDING_RECEPTORS	1.5478773	0.005882353	0.13683304	1
RHODES_UNDIFFERENTIATED_CANCER	1.5471098	0.004048583	0.13699232	1
ZHAN_MULTIPLE_MYELOMA_CD1_UP	1.5454564	0.021276595	0.13800354	1
TANG_SENESCENCE_TP53_TARGETS_DN	1.5445303	0.012269938	0.13831604	1
GREENBAUM_E2A_TARGETS_UP	1.5426041	0.026422765	0.13981529	1
WONG_ENDMETRIUM_CANCER_UP	1.5424033	0.028169014	0.13942364	1
HAN_JNK_SINGALING_UP	1.5362878	0.042105265	0.14566651	1
KEGG_B_CELL_RECEPTOR_SIGNALING_PATHWAY	1.5341367	0.00589391	0.14733325	1
GRAHAM_NORMAL_QUIESCENT_VS_NORMAL_DIVIDING_DN	1.5310887	0.009823183	0.15023647	1

WANG_BARRETTS_ESOPHAGUS_AND_ESOPHAGUS_CANCER_UP	1.530523	0.028355388	0.15026584	1
REACTOME_COBALAMIN_CBL_VITAMIN_B12_TRANSPORT_AND_METABOLISM	1.527235	0.054435484	0.1535503	1
ODONNELL_TFRC_TARGETS_DN	1.526841	0.003883495	0.15343583	1
FULCHER_INFLAMMATORY_RESPONSE_LECTIN_VS_LPS_DN	1.5264323	0	0.15322985	1
SERVITJA_LIVER_HNF1A_TARGETS_DN	1.5216709	0.007843138	0.1581521	1
ROY_WOUND_BLOOD_VESSEL_UP	1.5201737	0.023605151	0.15910855	1
EPPERT_CE_HSC_LSC	1.5196112	0.016632017	0.15906277	1
AFFAR_YY1_TARGETS_DN	1.5177302	0	0.16059296	1
ZWANG_EGF_PERSISTENTLY_UP	1.5175345	0.031746034	0.16014172	1
FLECHNER_BIOPSY_KIDNEY_TRANSPLANT_REJECTED_VS_OK_UP	1.5173904	0.009541985	0.15964912	1
KONG_E2F3_TARGETS	1.5158777	0.006036217	0.1608463	1
ZHANG_RESPONSE_TO_IKK_INHIBITOR_AND_TNF_UP	1.5152814	0.001984127	0.16094732	1
KEGG_SYSTEMIC_LUPUS_ERYTHEMATOSUS	1.5149252	0.015655577	0.16066203	1
ANDERSEN_CHOLANGIOCARCINOMA_CLASS2	1.5138248	0.001964637	0.16126926	1
KEGG_JAK_STAT_SIGNALING_PATHWAY	1.5118368	0.008316008	0.1628176	1
ZHONG_SECRETOME_OF_LUNG_CANCER_AND_MACROPHAGE	1.5107446	0.016393442	0.1634645	1
FOSTER_TOLERANT_MACROPHAGE_UP	1.5085534	0.00390625	0.16533762	1
ZHOU_INFLAMMATORY_RESPONSE_LPS_UP	1.5063673	0.001976285	0.1673532	1
BURTON_ADIPOGENESIS_PEAK_AT_24HR	1.5062038	0.021235522	0.16685314	1

ROZANOV_MMP14_TARGETS_DN	1.5046704	0.038306452	0.16820276	1
TAKEDA_TARGETS_OF_NUP98_HOXA9_FUSION_10D_DN	1.5021884	0.01010101	0.17055087	1
FIGUEROA_AML_METHYLATION_CLUSTER_5_DN	1.4987797	0.02970297	0.17402872	1
LU_TUMOR_VASCULATURE_UP	1.4962422	0.04312115	0.17662728	1
KEGG_GLYCINE_SERINE_AND_THREONINE_METABOLISM	1.4960216	0.044354837	0.17621914	1
MIKKELSEN_NPC_ICP_WITH_H3K4ME3	1.4943931	0	0.17761639	1
LEE_LIVER_CANCER_MYC_TGFA_DN	1.4897562	0.031558186	0.18275845	1
NABA_MATRISOME_ASSOCIATED	1.4875814	0	0.18513939	1
NABA_BASEMENT_MEMBRANES	1.4830935	0.047808766	0.1906846	1
SENGUPTA_NASOPHARYNGEAL_CARCINOMA_WITH_LMP1_UP	1.4829075	0	0.19013426	1
REACTOME_MOLECULES_ASSOCIATED_WITH_ELASTIC_FIBRES	1.480316	0.032786883	0.193033	1
HUANG_FOXA2_TARGETS_DN	1.4768016	0.04789272	0.1971309	1
RICKMAN_HEAD_AND_NECK_CANCER_D	1.4726437	0.0665362	0.20239632	1
SU_TESTIS	1.4706681	0.018828452	0.20432428	1
REACTOME_MET_ACTIVATES_PTK2_SIGNALING	1.4705129	0.052208837	0.20372781	1
LIAN_NEUTROPHIL_GRANULE_CONSTITUENTS	1.4700816	0.050403226	0.20355314	1
REACTOME_FGFR2_LIGAND_BINDING_AND_ACTIVATION	1.4694169	0.060311284	0.20365626	1
CHEMNITZ_RESPONSE_TO_PROSTAGLANDIN_E2_UP	1.4674361	0.011976048	0.20555206	1
PID_INTEGRIN1_PATHWAY	1.4669714	0.035433073	0.20541592	1
COATES_MACROPHAGE_M1_VS_M2_UP	1.4641922	0.011494253	0.20873573	1
VANTVEER_BREAST_CANCER_BRCA1_UP	1.4602537	0.040229887	0.21371785	1

WHITEFORD_PEDIATRIC_CANCER_MARKERS	1.4587082	0.003868472	0.2152782	1
NAKAMURA_CANCER_MICROENVIRONMENT_UP	1.4576564	0.05950096	0.21595868	1
LE_EGR2_TARGETS_UP	1.4571192	0.011650485	0.21592653	1
TAKEDA_TARGETS_OF_NUP98_HOXA9_FUSION_16D_DN	1.4553918	0.01775148	0.21770944	1
CAIRO_LIVER_DEVELOPMENT_DN	1.4532869	0.001953125	0.22011483	1
ZHENG_FOXP3_TARGETS_UP	1.4488583	0.055238094	0.22616921	1
DUTERTRE_ESTRADIOL_RESPONSE_24HR_UP	1.4483082	0.004048583	0.22624448	1
BIOCARTA_INTRINSIC_PATHWAY	1.4458243	0.061185468	0.22945103	1
KEGG_OLFACTORY_TRANSDUCTION	1.4444479	0.004056795	0.23083809	1
PETROVA_PROX1_TARGETS_UP	1.4444073	0.06042885	0.23004365	1
HUANG_DASATINIB_RESISTANCE_UP	1.4431871	0.01871102	0.23123395	1
BYSTROEM_CORRELATED_WITH_IL5_DN	1.4426343	0.0256917	0.23134637	1
LU_TUMOR_ANGIOGENESIS_UP	1.4419037	0.06854839	0.23166825	1
RICKMAN_HEAD_AND_NECK_CANCER_A	1.4393405	0.016359918	0.23504391	1
ZHONG_SECRETOME_OF_LUNG_CANCER_AND_FIBROBLAST	1.4364234	0.009823183	0.2389357	1
BROWN_MYELOID_CELL_DEVELOPMENT_UP	1.4339219	0.01048218	0.24224535	1
XU_CREBBP_TARGETS_UP	1.4330221	0.056640625	0.24286523	1
BURTON_ADIPOGENESIS_3	1.4318532	0.017374517	0.24396385	1
REACTOME_G_ALPHA_S_SIGNALLING_EVENTS	1.4316971	0	0.2433337	1
REACTOME_RESPIRATORY_ELECTRON_TRANSPORT_ATP_SYNTHESIS_BY_CHEMIOSMOTIC_COUPLING_AND_HEAT_PRODUCTION_	1.430145	0.022514071	0.24508418	1

BY_UNCOUPLING_PROTEINS				
MEISSNER_NPC_HCP_WITH_H3K27ME3	1.4300109	0.05668016	0.24442439	1
MULLIGHAN_NPM1_MUTATED_SIGNATURE_1_UP	1.4291614	0.001992032	0.24498336	1
YAMASHITA_METHYLATED_IN_PROSTATE_CANCER	1.4275005	0.03976143	0.246848	1
REACTOME_INTEGRIN_CELL_SURFACE_INTERACTIONS	1.4263513	0.024096385	0.24783216	1
BOHN_PRIMARY_IMMUNODEFICIENCY_SYNDROM_DN	1.4263283	0.056640625	0.24699305	1
ODONNELL_TARGETS_OF_MYC_AND_TFRC_DN	1.4251865	0.04315197	0.24799064	1
LEIN_PONS_MARKERS	1.4244528	0.032520324	0.24837147	1
HOLLERN_EMT_BREAST_TUMOR_UP	1.422103	0.016632017	0.24985772	1
***p53*$^{-/-}$ V-Fus CD4 naïve T cells vs *p53*$^{-/-}$ CD4 naïve T cells at non-tumor bearing status**	**NES**	**NOM p-val**	**FDR q-val**	**FWER p-val**
GAVIN_FOXP3_TARGETS_CLUSTER_P6	2.4609816	0	0	0
KEGG_TYPE_I_DIABETES_MELLITUS	2.2926378	0	4.09E-04	0.001
GOLDRATH_ANTIGEN_RESPONSE	2.2583098	0	5.42E-04	0.002
GAVIN_PDE3B_TARGETS	2.2093413	0	0.001221768	0.006
REACTOME_TNFS_BIND_THEIR_PHYSIOLOGICAL_RECEPTORS	2.1822565	0	0.001140655	0.007
REACTOME_OLFACTORY_SIGNALING_PATHWAY	2.125004	0	0.00298261	0.022
NAKAJIMA_MAST_CELL	2.10274	0	0.002670561	0.023
SANA_RESPONSE_TO_IFNG_UP	2.0753806	0	0.004677448	0.046
KLEIN_PRIMARY_EFFUSION_LYMPHOMA_DN	2.0732665	0	0.004246665	0.047
BROWNE_INTERFERON_RESPONSIVE_GENES	2.0520396	0	0.005607946	0.069

FLORIO_NEOCORTEX_BASAL_RADIAL_GLIA_DN	2.0518324	0	0.005098132	0.069
KUROZUMI_RESPONSE_TO_ONCOCYTIC_VIRUS	2.0448098	0	0.005758433	0.084
GAVIN_IL2_RESPONSIVE_FOXP3_TARGETS_UP	2.036178	0	0.00656399	0.101
KEGG_GRAFT_VERSUS_HOST_DISEASE	1.9894173	0	0.012949294	0.197
GAVIN_FOXP3_TARGETS_CLUSTER_T4	1.9689605	0	0.016562596	0.266
HANN_RESISTANCE_TO_BCL2_INHIBITOR_UP	1.9683245	0	0.01562825	0.268
ZHAN_MULTIPLE_MYELOMA_PR_UP	1.963644	0	0.015617113	0.278
GARGALOVIC_RESPONSE_TO_OXIDIZED_PHOSPHOLIPIDS_PINK_DN	1.960174	0.002583979	0.015380167	0.286
PLASARI_TGFB1_TARGETS_10HR_DN	1.9458071	0	0.018291181	0.342
LIAN_LIPA_TARGETS_6M	1.9149238	0	0.02574418	0.463
LI_INDUCED_T_TO_NATURAL_KILLER_UP	1.9133162	0	0.02494387	0.468
BOSCO_TH1_CYTOTOXIC_MODULE	1.910425	0	0.024624096	0.481
KIM_GLIS2_TARGETS_UP	1.8979495	0	0.02750314	0.538
NAKAYAMA_SOFT_TISSUE_TUMORS_PCA2_UP	1.8948809	0	0.02727885	0.55
ANDERSEN_CHOLANGIOCARCINOMA_CLASS2	1.8849798	0	0.02942638	0.596
GAVIN_FOXP3_TARGETS_CLUSTER_P4	1.8835677	0	0.028820578	0.604
KRASNOSELSKAYA_ILF3_TARGETS_UP	1.8645966	0	0.034679323	0.688
KEGG_ALLOGRAFT_REJECTION	1.8582741	0	0.03626084	0.719
HOFFMANN_SMALL_PRE_BII_TO_IMMATURE_B_LYMPHOCYTE_UP	1.8569223	0	0.035655957	0.724

MEISSNER_BRAIN_HCP_WITH_H3K27ME3	1.8550543	0	0.035119478	0.729
LIU_VAV3_PROSTATE_CARCINOGENESIS_UP	1.8449517	0.002659574	0.038720515	0.772
ICHIBA_GRAFT_VERSUS_HOST_DISEASE_D7_UP	1.8369209	0	0.04147175	0.806
SHIN_B_CELL_LYMPHOMA_CLUSTER_9	1.8346584	0.004385965	0.041172113	0.813
BOYLAN_MULTIPLE_MYELOMA_PCA1_UP	1.8324982	0	0.04101204	0.816
ROSTY_CERVICAL_CANCER_PROLIFERATION_CLUSTER	1.825257	0	0.04371365	0.845
PID_IL27_PATHWAY	1.8232684	0	0.04340172	0.852
GAURNIER_PSMD4_TARGETS	1.8208315	0	0.043262217	0.858
WIELAND_UP_BY_HBV_INFECTION	1.8174015	0	0.04352594	0.866
LIAN_LIPA_TARGETS_3M	1.8151937	0	0.043476492	0.871
KANG_DOXORUBICIN_RESISTANCE_UP	1.8137574	0	0.043178573	0.876
ONO_AML1_TARGETS_DN	1.809105	0	0.044205733	0.889
KEGG_CYTOKINE_CYTOKINE_RECEPTOR_INTERACTION	1.8041844	0	0.04510927	0.898
FONTAINE_THYROID_TUMOR_UNCERTAIN_MALIGNANCY_DN	1.7979383	0	0.04705327	0.912
RORIE_TARGETS_OF_EWSR1_FLI1_FUSION_DN	1.7758678	0.002298851	0.058805786	0.952
WENG_POR_TARGETS_GLOBAL_UP	1.7736459	0.008849558	0.0590868	0.956
LEE_EARLY_T_LYMPHOCYTE_UP	1.7621946	0	0.064742446	0.969
REACTOME_IMMUNOREGULATORY_INTERACTIONS_BETWEEN_A_LYMPHOID_AND_A_NON_LYMPHOID_CELL	1.7554277	0	0.06826724	0.976
LI_WILMS_TUMOR_ANAPLASTIC_UP	1.7538695	0.009153318	0.06809833	0.976
REACTOME_INTERFERON_GAMMA_SIGNALING	1.7469813	0	0.07153838	0.983

GAVIN_FOXP3_TARGETS_CLUSTER_P3	1.7431674	0	0.07296516	0.987
KONDO_PROSTATE_CANCER_WITH_H3K27ME3	1.7426466	0	0.07177239	0.987
BOSCO_INTERFERON_INDUCED_ANTIVIRAL_MODULE	1.7368311	0.005361931	0.07439018	0.99
WEBER_METHYLATED_HCP_IN_SPERM_UP	1.727065	0.009090909	0.080139525	0.993
BIOCARTA_TH1TH2_PATHWAY	1.7203859	0.004694836	0.08443967	0.997
MEISSNER_NPC_HCP_WITH_H3K27ME3	1.7164859	0.00257732	0.08562749	0.997
WANG_BARRETTS_ESOPHAGUS_AND_ESOPHAGUS_CANCER_UP	1.7146302	0.006818182	0.08551538	0.997
GREENBAUM_E2A_TARGETS_UP	1.7133105	0.004950495	0.08515572	0.997
MARKEY_RB1_ACUTE_LOF_DN	1.7132508	0	0.08371525	0.997
MIKKELSEN_MEF_LCP_WITH_H3K4ME3	1.7129911	0	0.08255605	0.997
PETROVA_PROX1_TARGETS_UP	1.7074852	0.014084507	0.085391626	0.998
VANASSE_BCL2_TARGETS_DN	1.7068089	0	0.08456264	0.998
WHITEFORD_PEDIATRIC_CANCER_MARKERS	1.7049253	0	0.08472997	0.998
YAN_ESCAPE_FROM_ANOIKIS	1.7035642	0.014423077	0.08447823	0.998
NAKAYAMA_SOFT_TISSUE_TUMORS_PCA1_UP	1.6990703	0.005509642	0.08656605	0.998
MCLACHLAN_DENTAL_CARIES_UP	1.6955476	0	0.088267826	0.998
CHIANG_LIVER_CANCER_SUBCLASS_INTERFERON_UP	1.6865243	0.011764706	0.09410631	0.999
PID_IL23_PATHWAY	1.6864005	0.007334963	0.09281071	0.999
AFFAR_YY1_TARGETS_DN	1.6833456	0	0.09427444	0.999
MORI_LARGE_PRE_BII_LYMPHOCYTE_DN	1.6808912	0.002610966	0.09478947	0.999
WUNDER_INFLAMMATORY_RESPONSE_AND_CHOLESTEROL_UP	1.6786027	0.00486618	0.09543958	0.999

MIKKELSEN_ES_ICP_WITH_H3K4ME3_AND_H3K27ME3	1.6737026	0	0.09840216	1
CHIANG_LIVER_CANCER_SUBCLASS_PROLIFERATION_UP	1.6686623	0	0.10178713	1
MIKKELSEN_IPS_WITH_HCP_H3K27ME3	1.6625504	0	0.10564245	1
REACTOME_PEPTIDE_LIGAND_BINDING_RECEPTORS	1.6613427	0	0.10523696	1
KEGG_ASTHMA	1.6599805	0.006802721	0.10502898	1
MIKKELSEN_ES_LCP_WITH_H3K4ME3	1.6567053	0	0.106601	1
HUANG_FOXA2_TARGETS_DN	1.6564227	0.006960557	0.105553545	1
OSADA_ASCL1_TARGETS_UP	1.6559151	0.007125891	0.10458392	1
KUROZUMI_RESPONSE_TO_ONCOCYTIC_VIRUS_AND_CYCLIC_RGD	1.6515052	0.01594533	0.10729362	1
FARMER_BREAST_CANCER_CLUSTER_2	1.6509031	0.014778325	0.10641734	1
SCIAN_CELL_CYCLE_TARGETS_OF_TP53_AND_TP73_DN	1.6486958	0.006993007	0.10724934	1
POOLA_INVASIVE_BREAST_CANCER_UP	1.6486621	0	0.10598173	1
LEE_LIVER_CANCER_MYC_TGFA_DN	1.6455729	0.002824859	0.10730972	1
ZHAN_MULTIPLE_MYELOMA_CD1_UP	1.644508	0	0.10709657	1
MEISSNER_BRAIN_HCP_WITH_H3K4ME2_AND_H3K27ME3	1.6410506	0.00234192	0.10896064	1
DUTERTRE_ESTRADIOL_RESPONSE_24HR_UP	1.640707	0	0.10797606	1
CROONQUIST_NRAS_SIGNALING_UP	1.6331279	0.012820513	0.11457331	1
PICCALUGA_ANGIOIMMUNOBLASTIC_LYMPHOMA_UP	1.63086	0	0.115496434	1
WORSCHECH_TUMOR_REJECTION_UP	1.630563	0.002450981	0.1144806	1
HAHTOLA_SEZARY_SYNDROM_DN	1.6303829	0.009345794	0.1134525	1

QI_PLASMACYTOMA_UP	1.627905	0	0.11453194	1
REACTOME_MET_ACTIVATES_PTK2_SIGNALING	1.6264181	0.013729977	0.11485305	1
MAEKAWA_ATF2_TARGETS	1.6242883	0.025	0.11554676	1
PID_INTEGRIN_CS_PATHWAY	1.6233352	0.014184397	0.1152416	1
GAL_LEUKEMIC_STEM_CELL_DN	1.6195939	0	0.11787682	1
KLEIN_TARGETS_OF_BCR_ABL1_FUSION	1.6180879	0.009852217	0.11838512	1
VALK_AML_CLUSTER_13	1.6168219	0.013186813	0.11841989	1
SERVITJA_LIVER_HNF1A_TARGETS_UP	1.6057584	0	0.12801889	1
LU_TUMOR_VASCULATURE_UP	1.5991826	0.021531101	0.1336919	1
KEGG_AUTOIMMUNE_THYROID_DISEASE	1.598355	0.023980815	0.13316575	1
CHIANG_LIVER_CANCER_SUBCLASS_CTNNB1_DN	1.5968419	0.002890173	0.13357712	1
MIKKELSEN_MCV6_ICP_WITH_H3K27ME3	1.5963955	0.002673797	0.13274628	1
REACTOME_DECTIN_2_FAMILY	1.5893923	0.021686748	0.13893402	1
KEGG_OLFACTORY_TRANSDUCTION	1.5882634	0	0.13886996	1
BOYLAN_MULTIPLE_MYELOMA_C_D_DN	1.5856516	0	0.14041033	1
MIKKELSEN_IPS_LCP_WITH_H3K4ME3	1.5851125	0	0.1396674	1
CROONQUIST_IL6_DEPRIVATION_DN	1.5815951	0	0.14204189	1
NABA_ECM_AFFILIATED	1.5814296	0.002801121	0.14091583	1
NABA_BASEMENT_MEMBRANES	1.5794954	0.011820331	0.1417829	1
REACTOME_INTERLEUKIN_6_FAMILY_SIGNALING	1.5791594	0.022883296	0.14086223	1
KEGG_AMINO_SUGAR_AND_NUCLEOTIDE_SUGAR_METABOLISM	1.5738902	0.012594459	0.14545795	1

VALK_AML_CLUSTER_4	1.5718138	0.02247191	0.14658101	1
SERVITJA_ISLET_HNF1A_TARGETS_UP	1.5717862	0	0.14531995	1
FLORIO_NEOCORTEX_BASAL_RADIAL_GLIA_UP	1.5689834	0	0.14740826	1
KIM_BIPOLAR_DISORDER_OLIGODENDROCYTE_DENSITY_CORR_DN	1.561211	0.007692308	0.15554905	1
KIM_MYC_AMPLIFICATION_TARGETS_DN	1.5609119	0.002724796	0.15458666	1
TANG_SENESCENCE_TP53_TARGETS_DN	1.5605235	0.018229166	0.15375781	1
EINAV_INTERFERON_SIGNATURE_IN_CANCER	1.5603956	0.025581395	0.15264146	1
REACTOME_G_ALPHA_S_SIGNALLING_EVENTS	1.5550104	0	0.15795867	1
KEGG_CELL_ADHESION_MOLECULES_CAMS	1.5517256	0	0.16103521	1
LU_TUMOR_ENDOTHELIAL_MARKERS_UP	1.547866	0.032183908	0.16450702	1
SAMOLS_TARGETS_OF_KHSV_MIRNAS_DN	1.5475546	0.028795812	0.16350445	1
IVANOVA_HEMATOPOIESIS_INTERMEDIATE_PROGENITOR	1.5467223	0	0.16326533	1
ZHOU_CELL_CYCLE_GENES_IN_IR_RESPONSE_24HR	1.5423851	0.011764706	0.16722648	1
ONO_FOXP3_TARGETS_DN	1.5395558	0.03255814	0.16965088	1
VERHAAK_GLIOBLASTOMA_MESENCHYMAL	1.534672	0	0.17472774	1
CLASPER_LYMPHATIC_VESSELS_DURING_METASTASIS_DN	1.5333022	0.020997375	0.17518638	1
BRUNO_HEMATOPOIESIS	1.5320746	0.002754821	0.17558926	1
ICHIBA_GRAFT_VERSUS_HOST_DISEASE_35D_UP	1.5310143	0	0.17563131	1
YAO_TEMPORAL_RESPONSE_TO_PROGESTERONE_CLUSTER_15	1.5300502	0.02189781	0.17542994	1
LINDSTEDT_DENDRITIC_CELL_MATURATION_D	1.5270253	0.010362694	0.17814079	1

HELLER_SILENCED_BY_METHYLATION_UP	1.5239711	0	0.18095939	1
HECKER_IFNB1_TARGETS	1.5229721	0.01055409	0.18097366	1
REACTOME_INTERLEUKIN_10_SIGNALING	1.5201783	0.025345622	0.18314987	1
SOTIRIOU_BREAST_CANCER_GRADE_1_VS_3_UP	1.5158671	0.003401361	0.18795668	1
HONRADO_BREAST_CANCER_BRCA1_VS_BRCA2	1.5140046	0.03736264	0.18914461	1
GRAHAM_CML_DIVIDING_VS_NORMAL_QUIESCENT_UP	1.5089718	0.003067485	0.19476457	1
EGUCHI_CELL_CYCLE_RB1_TARGETS	1.5086763	0.040865384	0.1938298	1
VALK_AML_CLUSTER_9	1.5057889	0.025761124	0.19646375	1
COATES_MACROPHAGE_M1_VS_M2_DN	1.5054512	0.016666668	0.19558278	1
REACTOME_MOLECULES_ASSOCIATED_WITH_ELASTIC_FIBRES	1.5039691	0.042410713	0.19631858	1
REACTOME_CLASS_A_1_RHODOPSIN_LIKE_RECEPTORS	1.5037361	0.003215434	0.19528872	1
MEISSNER_NPC_ICP_WITH_H3_UNMETHYLATED	1.5028751	0.04157044	0.19514282	1
LEIN_PONS_MARKERS	1.5007235	0.015544041	0.19680643	1
SMIRNOV_RESPONSE_TO_IR_2HR_DN	1.4998417	0.015957447	0.19665898	1
REACTOME_IL_6_TYPE_CYTOKINE_RECEPTOR_LIGAND_INTERACTIONS	1.4982133	0.045146726	0.19781254	1
CONCANNON_APOPTOSIS_BY_EPOXOMICIN_DN	1.4978226	0	0.19700618	1
FIGUEROA_AML_METHYLATION_CLUSTER_5_DN	1.4977059	0.0275	0.19588408	1
BERTUCCI_MEDULLARY_VS_DUCTAL_BREAST_CANCER_UP	1.496986	0.003412969	0.19557911	1
COATES_MACROPHAGE_M1_VS_M2_UP	1.4966935	0.00862069	0.19473508	1
MORI_IMMATURE_B_LYMPHOCYTE_UP	1.4938885	0.025575448	0.1976805	1

VANLOO_SP3_TARGETS_DN	1.4929363	0.008403362	0.1977511	1
REACTOME_INTERFERON_ALPHA_BETA_SIGNALING	1.4883733	0.016304348	0.20302084	1
KEGG_STEROID_BIOSYNTHESIS	1.4879581	0.038990825	0.20234136	1
ODONNELL_TARGETS_OF_MYC_AND_TFRC_DN	1.4852976	0.023923445	0.20469639	1
SASAKI_ADULT_T_CELL_LEUKEMIA	1.4844671	0	0.20452073	1
KEGG_INTESTINAL_IMMUNE_NETWORK_FOR_IGA_PRODUCTION	1.4829319	0.021428572	0.20524548	1
SHEPARD_BMYB_TARGETS	1.4826344	0.022408964	0.20440878	1
REACTOME_STING_MEDIATED_INDUCTION_OF_HOST_IMMUNE_RESPONSES	1.4821388	0.059382424	0.2038113	1
ODONNELL_TFRC_TARGETS_DN	1.4818972	0.009036144	0.20293756	1
MIKKELSEN_ES_HCP_WITH_H3K27ME3	1.4809111	0.029545454	0.20308287	1
MOHANKUMAR_HOXA1_TARGETS_DN	1.4787849	0	0.20494418	1
KORKOLA_YOLK_SAC_TUMOR	1.4748288	0.015463918	0.20962998	1
VISALA_AGING_LYMPHOCYTE_DN	1.4746819	0.042986427	0.20854436	1
REACTOME_ADP_SIGNALLING_THROUGH_P2Y_PURINOCEPTOR_1	1.4742516	0.059241705	0.2078392	1
MIKKELSEN_NPC_ICP_WITH_H3K4ME3	1.4738834	0	0.20724846	1
CROONQUIST_NRAS_SIGNALING_DN	1.4729023	0.008426966	0.2073719	1
REICHERT_MITOSIS_LIN9_TARGETS	1.4710367	0.04118993	0.20879252	1
BASSO_CD40_SIGNALING_UP	1.4709499	0.016759777	0.20770113	1
GRAHAM_CML_DIVIDING_VS_NORMAL_QUIESCENT_DN	1.4682815	0.005076142	0.21069889	1

REACTOME_CLASS_C_3_METABOTROPIC_GLUTAMATE_PHEROMONE_RECEPTORS	1.4657506	0.06146572	0.21329725	1
TAKEDA_TARGETS_OF_NUP98_HOXA9_FUSION_16D_DN	1.4638046	0.019607844	0.2149473	1
TARTE_PLASMA_CELL_VS_B_LYMPHOCYTE_DN	1.4637944	0.047505938	0.21372831	1
CADWELL_ATG16L1_TARGETS_UP	1.4626589	0.020114943	0.214398	1
GRAHAM_NORMAL_QUIESCENT_VS_NORMAL_DIVIDING_DN	1.4583338	0.016	0.21971142	1
PID_CONE_PATHWAY	1.4579908	0.048275862	0.21904087	1
KONG_E2F3_TARGETS	1.4560139	0.011764706	0.22076394	1
NABA_ECM_REGULATORS	1.4559964	0.016025642	0.21954189	1
BOYLAN_MULTIPLE_MYELOMA_D_DN	1.4544919	0.01344086	0.22054751	1
MIKKELSEN_NPC_LCP_WITH_H3K4ME3	1.4530977	0.020151133	0.221558	1
WANG_NFKB_TARGETS	1.452019	0.056737587	0.22195311	1
SHEN_SMARCA2_TARGETS_DN	1.4513962	0.003460208	0.22176453	1
BREDEMEYER_RAG_SIGNALING_NOT_VIA_ATM_DN	1.4507638	0.033854168	0.22158577	1
REACTOME_GPCR_LIGAND_BINDING	1.4499031	0.007352941	0.22163862	1
MEISSNER_NPC_HCP_WITH_H3_UNMETHYLATED	1.449874	0	0.22051044	1
CHEN_ETV5_TARGETS_SERTOLI	1.447093	0.056470588	0.22344981	1
WILENSKY_RESPONSE_TO_DARAPLADIB	1.4461164	0.034013607	0.22369257	1
OHGUCHI_LIVER_HNF4A_TARGETS_DN	1.4458239	0.0132626	0.22298163	1
GRAHAM_NORMAL_QUIESCENT_VS_NORMAL_DIVIDING_UP	1.4447597	0.034739453	0.22338958	1
RIZ_ERYTHROID_DIFFERENTIATION_APOBEC2	1.4420094	0.06954437	0.22645745	1

SAFFORD_T_LYMPHOCYTE_ANERGY	1.4413924	0.015503876	0.22630695	1
SCHUETZ_BREAST_CANCER_DUCTAL_INVASIVE_UP	1.4406245	0	0.2263668	1
LEE_TARGETS_OF_PTCH1_AND_SUFU_UP	1.4400913	0.033591732	0.22602335	1
CHICAS_RB1_TARGETS_GROWING	1.4395239	0.003584229	0.22572747	1
GENTLES_LEUKEMIC_STEM_CELL_UP	1.4392514	0.060606062	0.22497441	1
RICKMAN_HEAD_AND_NECK_CANCER_E	1.4391557	0.03233831	0.22397162	1
REACTOME_CHEMOKINE_RECEPTORS_BIND_CHEMOKINES	1.4370286	0.038659792	0.22581215	1
RIZ_ERYTHROID_DIFFERENTIATION_6HR	1.4368659	0.05378973	0.22494234	1
REACTOME_COMPLEX_I_BIOGENESIS	1.4344399	0.03021978	0.22745441	1
MIKKELSEN_MEF_ICP_WITH_H3K27ME3	1.4339058	0.00310559	0.22710161	1
BURTON_ADIPOGENESIS_3	1.4331824	0.008746356	0.22719173	1
MIKKELSEN_MEF_HCP_WITH_H3K27ME3	1.4324254	0	0.22735086	1
ZHOU_CELL_CYCLE_GENES_IN_IR_RESPONSE_6HR	1.4321058	0.018567638	0.22677523	1
LEIN_MIDBRAIN_MARKERS	1.4303442	0.021680217	0.22850797	1
PID_SYNDECAN_3_PATHWAY	1.4289105	0.075170845	0.22965318	1
GREENBAUM_E2A_TARGETS_DN	1.4263648	0.085011184	0.2324118	1
WANG_MLL_TARGETS	1.4253981	0	0.23292416	1
PLASARI_TGFB1_SIGNALING_VIA_NFIC_10HR_DN	1.4212114	0.053268764	0.23830496	1
FINETTI_BREAST_CANCER_KINOME_RED	1.4211339	0.06542056	0.23727694	1
OUILLETTE_CLL_13Q14_DELETION_DN	1.4194946	0.038560413	0.23870593	1
REACTOME_ENDOGENOUS_STEROLS	1.416934	0.07323232	0.24169172	1

KOHOUTEK_CCNT2_TARGETS	1.4168297	0.027624309	0.2407471	1
REACTOME_INTERLEUKIN_20_FAMILY_SIGNALING	1.4158943	0.058411215	0.24117129	1
HOLLEMAN_ASPARAGINASE_RESISTANCE_ALL_DN	1.4155505	0.087804876	0.24051134	1
FOSTER_KDM1A_TARGETS_UP	1.4128258	0.003333333	0.24372418	1
RICKMAN_HEAD_AND_NECK_CANCER_A	1.4104109	0.029569892	0.24668314	1
FONTAINE_PAPILLARY_THYROID_CARCINOMA_DN	1.4095042	0.03125	0.24703714	1
ABBUD_LIF_SIGNALING_1_DN	1.4077821	0.08144797	0.24874006	1
SENGUPTA_NASOPHARYNGEAL_CARCINOMA_UP	1.40683	0	0.24924707	1
***p53*$^{-/-}$ V-Fus CD4 memory T cells vs WT CD4 memory T cells at non-tumor bearing status**	**NES**	**NOM p-val**	**FDR q-val**	**FWER p-val**
BENNETT_SYSTEMIC_LUPUS_ERYTHEMATOSUS	2.298842	0	0	0
CROONQUIST_NRAS_SIGNALING_DN	2.1538405	0	0.00744025	0.018
CROONQUIST_IL6_DEPRIVATION_DN	2.149995	0	0.00523207	0.019
REACTOME_INTERFERON_ALPHA_BETA_SIGNALING	2.108988	0	0.010503752	0.051
MAEKAWA_ATF2_TARGETS	2.0928953	0	0.010538484	0.062
KIM_LRRC3B_TARGETS	2.0843596	0	0.00946979	0.067
BROWNE_INTERFERON_RESPONSIVE_GENES	2.0816116	0	0.00835514	0.069
GAVIN_FOXP3_TARGETS_CLUSTER_P6	2.0787444	0	0.007834083	0.074
ICHIBA_GRAFT_VERSUS_HOST_DISEASE_D7_UP	2.0782282	0	0.007055597	0.075
UROSEVIC_RESPONSE_TO_IMIQUIMOD	2.0708923	0	0.006930003	0.082
VILIMAS_NOTCH1_TARGETS_DN	2.0410504	0	0.009801956	0.122

ZHAN_MULTIPLE_MYELOMA_PR_UP	2.028427	0	0.011107302	0.148
HECKER_IFNB1_TARGETS	2.0133	0	0.012656835	0.185
MARKEY_RB1_ACUTE_LOF_DN	2.0079646	0	0.012571611	0.195
KRASNOSELSKAYA_ILF3_TARGETS_UP	2.0047565	0.002288329	0.012499092	0.208
REACTOME_PHOSPHORYLATION_OF_THE_APC_C	1.9861412	0	0.016241947	0.278
KIM_GLIS2_TARGETS_UP	1.9772102	0	0.01664941	0.299
FARMER_BREAST_CANCER_CLUSTER_1	1.9546739	0	0.02106717	0.377
WIELAND_UP_BY_HBV_INFECTION	1.910043	0	0.03472049	0.547
MOSERLE_IFNA_RESPONSE	1.9041648	0	0.036228064	0.577
FURUKAWA_DUSP6_TARGETS_PCI35_UP	1.8835597	0	0.04374788	0.659
BOYLAN_MULTIPLE_MYELOMA_PCA3_DN	1.8753222	0	0.046361767	0.702
ICHIBA_GRAFT_VERSUS_HOST_DISEASE_35D_UP	1.8648046	0	0.050732125	0.761
SANA_RESPONSE_TO_IFNG_UP	1.8640412	0.002493766	0.04892674	0.764
KONG_E2F3_TARGETS	1.858664	0	0.05049886	0.787
SOTIRIOU_BREAST_CANCER_GRADE_1_VS_3_UP	1.8538927	0	0.051619828	0.812
BOSCO_INTERFERON_INDUCED_ANTIVIRAL_MODULE	1.8491073	0	0.0524522	0.831
LY_AGING_MIDDLE_DN	1.8486277	0.004494382	0.0509916	0.833
LIU_VAV3_PROSTATE_CARCINOGENESIS_UP	1.8445642	0	0.052154772	0.852
VALK_AML_CLUSTER_3	1.836823	0.002132196	0.055040456	0.874
JIANG_HYPOXIA_CANCER	1.8336234	0	0.054856643	0.882
GRAESSMANN_RESPONSE_TO_MC_AND_SERUM_DEPRIVATION_U	1.8290334	0	0.055609927	0.888

P				
FLORIO_NEOCORTEX_BASAL_RADIAL_GLIA_DN	1.8272799	0	0.055052374	0.89
BURTON_ADIPOGENESIS_PEAK_AT_24HR	1.8228956	0	0.0556816	0.899
GREENBAUM_E2A_TARGETS_UP	1.8069612	0	0.063974865	0.934
YAN_ESCAPE_FROM_ANOIKIS	1.792967	0.002267574	0.07211592	0.962
REICHERT_MITOSIS_LIN9_TARGETS	1.785741	0.00877193	0.07571276	0.975
BOYLAN_MULTIPLE_MYELOMA_PCA1_UP	1.776144	0	0.0811287	0.983
ROSS_AML_WITH_MLL_FUSIONS	1.7620925	0	0.09122209	0.992
WORSCHECH_TUMOR_REJECTION_UP	1.7526537	0.002320186	0.09764391	0.997
AFFAR_YY1_TARGETS_DN	1.7456944	0	0.1018497	0.998
DAUER_STAT3_TARGETS_DN	1.7416044	0.002293578	0.10366578	0.999
LIAN_LIPA_TARGETS_6M	1.7397966	0	0.10286151	0.999
REACTOME_INHIBITION_OF_THE_PROTEOLYTIC_ACTIVITY_OF_APC_C_REQUIRED_FOR_THE_ONSET_OF_ANAPHASE_BY_MITOTIC_SPINDLE_CHECKPOINT_COMPONENTS	1.7380462	0.004494382	0.10252624	0.999
REACTOME_ANTIMICROBIAL_PEPTIDES	1.7369787	0.002386635	0.1011062	0.999
STEARMAN_TUMOR_FIELD_EFFECT_UP	1.7205875	0.006185567	0.116526745	0.999
RADAEVA_RESPONSE_TO_IFNA1_UP	1.7181855	0.007109005	0.11634395	0.999
GRAHAM_NORMAL_QUIESCENT_VS_NORMAL_DIVIDING_DN	1.7103583	0	0.122880176	0.999
COLINA_TARGETS_OF_4EBP1_AND_4EBP2	1.707183	0	0.12433775	0.999
REACTOME_IMMUNOREGULATORY_INTERACTIONS_BETWEEN_	1.7058533	0	0.123284094	0.999

A_LYMPHOID_AND_A_NON_LYMPHOID_CELL				
JECHLINGER_EPITHELIAL_TO_MESENCHYMAL_TRANSITION_UP	1.7034881	0	0.12360451	0.999
CHIARETTI_T_ALL_RELAPSE_PROGNOSIS	1.7034141	0.011682243	0.121320456	0.999
FERREIRA_EWINGS_SARCOMA_UNSTABLE_VS_STABLE_DN	1.6982014	0.00243309	0.12515807	0.999
TONKS_TARGETS_OF_RUNX1_RUNX1T1_FUSION_GRANULOCYTE_DN	1.6952765	0.012295082	0.12630485	0.999
BOSCO_TH1_CYTOTOXIC_MODULE	1.6941774	0	0.12511611	1
ZHOU_CELL_CYCLE_GENES_IN_IR_RESPONSE_24HR	1.6935759	0	0.12364986	1
GAVIN_IL2_RESPONSIVE_FOXP3_TARGETS_UP	1.678309	0.015086207	0.13856235	1
GAL_LEUKEMIC_STEM_CELL_DN	1.6755414	0	0.13986024	1
MCLACHLAN_DENTAL_CARIES_UP	1.6747867	0	0.1383155	1
ZHANG_INTERFERON_RESPONSE	1.6745609	0.016666668	0.13627043	1
YAO_TEMPORAL_RESPONSE_TO_PROGESTERONE_CLUSTER_15	1.6705332	0.006134969	0.1394238	1
CASTELLANO_NRAS_TARGETS_UP	1.66876	0.002369668	0.13949469	1
REACTOME_SIGNALLING_TO_ERKS	1.6672913	0.004405286	0.13896075	1
REACTOME_CONVERSION_FROM_APC_C:CDC20_TO_APC_C:CDH1_IN_LATE_ANAPHASE	1.6652815	0.021028038	0.13911253	1
FINETTI_BREAST_CANCER_KINOME_RED	1.6628909	0.006864989	0.13976343	1
ROSTY_CERVICAL_CANCER_PROLIFERATION_CLUSTER	1.6619208	0	0.13868245	1
LINDSTEDT_DENDRITIC_CELL_MATURATION_D	1.6534514	0.002212389	0.1472472	1
SHEPARD_BMYB_TARGETS	1.648274	0.002398082	0.15170144	1

BOYLAN_MULTIPLE_MYELOMA_D_DN	1.6454979	0	0.15283117	1
BAUS_TFF2_TARGETS_UP	1.6410189	0.012958963	0.15639886	1
ISHIDA_E2F_TARGETS	1.6362126	0.008830022	0.16053534	1
BURTON_ADIPOGENESIS_3	1.6327333	0.00248139	0.163025	1
TAKEDA_TARGETS_OF_NUP98_HOXA9_FUSION_3D_UP	1.6317143	0.002398082	0.16217759	1
NAKAYAMA_SOFT_TISSUE_TUMORS_PCA2_UP	1.6309186	0.002309469	0.16116557	1
MISSIAGLIA_REGULATED_BY_METHYLATION_DN	1.6283921	0.007194245	0.16243891	1
CADWELL_ATG16L1_TARGETS_UP	1.6282743	0.006928407	0.16048597	1
REACTOME_BIOSYNTHESIS_OF_SPECIALIZED_PRORESOLVING_MEDIATORS_SPMS	1.6262003	0.025229357	0.16137373	1
REACTOME_INTERFERON_GAMMA_SIGNALING	1.6244441	0.002358491	0.16172682	1
PID_PLK1_PATHWAY	1.6215063	0.00921659	0.16369255	1
WHITEFORD_PEDIATRIC_CANCER_MARKERS	1.6154327	0	0.16983528	1
LEE_EARLY_T_LYMPHOCYTE_UP	1.6098224	0.004938272	0.1756697	1
HANN_RESISTANCE_TO_BCL2_INHIBITOR_UP	1.602758	0.015765766	0.18372819	1
REACTOME_ACTIVATION_OF_APC_C_AND_APC_C:CDC20_MEDIATED_DEGRADATION_OF_MITOTIC_PROTEINS	1.5994742	0	0.186364	1
REACTOME_DEPURINATION	1.5945001	0.013452915	0.19210671	1
SMID_BREAST_CANCER_LUMINAL_A_DN	1.5873868	0.04506438	0.2020543	1
EINAV_INTERFERON_SIGNATURE_IN_CANCER	1.5813148	0.01843318	0.2101246	1
LIAN_LIPA_TARGETS_3M	1.580515	0.008888889	0.2091083	1

KANG_DOXORUBICIN_RESISTANCE_UP	1.5724418	0.014285714	0.22075492	1
HOFMANN_MYELODYSPLASTIC_SYNDROM_RISK_DN	1.5713836	0.03742204	0.22012351	1
BROWN_MYELOID_CELL_DEVELOPMENT_UP	1.5669459	0.002673797	0.22543076	1
WUNDER_INFLAMMATORY_RESPONSE_AND_CHOLESTEROL_UP	1.5637547	0.007177034	0.22831766	1
SENGUPTA_NASOPHARYNGEAL_CARCINOMA_UP	1.5588945	0	0.23475905	1
XU_AKT1_TARGETS_6HR	1.5558615	0.029850746	0.23769958	1
REACTOME_BASE_EXCISION_REPAIR_AP_SITE_FORMATION	1.5539317	0.018223235	0.23906758	1
BOYAULT_LIVER_CANCER_SUBCLASS_G5_DN	1.5497006	0.038116593	0.24450804	1
ZHENG_IL22_SIGNALING_UP	1.5482119	0.009925558	0.2445329	1
HOFFMANN_PRE_BI_TO_LARGE_PRE_BII_LYMPHOCYTE_UP	1.5441349	0.021321962	0.24954982	1
***p53*$^{-/-}$ V-Fus CD4 memory T cells vs *p53*$^{-/-}$ CD4 memory T cells at non-tumor bearing status**	**NES**	**NOM p-val**	**FDR q-val**	**FWER p-val**
nothing				

Supplementary Table 6: Somatic mutations detected by WES in 17 mice.

ID	Chr	Start	End	Ref	Alt	Gene	Type of mutation	Depth	P-value (fisher)	P-value (EBCall)
P53-2	14	77034157	77034157	G	A	Lacc1	nonsynonymous SNV	99	2.926	2.764
	7	126993672	126993677	CCT CCC	-	Mvp	nonframeshift deletion	40	2.987	3.345
	7	66888426	66888426	G	A	Adamts17	nonsynonymous SNV	28	3.545	3.448
	14	70491354	70491354	C	T	Bmp1	nonsynonymous SNV	72	4.275	4.213
	4	35708406	35708406	C	T	Lingo2	nonsynonymous SNV	112	4.715	4.014
	19	13530344	13530344	A	T	Olfr1480	nonsynonymous SNV	67	5.071	4.396
	6	142598164	142598164	G	A	Abcc9	nonsynonymous SNV	47	6.388	6.146
	2	88767620	88767620	G	A	Olfr1200	nonsynonymous SNV	115	6.881	5.371
	13	43668029	43668029	G	A	Rnf182	nonsynonymous SNV	17	13.206	10.887
	17	20278821	20278821	C	A	Vmn2r106	nonsynonymous SNV	68	14.813	10.391
P53-8	4	73403065	73403065	G	T	Gm11487	nonsynonymous SNV	238	2.081	3.154
	5	145147854	145147854	C	G	Bud31	nonsynonymous SNV	171	2.453	4.492
	1	186969056	186969056	A	G	D1Pas1	nonsynonymous SNV	58	2.62	3.528
	14	35580513	35580513	C	G	Grid1	nonsynonymous SNV	52	3.004	3.595
	18	13845409	13845409	A	G	Zfp521	nonsynonymous SNV	63	3.441	3.245
	5	12553136	12553136	T	C	Sema3d	nonsynonymous SNV	66	3.629	5.439
	11	70228682	70228682	-	C	Bcl6b	frameshift insertion	24	4.262	2.511
	2	120279266	120279266	C	A	Pla2g4d	nonsynonymous SNV	44	4.521	5.071

	9	111366696	111366696	C	G	Trank1	nonsynonymous SNV	43	5.686	4.542
	11	70228513	70228513	C	-	Bcl6b	frameshift deletion	67	6.088	4.502
	14	18871506	18871506	G	-	Ube2e2	frameshift deletion	146	8.75	4.585
	12	86244138	86244138	C	T	Gpatch2l	nonsynonymous SNV	59	15.005	11.073
P53-9	2	26468511	26468511	G	T	Notch1	nonsynonymous SNV	84	2.288	2.41
	7	111508067	111508067	C	T	Galnt18	nonsynonymous SNV	154	2.974	2.67
	15	100784858	100784858	G	C	Slc4a8	nonsynonymous SNV	64	4.168	3.093
	2	103976193	103976193	G	T	Lmo2	nonsynonymous SNV	47	11.61	7.111
	2	85647911	85647911	A	T	Olfr1002	nonsynonymous SNV	82	12.336	7.013
	13	27127351	27127351	A	C	Prl3d2	nonsynonymous SNV	99	14.716	8.014
	X	20670593	20670593	G	C	Uba1	nonsynonymous SNV	47	32.613	60
VDEL-8	X	43592647	43592647	A	C	Tex13c1	nonsynonymous SNV	14	2.397	2.404
	14	96152041	96152041	T	G	Klhl1	nonsynonymous SNV	51	2.605	2.895
	7	47427186	47427186	A	C	Mrgpra2a	nonsynonymous SNV	67	2.671	2.72
	5	25950884	25950884	A	G	Gm21671	nonsynonymous SNV	397	4.437	3.917
	2	180595328	180595328	G	A	Ogfr	nonsynonymous SNV	22	4.542	3.201
	2	88896904	88896904	C	T	Olfr1208	nonsynonymous SNV	76	4.928	3.229
	14	65054710	65054710	C	T	Extl3	nonsynonymous SNV	55	7.961	7.818
	4	131793625	131793625	G	T	Ptpru	nonsynonymous SNV	61	8.347	7.297
	7	10714842	10714842	A	T	Nlrp4b	nonsynonymous SNV	50	9.235	6.537
	13	38955779	38955779	G	A	Slc35b3	nonsynonymous SNV	62	10.06	7.09
	13	54683966	54683966	C	T	Rnf44	nonsynonymous SNV	72	11.72	8.416

	X	20670619	20670621	TTC	-	Uba1	nonframeshift deletion	108	41.218	13.371
VDEL-14	2	117153140	117153140	C	T	Spred1	nonsynonymous SNV	79	2.082	2.619
	1	9613400	9613400	G	A	Vxn	nonsynonymous SNV	24	2.46	2.708
	18	74218911	74218911	G	C	Cxxc1	nonsynonymous SNV	46	2.548	3.197
	7	4340889	4340889	A	T	Ncr1	nonsynonymous SNV	90	2.576	2.575
	10	86846917	86846917	C	G	Stab2	nonsynonymous SNV	38	3.874	3.899
	11	85912279	85912279	C	A	Tbx4	nonsynonymous SNV	38	4.361	4.382
	X	11318582	11318582	C	G	H2al1c;H2al1d;H2al1f;H2al1g;H2al1h;H2al1i	nonsynonymous SNV	19	5.145	4.785
	5	39615100	39615100	G	A	Hs3st1	nonsynonymous SNV	40	5.334	4.807
	18	10560455	10560455	T	C	Greb1l	nonsynonymous SNV	48	7.211	6.663
	X	13290522	13290522	A	G	Ddx3x	nonsynonymous SNV	40	13.931	12.866
	X	20672445	20672445	G	A	Uba1	nonsynonymous SNV	36	21.798	60
VDEL-15	2	26459954	26459954	-	CT	Notch1	frameshift insertion	94	4.14	2.633
VS2-1	11	3187308	3187308	G	T	Sfi1	nonsynonymous SNV	1585	2.004	2.315
	11	110250454	110250454	C	T	Abca6	nonsynonymous SNV	78	3.625	2.976
	X	120400453	120400453	A	-	Pcdh11x	frameshift deletion	30	4.648	3.728
	11	119463393	119463393	C	T	Rnf213	nonsynonymous SNV	62	7.714	5.876
	3	89141633	89141633	-	G	Pklr	frameshift insertion	29	8.139	4.384
	3	104462752	104462752	A	G	Lrig2	nonsynonymous SNV	37	8.621	5.995
	1	46612661	46612661	G	C	Dnah7c	nonsynonymous SNV	81	12.544	7.931
	17	56047318	56047318	C	T	Chaf1a	nonsynonymous SNV	51	13.228	7.686

VS2-2	9	15997209	15997209	T	A	Fat3	nonsynonymous SNV	62	2.403	2.668
	13	11750933	11750933	T	G	Ryr2	nonsynonymous SNV	78	4.343	4.264
	8	43626014	43626014	C	G	Adam34l	nonsynonymous SNV	131	7.107	6.25
	8	19064808	19064808	C	A	Defb39	nonsynonymous SNV	84	11.539	8.133
	19	12088109	12088109	C	T	Olfr1426	nonsynonymous SNV	134	15.518	9.612
VS2-6	7	105156863	105156863	T	C	Olfr684	nonsynonymous SNV	136	3.165	2.739
	10	34184085	34184085	-	C	Dse	frameshift insertion	69	4.125	2.541
	19	58799897	58799897	A	G	Hspa12a	nonsynonymous SNV	35	6.358	5.679
	11	101033964	101033964	G	A	Atp6v0a1	nonsynonymous SNV	55	12.993	9.709
VS2-17	1	90821978	90821978	A	C	Col6a3	nonsynonymous SNV	73	2.625	2.469
	1	54667543	54667543	C	G	Ankrd44	nonsynonymous SNV	66	2.645	3.205
	4	100441492	100441492	C	A	Ror1	nonsynonymous SNV	137	4.726	3.875
	7	9942330	9942330	A	C	Vmn2r48	nonsynonymous SNV	205	4.736	4.155
	X	145340757	145340757	C	T	Lhfpl1	nonsynonymous SNV	33	5.006	4.989
	2	73363978	73363978	T	C	Gpr155	nonsynonymous SNV	119	6.231	5.235
	3	133466879	133466879	G	A	Tet2	nonsynonymous SNV	83	8.91	6.342
	6	88764640	88764640	G	A	Mgll	nonsynonymous SNV	100	9.32	6.214
VDEL-4	12	75911116	75911116	C	T	Syne2	nonsynonymous SNV	53	2.566	3.04
	4	101163673	101163673	C	A	Jak1	nonsynonymous SNV	44	2.885	4.522
	7	50448915	50448915	G	A	Nell1	nonsynonymous SNV	75	3.932	3.895
	7	86394962	86394962	A	-	Olfr303	frameshift deletion	65	4.14	2.664
	8	120588767	120588767	T	C	Gins2	nonsynonymous SNV	51	6.315	5.09

	2	111944993	111944993	C	A	Olfr1307	nonsynonymous SNV	128	6.662	5.72
	3	64537760	64537760	G	T	Vmn2r6	nonsynonymous SNV	102	8.069	6.494
	6	59354651	59354651	C	T	Gprin3	nonsynonymous SNV	75	8.654	6.343
	7	63103815	63103815	G	T	Chrna7	nonsynonymous SNV	84	12.857	9.407
VDEL-11	6	121648151	121648151	G	A	A2m	nonsynonymous SNV	78	3.16	2.604
	17	18304169	18304169	A	-	Vmn2r93	frameshift deletion	95	3.177	2.245
	7	120283113	120283113	T	A	Abca14	nonsynonymous SNV	44	3.889	3.29
	1	24178311	24178311	G	A	Col9a1	nonsynonymous SNV	92	4.435	4.054
	2	120060267	120060267	G	-	Sptbn5	frameshift deletion	81	4.518	3.052
	7	42928038	42928038	A	C	Vmn2r63	nonsynonymous SNV	87	5.115	3.946
VS2-10	3	87088401	87088401	G	A	Kirrel	nonsynonymous SNV	31	2.031	3.454
	2	165146713	165146713	C	A	Cdh22	nonsynonymous SNV	45	2.056	2.763
	8	24823970	24823970	A	C	Adam5	nonsynonymous SNV	53	2.215	2.333
	16	94268061	94268061	T	A	Hlcs	nonsynonymous SNV	29	2.363	2.683
	14	56950203	56950203	C	-	Zmym2	frameshift deletion	58	2.674	2.888
	11	32735316	32735316	C	T	Fbxw11	nonsynonymous SNV	84	2.892	3.379
	9	58080820	58080820	C	G	Ccdc33	nonsynonymous SNV	69	3.274	4.004
VS2-11	19	44816000	44816000	C	T	Pax2	stopgain	60	2.195	2.925
	6	131309960	131309960	C	G	Styk1	nonsynonymous SNV	75	2.619	3.456
	X	48547275	48547275	G	A	Zfp280c	stopgain	30	3.413	2.821
	X	13289410	13289410	T	A	Ddx3x	nonsynonymous SNV	89	3.839	2.891
	X	7706732	7706732	G	T	Gpkow	nonsynonymous SNV	136	4.403	2.988

	9	120955227	120955227	C	G	Ctnnb1	nonsynonymous SNV	92	5.568	6.473
	9	7503521	7503521	G	T	Mmp10	nonsynonymous SNV	188	6.309	60
	1	175706024	175706024	T	-	Wdr64	frameshift deletion	75	6.664	4.081
VS2-15	11	88073613	88073613	C	T	Vezf1	nonsynonymous SNV	99	3.362	3.95
	17	40232588	40232588	A	C	Crisp3	nonsynonymous SNV	69	6.564	4.966
	2	52242019	52242019	G	A	Neb	stopgain	135	7.086	60
	17	53974059	53974059	T	-	Sult1c1	frameshift deletion	100	10.422	6.329
VS2-18	19	5607723	5607723	C	T	Kat5	nonsynonymous SNV	127	2.442	2.272
	12	13583520	13583520	C	T	Nbas	nonsynonymous SNV	104	3.425	3.281
	4	106771550	106771550	C	T	Acot11	nonsynonymous SNV	69	4.566	2.445
	8	61393779	61393779	C	T	Sh3rf1	nonsynonymous SNV	41	4.702	4.051
	11	75390310	75390310	C	G	Smyd4	nonsynonymous SNV	40	5.217	5.185
	1	32520951	32520951	G	T	Gm9839	nonsynonymous SNV	157	5.865	5.283
	17	35528160	35528160	C	T	Cchcr1	nonsynonymous SNV	85	6.176	4.431
	9	88715591	88715591	C	T	Mthfsl	nonsynonymous SNV	159	6.439	5.026
	3	53654825	53654825	C	A	Frem2	nonsynonymous SNV	84	9.731	6.429
	X	43591275	43591275	G	A	Tex13c1	nonsynonymous SNV	50	12.928	13.494
	10	24049962	24049962	C	A	Taar7f	nonsynonymous SNV	201	18.012	11.049
VS2-19	3	118797433	118797433	T	A	Dpyd	nonsynonymous SNV	63	2.433	3.024
	X	141723475	141723475	T	-	Irs4	frameshift deletion	75	3.11	2.381
	12	81421328	81421328	C	T	Adam4	nonsynonymous SNV	110	3.557	3.334
	1	3216173	3216173	C	A	Xkr4	nonsynonymous SNV	105	4.283	3.434

	18	37011132	37011132	G	A	Pcdha11	nonsynonymous SNV	565	8.213	13.61
	7	104768692	104768692	-	T	Usp17le	frameshift insertion	214	9.51	3.779
	7	104769614	104769614	-	GT	Usp17le	frameshift insertion	797	24.857	7.633

Supplementary Table 7: Lists of genes exhibiting chromosomal amplification or deletion.

Amplified genes					
14qE4	**chr14:114330002-116610000**				
1700100I10Rik	4930524C18Rik	Gpc5	Mir20a	Mir17	Mir92-1
4930505G20Rik	Mir17hg	Mir18	Mir19a	Mir19b-1	
15qD1	**chr15:60930002-63510000**				
Myc	Pvt1	H2afy3	D030024E09Rik	Gm20740	
Deleted genes					
6qB1	**chr6:40950002-41610000**				
Ephb6	Prss3	Trpv6	Try5	Gm5409	Gm5771
Prss2	Try4	2210010C04Rik	Prss1	Try10	Gm10334
14qC2	**chr14:52770002-54870000**				
Sall2	Olfr1508	Rab2b	Olfr1511	Tox4	
Mettl3	Olfr1509	Supt16	Olfr1510	Snord8	
Olfr1507	Chd8	Olfr1513	Olfr1512		
16qA1	**chr16:1-16350000**				
Adcy9	Snai2	Efcab1	Anks3	Dnaja3	Rbfox1
Ciita	Snn	Nudt16l1	1700037C18Rik	Mpv17l	Abat
Cebpd	Tnfrsf17	Bfar	4833415N18Rik	Pdxdc1	Gm1600
Socs1	Tnp2	Nde1	Glyr1	Txndc11	Tvp23a
Crebbp	Nubp1	2900011O08Rik	Parn	Zc3h7a	Zfp174
Dnase1	Pla2g10	Pkp2	Zfp263	Rrn3	Smim22

Emp2	Nagpa	Nmral1	Clec16a	Srl	Gm5766
Grin2a	Ercc4	Trap1	Snx29	Ubn1	A630010A05Rik
Gspt1	Carhsp1	Rpl39l	Ifitm7	Ubald1	Sec14l5
Hmox2	Slx4	1700123O21Rik	4930451G09Rik	Alg1	Mir365-1
Mcm4	Pmm2	1810013L24Rik	Cldn26	Rmi2	Mir484
Mgrn1	Mefv	2610020C07Rik	Naa60	Cpped1	Gm9961
Abcc1	Litaf	2310015D24Rik	Atf7ip2	Marf1	Gm4262
Myh11	Dexi	Yars2	1700003L19Rik	Spidr	Mir193b
Ntan1	Rogdi	Tekt5	4930455F16Rik	AU021092	Mir1945
Olfr15	Fopnl	Eef2kmt	Pla2g10os	Mettl22	Gm16861
Ppl	Rsl1d1	Ube2v2	Cluap1	Mkl2	Mir6365
Prkdc	Pam16	Zfp597	4930562C15Rik	Vasn	
Prm1	3110001I22Rik	Sept12	Coro7	Usp7	
Prm2	Cdip1	Mzt2	Tfap4	Olfr161	
Prm3	Tmem186	Shisa9	Glis2	Nlrc3	

1. Subramanian A, Tamayo P, Mootha VK, et al. Gene set enrichment analysis: a knowledge-based approach for interpreting genome-wide expression profiles. *Proc Natl Acad Sci U S A*. 2005;102(43):15545-15550.

2. Mootha VK, Lindgren CM, Eriksson KF, et al. PGC-1alpha-responsive genes involved in oxidative phosphorylation are coordinately downregulated in human diabetes. *Nat Genet*. 2003;34(3):267-273.

3. Zhou Y, Zhou B, Pache L, et al. Metascape provides a biologist-oriented resource for the analysis of systems-level datasets. *Nat Commun*. 2019;10(1):1523.

4. Heavican TB, Bouska A, Yu J, et al. Genetic drivers of oncogenic pathways in molecular subgroups of peripheral T-cell lymphoma. *Blood*. 2019;133(15):1664-1676.

5. LeBlanc RE, Lefterova MI, Suarez CJ, et al. Lymph node involvement by mycosis fungoides and Sezary syndrome mimicking angioimmunoblastic T-cell lymphoma. *Hum Pathol*. 2015;46(9):1382-1389.